MATHEMATICAL MODELING OF PHASE CHANGE HEAT TRANSFER PROCESS IN BIOLOGICAL TISSUES

Ph.D. THESIS

by

AJAY KUMAR

DEPARTMENT OF MATHEMATICS
INDIAN INSTITUTE OF TECHNOLOGY ROORKEE
ROORKEE – 247 667 (INDIA)
DECEMBER, 2017

MATHEMATICAL MODELING OF PHASE CHANGE HEAT TRANSFER PROCESS IN BIOLOGICAL TISSUES

A THESIS

Submitted in partial fulfilment of the requirements for the award of the degree

of

DOCTOR OF PHILOSOPHY

in

MATHEMATICS

by

AJAY KUMAR

DEPARTMENT OF MATHEMATICS
INDIAN INSTITUTE OF TECHNOLOGY ROORKEE
ROORKEE – 247 667 (INDIA)
DECEMBER, 2017

INDIAN INSTITUTE OF TECHNOLOGY ROORKEE
ROORKEE

CANDIDATE'S DECLARATION

I hereby certify that the work which is being presented in the thesis entitled "**MATHEMATICAL MODELING OF PHASE CHANGE HEAT TRANSFER PROCESS IN BIOLOGICAL TISSUES"** in partial fulfilment of the requirements for the award of the Degree of Doctor of Philosophy and submitted in the Department of Mathematics of the Indian Institute of Technology Roorkee, Roorkee is an authentic record of my own work carried out during a period from January, 2013 to December, 2017 under the supervision of Dr. V. K. Katiyar, Professor, Department of Mathematics, Indian Institute of Technology Roorkee, Roorkee and Dr. Shirley Telles, Director, Patanjali Research Foundation, Patanjali Yogpeeth, Haridwar, India.

The matter presented in this thesis has not been submitted by me for the award of any other degree of this or any other Institution.

(AJAY KUMAR)

This is to certify that the above statement made by the candidate is correct to the best of our knowledge.

(Dr. Shirley Telles)
Supervisor

(Dr. V. K. Katiyar)
Supervisor

The Ph.D. Viva-Voce Examination of **Mr. AJAY KUMAR**, Research Scholar, has been held on .....

Chairman, SRC

External Examiner

This is to certify that the student has made all the corrections in the thesis.

Supervisor

Head of the Department

Dated: .....

Abstract

Heat transfer involving phase change phenomena in biological tissues is a complex process. It involves several mechanisms such as thermal conduction, convection, radiation, metabolic heat generation, blood perfusion and phase change. The analysis of many biological heat transfer applications by the physiologists, physicians and engineers in the field of bio-heat transfer have resulted in improvement of treatment, preservation, destroying tumors and the protection of humans from extreme environmental conditions.

Phase change heat transfer problems are also known as moving boundary problems which are encountered in many practical applications like metal casting, environmental engineering, thermal energy storage system, freezing and thawing of foodstuff, cryopreservation and cryosurgery etc. Cryosurgery is a therapeutic technique that uses extreme freezing to treat the diseased tissues. The basic feature of this technique is that it is low invasive and offer the advantages of less expensive, shorter hospitalization and recovery period. The objective of cryosurgery is to treat the affected tissues and minimize the damage of healthy tissues in the vicinity of the tumor tissues. A number of investigations have been carried out to study the applications of cryosurgery.

Various heat transfer models are used to analyze phase change phenomena in heat transfer problems. The purpose of most of the heat transfer models is to find the temperature field and heat flux in a biological tissue under the set of constraints: general heat equation, initial and boundary conditions and distribution of sources or sinks, etc.

During phase change, interface between the frozen and unfrozen regions is moving with time and the boundary conditions at this interface require specific treatment. Except initial and boundary conditions, two more conditions are needed on the moving boundary, one to determine the boundary itself and another to complete the solution of the heat equation in each region. The phase change problems are non-linear in nature due to the unknown position of the freezing front and the direction of ice growth. In advance, it is difficult to predict the position and velocity of moving interface. The required mathematical analysis is much more complicated, when the physical properties of the system are temperature dependent.

Phase change heat transfer problems have a limited number of analytical solutions, which are confined up to one-dimensional problems along with some simple boundary conditions. Therefore, for solving such type of problems it is essential to employ the numerical methods because they appear to offer a more practical perspective. Based on front tracking, non-front tracing and fixed domain approaches, various numerical methods have been proposed for the solution of phase change problems. Numerical methods based on enthalpy and effective heat capacity formulation are well known methods to solve phase change heat transfer problems.

The present thesis deals with some Mathematical models to study phase change heat transfer problems in biological tissues during cryosurgery. The study of the thermal gradient inside the tissue is an important issue for the optimization of cryosurgery. The transient temperature profiles in tumor and normal tissue are useful to diagnose whether the tumor is damage or not and also try to minimize injury to healthy tissues during cryosurgery. Numerical solutions are obtained using finite difference method based on temperature dependent enthalpy. A computer code has been developed using MATLAB software on "Intel core i5 processor @ 3.30 GHz with 6GB RAM". Results obtained are interpreted in the graphical form.

The present thesis is compiled in six chapters and the chapter wise description is given below.

Chapter 1 is an introductory and contains some basic concepts of heat transfer. Different heat transfer models are also discussed in this chapter. It gives a brief description of freezing process of biological tissue during cryosurgery, mechanism and mathematical formulation of cryosurgery and the solution methodology.

In **Chapter 2**, a two-dimensional hyperbolic bio-heat model is developed by modifying the classical Pennes bio-heat model. Non-ideal property of tissue, metabolic heat generation and blood perfusion are also taken into consideration to study the phase change heat transfer during cryosurgery process of lung cancer. An enthalpy based finite difference scheme is adopted to solve the present model. We have examined the effect of different values of relaxation time on transient temperature, lower and upper interfaces during freezing process. Information obtained is useful to predict that the tumor tissue has been damaged or not and minimization of the damage of surrounding normal tissues by over-freezing, which could be helpful to improve the treatment planning.

In **Chapter 3**, a two-dimensional dual phase lag model is proposed to study the phase change heat transfer process during cryosurgery of lung tumor tissue. This model is based on dual phase lag constitutive relation and also includes the discontinuity of temperature at the frozen-unfrozen interface. The temperature dependent enthalpy formulation and finite difference method is used to solve the mathematical model. The effects of phase lag of heat flux and temperature gradient on temperature profiles and position of phase change interfaces have been studied numerically. The results of this study are significant for successful cryosurgical treatment.

In **Chapter 4**, we have studied the freezing behavior of triple layer skin tissue using a three-dimensional hyperbolic bio-heat model. The complexities of the problem are due to moving interface, discontinuity in the temperature at interface and triple layer skin tissue which has different thermal properties in different layers. The finite difference method is adopted to analyze the effect of relaxation time on freezing interfaces and temperature distribution in skin tissue. It is noted that relaxation time has important effect on phase change interfaces and temperature distribution.

In **Chapter 5**, to study the effects of two phase lags in triple layer skin tissue freezing, a three-dimensional dual phase lag model is proposed. The difficulties of the problem are temperature discontinuity and movement of freezing interfaces and different thermal properties of layers of skin tissue. The finite difference approximation based on temperature dependent enthalpy has been used to solve the dual phase lag model. Temperature profiles and motion of freezing interface are plotted to see the effects of both the phase lags in freezing procedure. It is found that the freezing is fast for small value of phase lag of heat flux.

Finally, **Chapter 6** presents the conclusion drawn from the thesis and possible directions of the future scope.

ACKNOWLEDGEMENTS

It is a pleasure to convey my gratitude, to few of the many sources of inspiration for me, to all the people who have helped in successful realization of this Thesis.

First and foremost I thank the incessant source of divine blessings, the almighty God, who always motivates me to move forward with his omens and love.

I express my deep sense of gratitude to my supervisors Dr. V.K. Katiyar, Professor, Department of Mathematics, Indian Institute of Technology Roorkee and Dr. Shirley Telles, Director, Patanjali Research Foundation, Patanjali Yogpeeth, Haridwar. I feel privileged to express my sincere regards to my guides for their valuable guidance, support and constant encouragement throughout the course of my research work. Their truly scientific intuition and broad vision inspired and enriched my growth as a student and researcher. The critical comments, rendered by them during the discussions are deeply acknowledged.

I express my regards to Prof. R. C. Mittal, former Head of the Department, Prof. Tanuja Srivastava, DRC Chairperson, Prof. Kusum Deep, former DRC Chairperson and Prof. P.N. Agarwal, former DRC Chairperson, for their support. Special thanks to my SRC members: Prof. N. Sukavnam, Prof. M. Parida and Prof. Kusum Deep for spending their valuable time during the discussions over seminars.

It is my pleasure to express my gratitude to Dr. Sushil kumar, Assistant Professor, SVNIT Surat for his guidance, encouragement and support. I also acknowledge to Dr. Kranti Kumar for their affection and care for me like my elder brother.

I am thankful to my lab seniors Dr. Anju Saini, Dr. Dev Datta, Dr. Fateh Singh, Dr. Venkatesh Kajjam, Dr. Shashi Sharma, Dr. Virendra Kumar and lab colleagues Mr. Rahul Shukla and Mr. Endalew Getnet for providing their cooperation, support, healthy and progressive research environment.

I am especially thankful to the members of CFD Lab Dr. Manish Khandelwal, Dr. Abhishek Kumar Sharma and Mr. Arshan Khan for their cooperation and constant support.

I consider myself truly blessed as I have always been in a good company of friends. Their love, inspiration, support and cooperation is beyond the scope of my acknowledgement, yet I would like to express my heartfelt gratitude to my friends Harshit, Tajinder, Kiran, Rakesh, Kalu Ram, Harish and Amit.

I feel a deep sense of gratitude for my highly respectable father, Sh. Som Lal and mother, Smt. Parveen Bala who raised me with their unconditional love, inculcated in me the values that really matter in life, formed part of my vision and taught me to always believe in myself. Words can never express my feelings for them. I am also thankful to my younger brothers Jeevan Kumar, Rohit Kumar and Sister Rehina Devi for their love, moral support and encouragement.

Financial assistance from MHRD, New Delhi, India in the form of JRF and SRF is also gratefully acknowledged.

With profound gratitude, love and devotion, I dedicate this Thesis to my parents.

IIT Roorkee

Dated: **(AJAY KUMAR)**

Table of Contents

List of Figures

List of Tables

Nomenclature

T temperature (^0C)

t time (s)

ρ density (kg/m^3)

c specific heat (J/kg ^0C)

k thermal conductivity (W/m ^0C)

L latent heat (kJ/kg)

Q_m metabolic heat generation (W/m^3)

w_b blood perfusion in tissue (ml/s/ml)

T_b arterial blood temperature (^0C)

T_c cryoprobe temperature (^0C)

$S(t)$ position of freezing interface

q heat flux

H enthalpy

τ_q heat flux relaxation time (s) or phase lag of heat flux

τ_T phase lag of temperature gradient (s)

v_n normal velocity of phase change interface

f^* fraction

Subscripts

f frozen state

u unfrozen state

ph phase change

b blood

c cryoprobe

ml upper limit of phase change

ms lower limit of phase change

e epidermis

d dermis

s subcutaneous

Superscript

n time step

List of Publications

The following is a list of papers published/communicated from the thesis.

1. **Ajay Kumar**, Sushil Kumar, V. K. Katiyar, and Shirley Telles. Phase change heat transfer during cryosurgery of lung cancer using hyperbolic heat conduction model. *Computers in Biology and Medicine*, 84 (2017): 20-29. **Elsevier, I.F-1.836**.

2. **Ajay Kumar**, Sushil Kumar, V. K. Katiyar, and Shirley Telles. Dual phase lag bio-heat transfer during cryosurgery of lung cancer: Comparison of three heat transfer models. *Journal of Thermal Biology*, 69 (2017) 228–237. **Elsevier, I.F-2.157.**

3. **Ajay Kumar**, Sushil Kumar, V. K. Katiyar, and Shirley Telles. Three dimensional study on hyperbolic bio-heat model for triple layer skin tissue freezing. **Submitted to Journal**.

4. **Ajay Kumar**, Sushil Kumar, V. K. Katiyar, and Shirley Telles. Three dimensional study on dual phase lag model for freezing behavior of triple layer skin tissue. **Submitted to Journal**.

Chapter 1

General Introduction

1.1 Introduction

Mathematical modeling is the branch of mathematics through which we explain and predict real world behavior. Basically, it is a process which includes the transformation of real world problems into mathematical form, solving the mathematical problems and converting the solutions of these problems in the real world language [56]. In broad sense, a model is a simplified representation of an object or system that we want to investigate. Mathematical models are used in various disciplines like physics, biology, electrical engineering and the natural sciences etc.

In Mathematical Biosciences, we study the applications of mathematical modeling and mathematical techniques to get an insight into the problems of biosciences. Mathematical modeling of the lung, liver, skin tissue, conduction of current in nerve cells, exchange of oxygen and carbon dioxide in the human respiratory system, functioning of various organs, infectious diseases and flow of fluid in human arteries, plays a dominant role in control of diseases of the above systems [40-41, 70, 74-76, 88-89].

Mathematical models necessarily involves quantifiable phenomenon. Such a model will likely involve parameters, independent variables and dependent variables. In this thesis we have focused and investigated only mathematical models which represent the heat transfer involving phase change phenomena in biological tissues during cryosurgery.

Heat transfer concerns the exchange of thermal energy within the physical system or between the considered mediums. Heat transfer takes place from higher temperature to lower temperature region due to difference in temperature between the regions. The heat transfer can also take place within the system due to difference in temperature at various points inside the system. The temperature difference is considered to be potential that causes the transfer of heat. The problem of heat transfer is classified in three different modes: conduction, convection and radiation [107].

Conduction: Fourier's Law of Conduction

Conduction is the mode of heat transfer in which flow of heat takes place through molecular transport of heat, there is not necessarily any motion in the conducting medium. Conduction is the most significant means of heat transfer within a medium or between two or more mediums which are in thermal contact with each other. Transfer of thermal energy occurs from a region of higher kinetic energy to that of lower kinetic energy region [107]. A temperature gradient is the continuously transfer of energy in the direction of decreasing temperature.

The Fourier's law of heat conduction is given as

$$q_x = -k\frac{dT}{dx} \tag{1.1}$$

where, the heat flux, q_x is the heat flow rate per unit area normal to the direction of heat flow, and k is the thermal conductivity of material.

Convection: Newton's Law of Cooling

Convection is the transfer of energy between the solid and liquid surface. In convection heat transfer between solid and fluid occurs as a consequence of the motion of fluid relative to the solid surface. According to Newton's law of cooling, flux in convection is directly proportional to the temperature difference between solid and surrounding fluid [107].

$$q_s = h\left(T_s - T_\infty\right) \tag{1.2}$$

where, q_s is surface heat flux, h is the heat transfer coefficient, T_s is temperature of the surface and T_∞ is the surrounding fluid temperature.

Radiation: Stefan-Boltzmann Law

Radiation is the mode of heat transfer in which radiation energy is transferred through electromagnetic waves; it does not require a medium. These waves carry the energy away from the emitting object and it propagates best in a vacuum [107]. Stefan-Boltzmann law states that the radiant heat flux from a body is proportional to the fourth power of its absolute temperature

$$q_b = \sigma T_s^4 \tag{1.3}$$

where, q_b is the radiant heat flux, σ is the Stefan-Boltzmann constant; its value is $\sigma = 5.67 \times 10^{-8} W/m^2 - K^4$ and T_s is the absolute temperature.

1.2 Freezing Process

Freezing process is the phase transition process, in which one phase changes to another phase. One has to study the phenomena of heat extraction from the liquid region, as the phase transition can occur only by lowering of free energy of the system. The motion of interface between liquid and solid phase including the absorption or releasing effect of latent heat increased the complexity of heat conduction problem with phase change phenomena [24]. Phase change problems are also referred as "Moving Boundary Problems". These problems are time dependent boundary value problems and moving interface has been determined by a function of time and space. Such type of problem was first studied by Stefan, therefore it is also called as "Stefan problem" [138]. In his research, he had studied the thickness of polar ice.

Solidification of pure substance and solidification of impure substance are the two major categories of freezing process. In solidification of pure substance, freezing occurs at a discrete temperature and it gives a sharp liquid/solid interface. On the other hand in solidification of impure substance freezing occurs over an extended temperature range and it gives mixed phase region. The mixed phase region known as mushy region is a combination of liquid solute and solid crystals [3].

There are two types of region in phase change problem, one is frozen region and other is known as unfrozen region. Interface between these two regions is moving with time and the boundary conditions at this interface require special attention. Except initial and boundary conditions, two more conditions are needed on the moving boundary, one to determine the boundary itself and another to complete the solution of the heat equation in each region.

For one-dimensional phase change problem with cooling at $x = 0$ and its moving interface, $x = s(t)$, energy equations are as follows [84]:

In frozen region

$$\rho_f c_f \frac{\partial T_f}{\partial t} = \frac{\partial}{\partial x}\left(k_f \frac{\partial T_f}{\partial x} \right) \qquad 0 \le x \le s(t), \qquad (1.4)$$

In unfrozen region

$$\rho_u c_u \frac{\partial T_u}{\partial t} = \frac{\partial}{\partial x}\left(k_u \frac{\partial T_u}{\partial x} \right) \qquad s(t) \le x \le l. \tag{1.5}$$

where, T is the temperature; L, latent heat; ρ, density; c, specific heat; k, thermal conductivity; l, length of the whole region.

In phase change process, the interface between frozen and unfrozen phase moves with time and the interface boundary condition on moving boundary needs two more conditions other than initial and boundary conditions. One condition determines the boundary itself and another to complete the solution of heat equation in each region. Therefore, the energy balance conditions at moving interface are given as

$$k_f \frac{\partial T_f}{\partial x} - k_u \frac{\partial T_u}{\partial x} = \rho L \frac{ds(t)}{dt} \qquad \text{at } x = s(t), \tag{1.6a}$$

$$T_u = T_f = T_{ph} \qquad \text{at } x = s(t). \tag{1.6b}$$

Main applications of freezing process are in metal casting [155], environmental engineering [85], thermal energy storage system [49], aerodynamic ablation, freezing and thawing of foodstuff [26], cryopreservation [117], cryosurgery [31, 157] and numerous others.

1.3 Heat Transfer in Biological Tissues

Heat transfer in living biological tissues is a complex process. This complexity arises due to thermal conduction in tissues, convection, anisotropic blood flow in the network of arteries and veins, blood perfusion rate and variable metabolic heat generation and tissue physiological condition. Heat transfer in biological tissues is usually referred to as bio-heat equation. Various mathematical models have been formulated to describe the heat transfer within living biological tissues. The determination of temperature through these models has been generally used in several medical therapies and physiological studies. The nature of heat transfer in living tissue contains the basic elements of the process of heat transfer.

Heat transfer models for blood perfused tissues have been used in different applications in temperature regularization [101, 109-110, 140], tumor detection [50-51, 98-99,111], cryosurgery [9, 11, 14, 35, 39, 68-69], etc. In order to describe the bio-heat

transfer, various mathematical models such as Pennes bio-heat model, Chen-Holmes model, Weinbaum, Jiji and Lemons model and Weinbaum-Jiji model have been proposed.

1.3.1 Pennes Bio-heat Transfer Model

In 1948, Harry H. Pennes [112] developed a bio-heat model for analysis of heat transfer in human forearm, which is given as

$$\rho c \frac{\partial T}{\partial t} = \nabla \cdot k \nabla T + \rho_b c_b w_b (T_b - T) + Q_m . \tag{1.7}$$

where, ρ and c are the density and specific heat of the tissue, whereas ρ_b, w_b and c_b are the density, perfusion rate and specific heat of the blood, respectively. T is the temperature, T_b is the arterial temperature, t is the time and Q_m is the metabolic heat generation due to organic process activity in body. The term $\nabla \cdot k \nabla T$ in equation (1.7) is referred as conduction term and $\rho_b c_b w_b (T_b - T)$ as blood perfusion term.

According to Pennes model, heat transfer occurs in a tissue only in capillaries at arterial temperature. Since porous capillary beds supply blood to different tissues, therefore these capillaries provide larger area for heat transfer between blood and tissues. Pennes assumed that the arterial blood temperature T_b is uniform throughout the tissue, while he considered the vein temperature to be equal to the tissue temperature which is denoted by T at the same point. Due to simplicity and ease of application under certain conditions, this model has been used for various applications such as cryosurgery [124], tissue ablation [52] and therapeutic hyperthermia [123]. It is a continuum model, which considers the effect of blood flow in the conduction equation without consideration of flow of each vessel individually.

1.3.2 Chen-Holmes Bio-heat Transfer Model

Chen and Holmes [20] assumed that all tissue-arterial blood heat exchange occurs along the circulatory network after the blood flows through the terminal arteries and before it reaches the level of the arterioles. In Chen-Holmes model, total tissue control volume is subdivided to the solid tissue sub volume and blood sub volume and blood perfusion term takes into consideration the direction of blood flow and vascular geometry, which is given by the following equation

$$\rho c \frac{\partial T}{\partial t} = \nabla \cdot k_p \nabla T + \rho_b c_b w^*_b (T^*_b - T) - \rho_b c_b \bar{u} \cdot \nabla T + \nabla \cdot k_p \nabla T + Q_m . \quad (1.8)$$

where, the term $\rho_b c_b w^*_b (T^*_b - T)$ is different to blood perfusion term of Pennes model because w^*_b is the rate of perfusion at the local generation of vessel branching and T^*_b is the temperature of blood upstream of the arterioles. The term $\nabla \cdot k_p \nabla T$, where k_p is perfusion conductivity, represents conduction mechanisms associated with small temperature fluctuations in equilibrated blood. $\bar{u}$ is the volumetric blood flow rate per unit area in particular direction and the term $\rho_b c_b \bar{u} \cdot \nabla T$ describes the energy convected due to equilibrated blood.

To apply the Chen-Holmes model, the detailed knowledge of the vascular network and blood perfusion is needed. Therefore, it is more difficult to use as compared to the Pennes bio-heat model.

1.3.3 Weinbaum, Jiji and Lemons (WJL) Model

Since the Chen-Holmes model does not explicitly address the modeling of countercurrent vascular system. In 1984, three researchers Weinbaum, Jiji and Lemons proposed a vascular bio-heat model based on the assumption that small arteries and veins are parallel and not with heat exchange at the capillaries level [55]. The blood flows in countercurrent direction which results in counterbalance of cooling–heating effect. The energy conservation equations for a thermally significant artery and vein neglecting axial conduction are as follows

$$\pi (\rho c)_b \frac{d(n r_b^2 \bar{V} T_a)}{ds} = - n q_a - 2\pi (\rho c)_b n r_b g T_a , \quad (1.9a)$$

$$\pi (\rho c)_b \frac{d(n r_b^2 \bar{V} T_v)}{ds} = - n q_v - 2\pi (\rho c)_b n r_b g T_v . \quad (1.9b)$$

In equation (1.9), left side terms are heat convection terms along the path of arteries and veins respectively within the control volume, where r_b is the vessel radius, n is the vessel number density and $\bar{V}$ blood flow velocity within the vessel. The first term on the right side of equation represents the conduction process through the vessel wall and second term represents energy carried out, or into the blood vessel. The mass conservation law is given as

$$\frac{d(nr_b^2\bar{V}T_a)}{ds} = -2nr_b g\,. \tag{1.10}$$

Equation (1.9) can be simplified by substituting equation (1.10) in equation (1.9) for the tissue control volume and the following set of three coupled equations is obtained

$$(\rho c)_b \pi r_b^2 \bar{V} \frac{dT_a}{ds} = -q_a\,, \tag{1.11a}$$

$$(\rho c)_b \pi r_b^2 \bar{V} \frac{dT_v}{ds} = -q_v\,, \tag{1.11b}$$

$$\rho c \frac{\partial T}{\partial t} = \nabla \cdot k\nabla T + \left\{ ng(\rho c)_b \cdot (T_a - T_v) - n\pi r_b^2 (\rho c)_b \bar{V} \frac{d(T_a - T_v)}{ds} \right\} + Q_m\,. \tag{1.11c}$$

The equations (1.11a) and (1.11b) represent the heat transfer in thermally significant artery and vein respectively. The equation (1.11c) represents the tissue surrounding the artery-vein pair. The left hand side of equation (1.11c) represents the heat transfer in the tissue control volume. The first term of right side of equation (1.11c) represents the heat conducted in the direction of vessel path. The middle term of right side of equation (1.11c) refers the capillary bleed of energy exchange and net heat exchange between the tissue and artery-vein pair respectively. The second term on the right-hand side of equation (1.11c) is similar to perfusion term of Pennes except the bleed-off mass flow (g).

WJL model is more significant in the deep muscles tissues because the countercurrent vessels are small in the peripheral tissue and contribute less in heat transfer.

This theoretical model lacks experimental validation due to its complexity and detailed description is required for associated vascular network to a meaningful application. These limitations make this model difficult to apply for most tissues or a variety of thermal conditions.

1.3.4 Weinbaum and Jiji (WJ) Bio-heat Transfer Model

The above three temperature models are more complex; therefore Weinbaum and Jiji [150] derived a simplified bio-heat model. This model considered the effect of number of countercurrent blood vessel pairs, blood vessel diameters and the blood velocity, while predicting temperature field in vascularized biological tissue.

The assumption of this model was that the tissue temperature is approximated by the average temperatures of the local artery and vein.

$$T \approx \frac{(T_a + T_b)}{2}. \tag{1.12a}$$

Further they also assumed that heat conducted from arteries to the corresponding paired veins, such that

$$q_a \approx q_v \approx \sigma k(T_a - T_v). \tag{1.12b}$$

On substituting equation (1.12) in WJL model, it reduces to the following bio-heat equation as

$$\rho c \frac{\partial T}{\partial t} = \frac{\partial}{\partial t}\left(k_{eff} \frac{\partial T}{\partial x} \right) + Q_m, \tag{1.13}$$

where, k_{eff} is the effective thermal conductivity of the tissue which is a function of different tissue-blood vessel configurations, and is given as

$$k_{eff} = k\left[1 + \frac{n\left\{ \pi r_b^2 (\rho c)_b V \cos\gamma \right\}^2}{\alpha . k^2} \right].$$

A review of the chronological development of mathematical models of bio-heat transfer has been given by Charny and Levin [19]. Computer simulated results obtained by Baish et al. and Wissler et al. [8, 151] show that the Weinbaum and Jiji model is applicable to muscle tissue that contains blood vessels with diameter, $d < 0.2\,mm$.

Hence, Weinbaum and Jiji model is not an accurate model to predict the temperature field. The Pennes model is still the most commonly used model for thermal energy transport in biological tissues because of its simplicity.

1.4 Cryosurgery

Cryosurgery is a medical technique to treat the tumor tissues, in which extremely low temperature is used to destroy the diseased tissues. It is also known as cryotherapy or cryoablation. Cryosurgery has many advantages over other medical treatments, such as less pain, less invasiveness, cheap price, safe, effective and less time hospital stay and recovery period [30, 72]. Besides this, one of the main advantages of cryosurgery is that it localizes the cell destruction, which in turn minimizes damage to the neighboring normal tissues. It is used in the treatment of many types of tumors, e.g., lung, liver, skin cancer,

bone tumors, hemorrhoids and prostate cancer, etc. The development of this technique was reported in the middle of 19^{th} century. The first successful treatment of cancer was done by James Arnott, an English physician, who used iced saline solution to treat malignant tumor [6].

The era of modern cryosurgery began in 1961, when Irving Cooper [23], an American neurosurgeon, developed a liquid nitrogen-based cryosurgical equipment [131]. In cryosurgery process, liquid nitrogen as a cryogen is introduced on or within the diseased tissues through an instrument known as cryoprobe. Cryoprobe is a hollow instrument made of specific metal. Although there are other cryogens like liquid argon (-187 ^0C), nitrogen oxide (-89.5 ^0C) and solid carbon dioxide (-79.5 ^0C) used in cryosurgery [10], but due to minimum boiling temperature (-196 ^0C), liquid nitrogen is most widely used as cryogen [4]. This cryogen has greatest freezing capability and it is non-toxic, cheap and easily available. A low temperature area in the effected tissue region is generated by the tip of cryoprobe. The cryoprobe removes heat from the tissue and freezing interface propagates from probe into the tissue surface damaging the diseased tissue along the way. The probe is removed after the desired region is frozen and leaves the frozen tissue for thawing [12].

1.4.1 Mechanism of Tissue Injury during Cryosurgery

The physical effect of cryosurgery is cell destruction and it is directly related to in the formation of ice crystals. In cryosurgery process, water in the tissue gets crystallized when the tissue temperature falls into the freezing range. Immediate and delayed effects are the two major mechanisms (Figure 1.1) towards the destructive effect of freezing in cryosurgery [38]. The immediate effect occurs due to direct destruction of cells through the effect of cooling and freezing. Whereas the delayed effect of cell injury appears due to the progressive failure of microcirculation and vascular stasis, which can last up to many hours after the completion of cryosurgical procedure [38, 90-91]. The immediate mechanism of cell destruction is injurious effect of freezing. Gage et al. [38] have showed in their study that -50 ^0C is the cell death temperature.

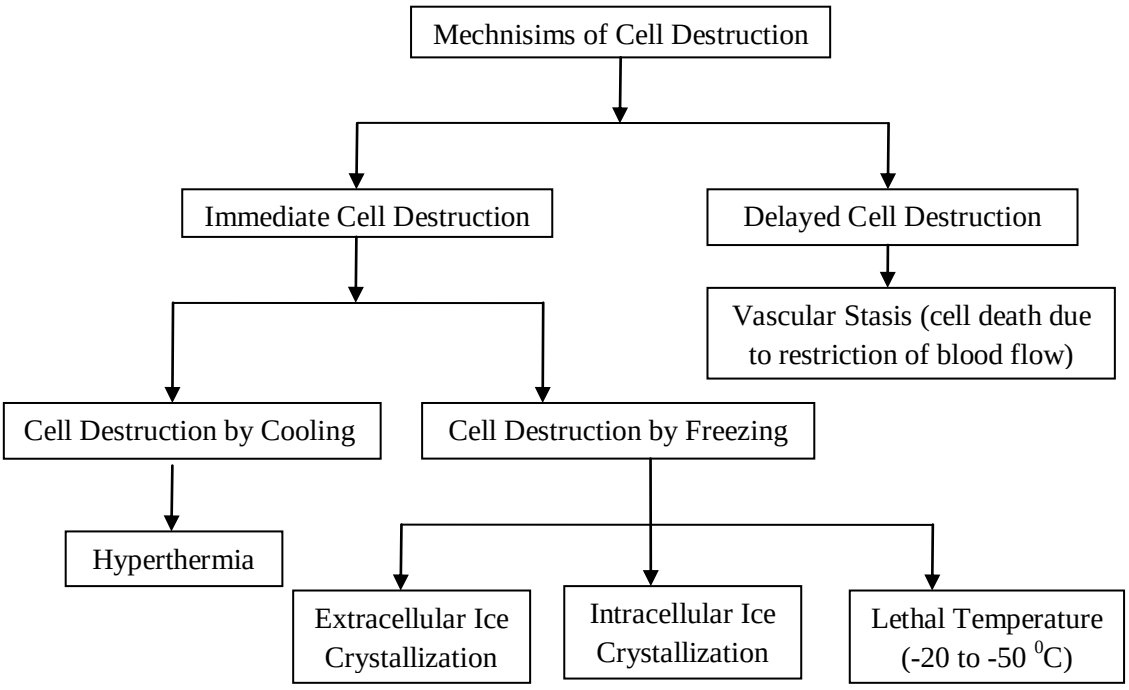

Figure 1.1: Mechanism of Cryosurgery [21].

1.4.2 Extracellular and Intracellular Ice Crystallization

Two biophysical changes in tissues during the freezing-induced cell injury in freezing process are extracellular ice formation (EIF) and intracellular ice formation (IIF). These two are important freezing response experienced by cells. Extracellular ice crystallization takes place when the cooling rate is slow. While at fast cooling rate, intracellular ice formation is achieved. The rates of freezing are high sufficient to induce intracellular ice formation (IIF) along with surrounding area of the cryoprobe. Formation of ice crystals begins in extracellular space, as the tissue temperature falls a few degree below to 0 ^0C. Therefore, solute concentration increases and water gets removed from the cells. As a result, the cells shrink and membrane and constituents get damaged [21].

During the high cooling rate, the extracellular ice crystallization does not have enough time to form. In this situation, removal of water from the cells is not fast enough to achieve the equilibrium across the cell membrane. Therefore, osmotic equilibrium is maintained by intracellular crystallization of ice in both inside and outside of the cells. During freezing, the cell volume expands which damage the cell membrane i.e., causes destruction of cells [21].

The difference between the intracellular and extracellular osmotic pressure increases with an increase in cooling rate. Hence, the difference in temperature between the actual temperature of the cytoplasm and its freezing point increases (the degree of under cooling in the cytoplasm increases). In both extracellular and intracellular ice crystallization, water is removed from the biological system and dehydration results in cell death. The fraction of unfrozen water is an important factor in cell death or survival. Moreover, the deleterious effect of cell shrinkage and expansion may be sufficient to explain cell death [90-91].

1.4.3 Mathematical Formulation of Cryosurgery

For a cryosurgical treatment, the most desirable things are to compute the freezing propagation and effect of temperature inside the freezing surface. Computerized planning helps cryosurgeons in the pre-planning of cryosurgery. Imaging techniques like Ultrasound, Electrical Impedance Tomography (EIT) and Magnetic Resonance Imaging (MRI) are not able to provide the thermal history inside the frozen tissues, as these techniques only capture the outer freezing front.

Then mathematical models came into existence to predict the thermal information and extent of freezing within the subjected tissue. Heat transfer models based on bio-heat equation have been developed to explain cryosurgery process mathematically. During cryosurgery, it is assumed that heat transfer takes place only by conduction and classical Pennes bio-heat equation [112] is generally used to formulate the mathematical model in cryosurgery. It is given as

(a) In unfrozen region

$$\rho_u c_u \frac{\partial T_u(S,t)}{\partial t} = \nabla k_u \cdot \nabla T_u(S,t) + (\rho c)_b \, w_b (T_b - T_u(S,t)) + Q_m \qquad S \in D_u(t) \qquad (1.14)$$

where, ρ_u, c_u and k_u are density, specific heat and thermal conductivity of unfrozen region, ρ_b is density of blood, c_b is specific heat of blood, w_b is blood perfusion rate, Q_m is the metabolic heat generation in tissue, $T_u(S,t)$ is the temperature in unfrozen region, T_b is the arterial blood temperature and $D_u(t)$ denotes the unfrozen domain at time *t*.

(b) In frozen region

Due to absence of blood perfusion and metabolism, the heat balance equation can be written as

$$\rho_f c_f \frac{\partial T_f(S,t)}{\partial t} = \nabla k_f \cdot \nabla T_f(S,t) \qquad S \in D_f(t) \tag{1.15}$$

where, ρ_f, c_f and k_f are density, specific heat and thermal conductivity of frozen region. $T_f(S,t)$ is the temperature in frozen region and $D_f(t)$ denotes the frozen domain at time *t*.

(c) Conditions at interfaces are given by

$$T_u(S,t) = T_f(S,t) = T_{ph}(S,t) \tag{1.16}$$

$$k_f \frac{\partial T_f(S,t)}{\partial n} - k_u \frac{\partial T_u(S,t)}{\partial n} = \rho L v_n \tag{1.17}$$

where, T_{ph}, n, L, and v_n denote phase change temperature, unit outward normal, latent heat and normal velocity of phase change interface, respectively.

1.5 Solution Methodology

1.5.1 Introduction

The moving boundary between solid and liquid phase is the characteristic of the freezing or solidification. The nature of these problems is non-linear due to the unknown position of freezing front and the direction of ice growth. The position of moving interface is found out by the continuation of solution of problem, as it is difficult to predict in advance. The physical properties of the system are temperature dependent therefore mathematical study becomes still more complicated. Many researchers have studied in this direction, their study is based on analytical as well as numerical techniques but restricted to some simple assumptions.

1.5.2 Analytical Solutions

The existing analytical solutions for phase change problem are limited to one-dimensional, semi-infinite and infinite region with simple boundary conditions. These solutions are usually in the form of similarity variable and are referred as similarity solutions. In 1860, Neumann [97] gave the solution of phase change problem in a semi-infinite region but his

work was not published until 1912. The earliest exact solution of phase change problem was given by Stefan [138]. In his work, he used freezing of semi-infinite liquid region. Carslaw and Jaegar [17] have further generalized the Neumann solution.

Formulation of moving boundary problems in terms of integral equations was also found useful. Evans et al. [37] obtained an integral form for one-phase moving boundary problems using Laplace transforms. Generalized Laplace transform for phase change problems was given by Ku and Chen [58]. Selim and Seagrave [126] used integral transform for the solution of plane cylindrical and spherical moving boundary. The solution of heat flow problems subjected to fixed boundary conditions with the use of Green's function is well known. Liu and Zhou [78] studied the freezing and thawing process of biological skin tissue using the Green's function. This method is also used by Muehlbaur et al. [95] and Katiyar and Mohanty [57] in the transient heat transfer analysis of alloy solidification.

It is easy to obtain the solution of quasi-steady approximation of Stefan problem, but the validity of the solution is limited as the initial condition could not be taken in this method. Caldwell and Kwan [15] used perturbation method to solve quasi-steady approximation of Stefan problem. Jiji and Gaye [54] studied the freezing and melting of phase change materials with energy generation using quasi-steady approximation.

Some authors have studied analytically the heat transfer phenomena in biological tissues. Among them, Shih et al. [132] have performed analytical study of Pennes bio heat equation using Laplace transform assuming the sinusoidal heating on the surface of the skin. Their analysis showed that the temperature oscillation is unstable at the initial stage due to effect of the sinusoidal heat flux on the surface of skin tissue. An extensive study is made by Ahmadikia et. al. [1], they examined the heat transfer effect in skin tissue due to laser heating, and solved two bio-heat models analytically using Laplace transform method. Mahjoob and Vafai [86] investigated analytically bio-heat transfer phenomena within the biological tissue which arises in the therapeutic applications like hyperthermia treatment.

1.5.3 Numerical Solution

Since the moving boundary problems and phase change heat transfer phenomena are non-linear, it is difficult to arrive at the solution by analytical methods. Therefore, for solving such type of problems it is necessary to employ the numerical method. In literature, different methods have been proposed for the numerical solution of phase change

problems [116, 118, 158, 156]. They differ primarily in the way that heat transfer on the phase boundary is modeled. Existing numerical methods have been categorized as follows

Front Tracking Method

Front tracking method is used to find the interface between liquid and solid phases using the Stefan condition and recognize the interface as boundary. In this method, boundary conditions at interface are fixed and different sets of conservation equations are solved. Front tracking method does not need initial information of the interfaces, and multiple fronts can also occur. Fixed finite difference grid methods, modified grid using variable space grids or variable time steps, adaptive grid methods and methods of lines are some examples of front tracking method [22, 43, 103].

Front Fixing Method

In front fixing method boundaries of phase change are fixed by a change of variable which considerably simplifies the numerical computation. This method includes body-fitted curvilinear coordinates and isotherm migration methods.

Fixed Domain Method

In both front tracking and front fixing methods, it is required to satisfy the "Stefan condition" on the moving boundary. Moreover, when the moving boundary does not move smoothly with time, sometimes it may be very difficult to find the position of moving boundary. The moving boundary may have double back, or sharp peaks or it may even disappear. Therefore, the problem is formulated in such a way that the Stefan conditions can be bound implicitly in the form of new equations, which applies over the whole of a fixed domain. This is fulfilled by introducing enthalpy function or effective heat capacity [36].

1.5.4 Enthalpy Method

To solve the phase change problems in which the substance does not have a separate solid-liquid interface, several researchers have used the enthalpy method. In this method an enthalpy function is used as dependent variable together with temperature and only a single energy equation works for both liquid and solid phases. Enthalpy method is applicable in different phase change problems and provide more exact solution than the other methods [145].

The basic feature of enthalpy method is that the evaluation of latent heat is computed by the enthalpy and its relation with temperature. The relationship is assumed to be step function and linear function for isothermal and non-isothermal phase change problems respectively, given as [24].

(a) For isothermal phase change

$$H = \begin{cases} c_f (T - T_m) & T \le T_m \\ c_u (T - T_m) + L & T > T_m \end{cases} \tag{1.18a}$$

(b) For non-isothermal phase change

$$H = \begin{cases} c_f (T - T_{ms}) & T < T_{ms} \\ (T - T_{ms}) \left(\frac{1}{2}(c_f + c_u) + \frac{L}{(T_{ml} - T_{ms})} \right) & T_{ms} \le T \le T_{ml} \\ L + \frac{1}{2}(c_f + c_u)(T_{ml} - T_{ms}) + c_u (T - T_{ml}) & T > T_{ml} \end{cases} \tag{1.18b}$$

where, L stands for latent heat, T_{ml} and T_{ms} are temperature of liquid and solid phase respectively.

Using enthalpy, H (Equation 1.18), the Stefan equations (1.4) – (1.6) reduces to a single equation

$$\rho \frac{\partial H}{\partial t} = \nabla k . \nabla T \tag{1.19}$$

while equations (1.14) – (1.17) reduces to

$$\rho \frac{\partial H}{\partial t} = \nabla k \cdot \nabla T + (\rho c)_b \, w_b (T_b - T) + Q_m \tag{1.20}$$

Enthalpy formulation is used in various studies of phase change problems such as in metal casting, freezing and thawing of food, cryosurgery and thermal energy storage system [31, 69, 71, 108, 127, 145-147].

The advantages of this method are following [145]:

(i) There are no conditions to be satisfied at the position of phase change interface.

(ii) There is no need to consider frozen and unfrozen regions separately.

(iii) There is no need to perfectly track the phase change boundary.

(iv) One can fix the no. of grids for calculation purpose.

(v) It is easy to deal with the cases where phase change occurs over a wide range rather than at a single point.

In the above method whole region is divided into finite number of elements and the heat balance equations (1.19) and (1.20) give accurate value of the enthalpy of each element. After obtaining the enthalpy of an element, temperature can be evaluated by reverting equation (1.18). Equations (1.19) and (1.20) can be solved using many numerical methods such as finite difference method (FDM) [32-34, 69, 73, 116], finite element method (FEM) [46, 61, 83, 100,103, 149], boundary element method (BEM) [29, 48] and finite volume method (FVM) [64-66]. The finite element method, boundary element method and finite volume method successfully handle complex geometries, but it is found that they are consuming more time in computing and programming. On the other hand, finite difference techniques are still the most popular at present because of their simplicity and less time consumption in formulation and programming [32, 34, 62, 113].

1.5.5 Finite Difference Method

Finite difference methods are numerical methods which are used to solve the differential equations where the derivatives are approximated by finite difference equations. In the finite difference simulation, a physical problem containing the continuous variation of a field variable $f(x, y, z, t)$, is converted into an approximate value of f at nodes (x_i, y_i, z_i) and the time level t_n [148]. These methods approximate the solution of differential equations by replacing the derivatives of different order by suitable finite difference approximation [122, 106, 125, 137].

The first derivative of a function T is

$$T'(x) = \lim_{h \to 0} \frac{T(x+h) - T(x)}{h} + \mathrm{O}(h) \tag{1.21}$$

Neglecting the error term $\mathrm{O}(h)$ gives

$$T'(x) \approx \frac{T(x+h) - T(x)}{h} \tag{1.22}$$

Equation (1.22) is called a first order forward difference approximation to $T'(x)$. Similar formulae are used to replace derivative expressions in differential equations.

Let *T* be a function of the independent variable *x* and *t*. Subdivide the *x* - *t* plane into sets of equal rectangles of sides $\delta x = h$, $\delta t = k$ by equally spaced grid lines parallel to *OX* , defined by $x_i = ih$, i = 0,1,2,...,*N* and equally spaced grid lines parallel to *OY*, defined by $t_n = nk$, n = 0,1,2,…,*N*. The value of *T* at the representative mesh point $T(ih, nk) = T_{i,n}$, by Taylor's theorem,

$$T(x+h,t)=T(x,t)+hT'(x,t)+\frac{1}{2}h^2T''(x,t)+\frac{1}{6}h^3T'''(x,t)+--- \tag{1.23}$$

$$T(x-h,t)=T(x,t)-hT'(x,t)+\frac{1}{2}h^2T''(x,t)-\frac{1}{6}h^3T'''(x,t)+--- \tag{1.24}$$

Equation (1.23) gives forward difference approximation

$$\frac{\partial T}{\partial x}=T'(x,t)=\frac{\{T(x+h,\,t)-T(x,t)\}}{h}+\mathrm{O}(h) \tag{1.25}$$

Equation (1.24) gives backward difference approximation

$$\frac{\partial T}{\partial x}=T'(x,t)=\frac{\{T(x,t)-T(x-h,t)\}}{h}+\mathrm{O}(h) \tag{1.26}$$

Equations (1.23) and (1.24) give central difference approximation for first order derivative as

$$\frac{\partial T}{\partial x}=T'(x,t)=\frac{\{T(x+h,t)-T(x-h,t)\}}{2h}+\mathrm{O}(h^2) \tag{1.27}$$

Equations (1.23) and (1.24) give central difference approximation for second order derivative as

$$\frac{\partial^2 T}{\partial x^2}=T''(x,t)\;=\;\frac{\{T_{i+1,n}-2T_{i,n}+T_{i-1,n}\}}{h^2}+\mathrm{O}(h^2) \tag{1.28}$$

$$\frac{\partial^2 T}{\partial t^2}\;=T''(x,t)=\frac{\{T_{i,n+1}-2T_{i,n}+T_{i,n-1}\}}{k^2}+\mathrm{O}(k^2) \tag{1.29}$$

$$\frac{\partial^2 T}{\partial x\partial t}=\frac{\{T_{i+1,n+1}-T_{i+1,n-1}-T_{i-1,n+1}+T_{i-1,n-1}\}}{4hk} \tag{1.30}$$

The central difference approximation to the third order derivative is

$$\frac{\partial^3 T}{\partial x^3} = \frac{\left\{T_{i+2,n} - 2T_{i+1,n} + 2T_{i-1,n} - T_{i-2,n}\right\}}{2(\delta x)^3} \tag{1.31}$$

Similar approximation can be obtained to higher order derivatives.

Finite difference methods using enthalpy formulation of phase change problems include explicit method, semi implicit method, and fully implicit method. The explicit method is conditionally stable, while others are unconditional stable [102].

1.6 Objective of the Study

Heat transfer with phase change in living biological tissues is an important area of research due to its wide applications in disease diagnostic, burn injury evaluation, cryosurgery, cancer hyperthermia and cryopreservation. At the present time, the controlled destruction of tissues by freezing is commonly used in medicine. Cryosurgery has become a well-established technique for the ablation of undesirable tissues.The motivation for this study is to improve the efficacy and safety of this technique. On the basis of available literature (see introduction of chapter 2), we have used the hyperbolic bio-heat model for the numerical study of phase change heat transfer during cryosurgical treatment of lung tumor tissue. The literature review also reveals that the numerical study of phase change heat transfer in cryosurgery of lung cancer can be explored further using dual phase lag model. Apart from this, the three-dimensional hyperbolic bio-heat model and dual phase lag model could be helpful in analyzing the freezing behavior of the triple layer skin tissue. Therefore, the objectives of the present thesis are

- To study the effect of relaxation time on temperature distribution and phase change interfaces interface during cryosurgical treatment of lung tumor tissue, a two-dimensional hyperbolic bio-heat model has been developed.
- To examine the effect of phase lags in heat flux and temperature gradient on freezing interfaces and distribution of temperature during cryosurgery of lung cancer, a two-dimensional dual phase lag model has been presented.
- To study the freezing behavior of triple layer skin tissue, a three-dimensional hyperbolic bio-heat model has been proposed.

- To study the effect of two phase lags in freezing of triple layer skin tissue using a three-dimensional dual phase lag model.

Chapter 2

Hyperbolic Bio-heat Model for Phase Change Heat Transfer during Cryosurgery of Lung Cancer

2.1 Introduction

Lung cancer is one of the major causes of death among all types of cancer. Every year a large number of people die due to this cancer disease. Lung cancer is an uncontrolled growth of diseased or abnormal tissues in the lungs. As per the report of the World Health Organization (WHO), around 20 % people (1.59 million) die due to lung cancer every year [42]. According to cancer death report 2017 by the American Cancer Society [16], around 222,500 cases of the lung cancer are expected in 2017. Out of these cases 155,870 are expected death cases in 2017. Cigarette smoking, passive smoking, air pollution, especially small particulates, asbestos, exposure to radon, some organic chemicals and genetic susceptibility are the main causes of lung cancer. There are many medical treatments like surgery, radiotherapy and chemotherapy, etc., available to cure lung cancer [121]. These treatments have some calamitous side effects. Cryosurgery is one of the important surgical techniques, which is safe and effective method of tumor treatment as compared to the other treatments.

The main aim of cryosurgery is to destroy the tumor tissue while minimizing the damage to healthy lung tissues. A good knowledge of temperature distribution and positions of phase change interface in lung-tumor tissue is required for a successful cryosurgical treatment. A brief description of literature in the direction of cryosurgery in biological tissues is given below.

To predict the thermal reaction of tumor and normal tissues in cryosurgical treatment, Hoffmann and Bischof [47] have proposed a cryosurgical model using a dorsal skin flap chamber. Chua et al. [21] have presented the detailed analysis of rate of cell destruction and temperature distribution in the tumor tissue during cryosurgery. In their study, they observed that in comparison with multiple cryoprobes, a single cryoprobe having large diameter works efficiently in destroying the tumor tissue while preserving the healthy tissues.

To see the freezing effect in tumor tissue, Nakayama et al. [96] have studied numerically the growth of ice-ball and location of freezing front with time and compared with analytical one. They reported the existence of a tumor tissue of limiting size, which can be frozen upto maximum by a single cryoprobe. Niu et al. [104] have made an experiment using different freeze-thaw cycles and analyze the lung necrosis during cryosurgery in lung cancer. They observed that for complete destruction of lung cancer cells, three freeze-thaw cycles are required. Tarwidi [141] investigated the Cryosurgical simulation of lung cancer based on efficient freezing time. He reported that temperature distribution and solid-liquid interface in tissue can be used to maximize the damage rate of tumor tissue and minimize the injury to normal tissue. Recently, Hafid and Lacroix [44] presented an inverse heat transfer method for monitoring the motion of the freezing front in cryosurgery, with the help of a thermocouple inserted into the layer of diseased tissue. This information is then fed to the Pennes bio-heat equation that calculates the time-varying temperature distribution inside the layer of tissue and predicts the motion of the freezing front. Results have shown that the proposed inverse method is a promising alternative to ultrasound and MRI for monitoring the motion of the freezing front.

In their studies, most of the above authors have used Pennes bio-heat model [112], which is given as

$$\rho c \frac{\partial T}{\partial t} = -\nabla q + \rho_b c_b w_b \left(T_b - T\right) + Q_m , \tag{2.1}$$

where c, ρ, ρ_b, c_b , w_b , T, t, T_b and Q_m have the same meaning as in equation (1.7). This model is also called parabolic bio-heat model.

The above Equation (2.1) is based on the Fourier's law,

$$q\left(S,t\right) = -k\nabla T\left(S,t\right), \tag{2.2}$$

where, k denotes the thermal conductivity of tissue, $T\left(S,t\right)$ and $q\left(S,t\right)$ are temperature and heat flux at position $S\left(x,y,z\right)$ at time t respectively.

According to Fourier's law of heat conduction, a thermal signal propagates with infinite speed in the medium [77]. Which is not true in reality, the propagation speed of a thermal signal is finite because biological tissues have non-homogeneous structure and they require a relaxation time to acquire a proper amount of energy to transfer to the

neighboring element [82]. The paradox which occurred in Pennes bio-heat transfer model was solved by Cattaneo [18] and Vernotte [144]. They simultaneously proposed a modified form of Fourier's law as

$$q(S,t+\tau_q) = -k\nabla T(S,t), \tag{2.3}$$

where, τ_q stands for the relaxation time for heat flux. Using Taylor series expansion, the equation (2.3) can be written as follows

$$q(S,t)+\tau_q \frac{\partial q(S,t)}{\partial t} = -k\nabla T(S,t), \tag{2.4}$$

Equation (2.4) is called as Cattaneo-Vernotte's constitutive equation. Using equations (2.1) and (2.4), we get the following equation which is known as hyperbolic bio-heat equation,

$$\tau_q \rho c \frac{\partial^2 T}{\partial t^2} + \left(\rho c + \tau_q \rho_b c_b w_b\right)\frac{\partial T}{\partial t} = k\left(\frac{\partial^2 T}{\partial x^2} + \frac{\partial^2 T}{\partial y^2}\right) + \rho_b c_b w_b \left(T_b - T\right) + Q_m . \tag{2.5}$$

If $\tau_q = 0$, then the above equation is converted into parabolic bio-heat equation.

Many studies are available in the literature [5, 82, 134-135], in which researchers have used hyperbolic bio-heat model with freezing condition. Among others, Deng and Liu [28] have studied phase change heat transfer and thermal stress inside the skin tissue during freezing process. In their study, they have not included the discontinuous nature of temperature at the phase change interface. Zhou et al. [163] presented a two-dimensional non-Fourier bio-heat model to investigate the thermal damage and temperature distribution in laser-irradiated biological tissues. To describe non-Fourier effect of biological tissue during freezing process Ahmadikia and Moradi [2] studied hyperbolic heat conduction model along with discontinuous nature of temperature at liquid-solid interface but did not consider the heat source term due to blood perfusion and metabolic heat generation. Metabolic heat generation and blood perfusion also have significant effect on heat transfer in tissues [119-120]. In cryosurgery during freezing, some healthy tissues may also freeze. These frozen tissues can resume their state due to heat supply by body metabolism and blood perfusion. Negligence of these terms can result up to 20% error in the result.

In this chapter, a 2D hyperbolic bio-heat model is developed by modifying the classical Pennes bio-heat model. Non-ideal property of tissue, metabolic heat generation

and blood perfusion are also taken into account to study the cryosurgery process of lung cancer. A finite difference approximation based on enthalpy method is employed to solve the above model. To study the effect of relaxation time for heat flux on movement of interfaces and temperature distribution in the tissue are obtained for different values of relaxation time.

2.2 Problem Description

We have considered a tumor tissue of dimension $1.5\,cm \times 1.5\,cm$, which is embedded in a lung tissue of dimension $4.0\,cm \times 4.0\,cm$. A cryoprobe is located at the position $x = 0$, $1.8\,cm \le y \le 2.2\,cm$.The physical configuration of the present problem is given in figure 2.1 [69].

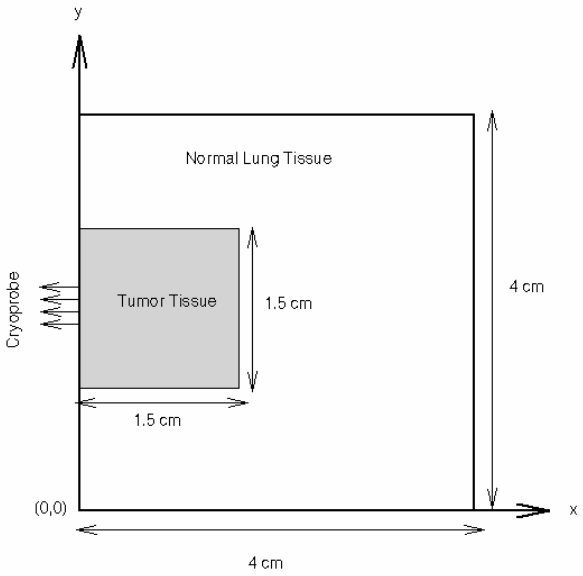

Figure 2.1: Schematic diagram of physical problem.

2.3 Mathematical Formulation

2.3.1 Assumptions

The following assumptions are considered to solve the two-dimensional hyperbolic bio-heat transfer model.

- Heat conduction in tissue takes place through non-Fourier conduction [2].

- When tissue is in unfrozen state, heat generation occurs in tissue due to metabolism and blood perfusion [27, 29].
- The initial temperature of tissue is considered as an arterial temperature (37 ^0C).
- Non-ideal property of tissue is used with upper and lower phase change interface at temperature -1^0C and -8^0C respectively [114].
- Outer boundary is far away from cryoprobe, so assumed at body core temperature (37 ^0C).
- Thermo-physical properties of normal lung and tumor tissue are taken as

$$(k)_e = \begin{cases} (k_f)_e & T < T_{ms} \\ \frac{1}{2}\left\{(k_f)_e + (k_u)_e\right\} & T_{ms} \le T \le T_{ml}, \\ (k_u)_e & T > T_{ml} \end{cases}$$

$$(\rho)_e = \begin{cases} (\rho_f)_e & T < T_{ms} \\ \frac{1}{2}\left\{(\rho_f)_e + (\rho_u)_e\right\} & T_{ms} \le T \le T_{ml}, \\ (\rho_u)_e & T > T_{ml} \end{cases}$$

$$(c)_e = \begin{cases} (c_f)_e & T < T_{ms} \\ \frac{1}{2}\left\{(c_f)_e + (c_u)_e\right\} & T_{ms} \le T \le T_{ml}, \\ (c_u)_e & T > T_{ml} \end{cases}$$

where subscripts $e = l$ and t are for lung and tumor respectively.

2.3.2 Governing Equations

The governing equations of 2D hyperbolic bio-heat model for lung tumor tissue for both the regions frozen and unfrozen are given as:

$$\tau_q \rho_f c_f \frac{\partial^2 T_f}{\partial t^2} + \rho_f c_f \frac{\partial T_f}{\partial t} = k_f \left(\frac{\partial^2 T_f}{\partial x^2} + \frac{\partial^2 T_f}{\partial y^2} \right), \tag{2.6}$$

$$\tau_q \rho_u c_u \frac{\partial^2 T_u}{\partial t^2} + \left(\rho_u c_u + \tau_q \rho_b c_b w_b \right) \frac{\partial T_u}{\partial t} = k_u \left(\frac{\partial^2 T_u}{\partial x^2} + \frac{\partial^2 T_u}{\partial y^2} \right) + \rho_b c_b w_b \left(T_b - T_u \right) + Q_m, \tag{2.7}$$

respectively. The symbols used in above equations are already defined in the nomenclature.

The conditions at phase change interface are given as

$$k_f \frac{\partial T_f(S,t)}{\partial n} - k_u \frac{\partial T_u(S,t)}{\partial n} = \rho L v_n + \tau_q \rho L \dot{v}_n, \tag{2.8}$$

$$T_u(S,t) = T_f(S,t) = T_{ph}. \tag{2.9}$$

where $v_n = \frac{\partial S}{\partial t}$, $\dot{v}_n = \frac{\partial^2 S}{\partial t^2}$, n is the unit outward normal, L represents the latent heat of fusion.

Using void fractioning volumetric averaging technique [84], macroscopic properties of lung are computed as [12]

$$\begin{aligned} \rho_l &= \rho_w f_w^* + \rho_a f_a^* \\ c_l &= c_w f_w^* + c_a f_a^* \\ k_l &= k_w f_w^* + k_a f_a^* \end{aligned} \tag{2.10}$$

where, f^* denotes fraction and subscripts *l*, *w* and *a* represent lung, tissue and air.

To avoid the discontinuity of temperature at phase change interface and unknown position of the solid-liquid interface, we consider enthalpy formulation to solve the present model. Temperatures of frozen, mushy and unfrozen regions are expressed into enthalpies by using the definition of enthalpy, $H(T) = \int_{T_r}^{T} c\, dT$, where T_r is the reference temperature:

(i) Frozen region ($T < T_{ms}$):

$$H = \int_{T_{ms}}^{T} c_f dT = c_f (T - T_{ms}).$$

(ii) Mushy region ($T_{ms} \le T \le T_{ml}$):

$$H = \frac{1}{2}\int_{T_{ms}}^{T} (c_f + c_u) dT + \frac{L}{(T_{ml} - T_{ms})}\int_{T_{ms}}^{T} dT = (T - T_{ms})\left\{\frac{1}{2}(c_f + c_u) + \frac{L}{(T_{ml} - T_{ms})}\right\}.$$

(iii) Unfrozen region ($T > T_{ml}$):

$$H = L + \frac{1}{2}\int_{T_{ms}}^{T_{ml}} (c_f + c_u) dT + \int_{T_{ms}}^{T} c_u\, dT = L + \frac{1}{2}(c_f + c_u)(T_{ml} - T_{ms}) + c_u (T - T_{ms}).$$

Thus, tissue temperature and enthalpy can also be written in combined form as follows

$$H = \begin{cases} c_f (T - T_{ms}) & T < T_{ms} \\ (T - T_{ms}) \left\{ \frac{1}{2}\left(c_f + c_u\right) + \frac{L}{(T_{ml} - T_{ms})} \right\} & T_{ms} \le T \le T_{ml}, \\ L + \frac{1}{2}\left(c_f + c_u\right)(T_{ml} - T_{ms}) + c_u (T - T_{ml}) & T > T_{ml} \end{cases} \tag{2.11}$$

where, T_{ms} and T_{ml} are solidus (-8 ^0C) and liquidus (-1 ^0C) temperatures. Using equation (2.11), equations (2.6) – (2.9) reduce to a single equation as

$$\tau_q \rho \frac{\partial^2 H}{\partial t^2} + \left(\rho + \frac{\tau_q \rho_b w_b c_b}{c} \right) \frac{\partial H}{\partial t} = k \left(\frac{\partial^2 T}{\partial x^2} + \frac{\partial^2 T}{\partial y^2} \right) + \rho_b w_b c_b \left(T_b - T \right) + Q_m. \tag{2.12}$$

2.3.3 Initial and Boundary Conditions

(a) The condition at initial time $t = 0$ as follows:

$$T_f (x, y, 0) = T_0 = 37\ ^0C \quad \text{and} \quad \left. \frac{\partial T_f}{\partial t} \right|_{t=0} = 0,$$

$$T_u (x, y, 0) = T_0 \quad \text{and} \quad \left. \frac{\partial T_u}{\partial t} \right|_{t=0} = 0,$$

(b) The conditions on the boundary of the tissue are defined as follows:

(i) At $x = 0$ and $1.8cm \le y \le 2.2cm$

$$T(0, y, t) = T_c = -196\ ^0C.$$

(ii) At $x = 0, 0 \le y < 1.8cm$ and $2.2cm < y \le 4.0cm$, adiabatic condition has been assumed, i.e.,

$$\frac{\partial T(x, y, t)}{\partial x} = 0.$$

(iii) At $y = 0, y = 4.0cm$ and $0 \le x \le 4.0cm$; $x = 4.0\ cm,\ 0 \le y \le 4.0cm$

$$T\ (x, y, t) = 37\ ^0C.$$

(iv) At y = 1.25 cm, y = 2.75 cm and $0 \le x \le 1.5\,cm$; x = 1.5 cm, $1.25\ cm \le y \le 2.75\,cm$,

Continuity condition for heat flux and temperature at common boundary lung and tumor is given as

$$k_t \frac{\partial T_t(x,y,t)}{\partial x} = k_l \frac{\partial T_l(x,y,t)}{\partial x} \qquad \text{and } T_t = T_l$$

where, subscripts t and l stand for tumor and normal lung tissue, respectively.

2.4 Numerical Solution

Finite difference explicit approximation has been used to solve the presented model. Considering $x_i = i\delta x,\ y_j = j\delta y (\delta x = \delta y)$ *and* $t_n = n\delta t$, where i, j and n are the space and time index respectively; $\delta x, \delta y$ and δt are the increment in x-axis, y-axis and time respectively. Applying forward difference approximation to first order time derivative and second order central difference approximation to time and space derivatives at point (x_i, y_j, t_n) in equation (2.12), we get

$$\begin{aligned} H_{i,j}^{n+1} = {} & \left(1 + A_{i,j}^n F_{i,j}^n\right) H_{i,j}^n - A_{i,j}^n F_{i,j}^n H_{i,j}^{n-1} + D_{i,j}^n F_{i,j}^n (T_{i+1,j}^n + T_{i-1,j}^n - 4T_{i,j}^n + T_{i,j+1}^n + T_{i,j-1}^n) \\ & + E_{i,j}^n F_{i,j}^n (T_b - T_{i,j}^n) + F_{i,j}^n Q_{mi,j}^n, \end{aligned} \tag{2.13}$$

where,

$$A_{i,j}^n = \frac{\tau_q \rho_{i,j}^n}{(\delta t)^2};\ \ B_{i,j}^n = \left\{ \frac{\rho_{i,j}^n}{(\delta t)} + \frac{\tau_q \rho_b c_b w_{bi,j}^n}{c_{i,j}^n (\delta t)} \right\};\ D_{i,j}^n = \frac{k_{i,j}^n}{(\delta x)^2};\ E_{i,j}^n = \rho_b c_b w_{bi,j}^n;\ F_{i,j}^n = \frac{1}{A_{i,j}^n + B_{i,j}^n}.$$

Equation (2.13) gives the enthalpy at the $(n+1)^{th}$ time level in terms of enthalpy and temperature at n^{th} time level. A stability criteria for numerical solution is used to manage the space and time increments, which is given as

$$\max\left\{ \frac{(\delta t)^2 \left\{4k + \rho_b\, w_b\, c_b\, (\delta x)^2\right\}}{(\delta x)^2 \left\{2c\tau_q\rho + c\rho(\delta t) + \tau_q \rho_b\, w_b\, c_b\, (\delta t)\right\}}, \frac{(\delta t)^2 \left\{4k + \rho_b\, w_b\, c_b\, (\delta y)^2\right\}}{(\delta y)^2 \left\{2c\tau_q\rho + c\rho(\delta t) + \tau_q \rho_b\, w_b\, c_b\, (\delta t)\right\}} \right\} \le 1.$$

After finding the enthalpy at $(n+1)^{th}$ time level, one can obtain the temperature at $(n+1)^{th}$ time level by inverting the equation (2.11) as follows:

$$T=\begin{cases}\dfrac{H}{c_f}+T_{ms}, & H<0\\ \dfrac{2H(T_{ml}-T_{ms})}{\left(c_f+c_u\right)\left(T_{ml}-T_{ms}\right)+2L}+T_{ms}, & 0\le H\le L+\dfrac{1}{2}\left(c_f+c_u\right)\left(T_{ml}-T_{ms}\right).\\ \dfrac{H}{c_u}-\dfrac{L}{c_u}-\dfrac{\left(c_f+c_u\right)}{2c_u}\left(T_{ml}-T_{ms}\right)+T_{ml}, & H>L+\dfrac{1}{2}\left(c_f+c_u\right)\left(T_{ml}-T_{ms}\right)\end{cases} \quad (2.14)$$

Once the new temperature field is known from the enthalpies, the procedure is repeated. The position of upper and lower phase change interfaces is given by isotherms at -1 ^0C and -8 ^0C.

2.4.1 Numerical Code Validation

The validity and accuracy of the numerical code for the present problem are checked by comparing our particular results with the published results [69]. Results are compared with parabolic bio-heat model as a special case ($\tau_q = 0s$). Solution generated by present code is in good agreement with the published results (see Table 2.1). Apart from this, grid independence of the solution is also checked for various grid sizes in the *x* and *y* directions. We found that the results remain consistent when the grid size is 40 x 40 or more. Therefore, all the computations are reported by taking the grid size as 40 x 40.

Table 2.1: Comparison between published and present results at $\tau_q = 0\,s$.

Published results [69]			**Present results**	
Time (s)	Lower Interface (cm)	Upper Interface (cm)	Lower Interface (cm)	Upper Interface (cm)
25	0.30	0.34	0.30	0.34
50	0.40	0.43	0.39	0.42
75	0.46	0.52	0.47	0.51
100	0.51	0.56	0.52	0.57
125	0.56	0.60	0.57	0.62
150	0.59	0.65	0.60	0.66
175	0.65	0.70	0.66	0.71
200	0.67	0.71	0.69	0.73

2.5 Results and Discussion

In this section, we illustrate the numerical results for hyperbolic bio-heat model with phase change during cryosurgical treatment of lung cancer. Present problem is solved with dimensional parameters. The values of dimensional parameters for both tumor and lung tissue based on equation (2.10) are given in Table 2.2 [12, 67, 69, 114]. The values of relaxation time for heat flux are considered as $\tau_q = 0s, 1s, 5s, 10s$ and $15s$ [2, 28, 77, 94].

To implement cryosurgery precisely, the temperature distribution and propagation of freezing interface in tissue are important to monitor the tumor damage and sparing healthy tissue. The effect of different values of relaxation time on temperature profiles and freezing interfaces has been obtained.

Table 2.2: Thermo-physical properties of tissues [12, 67, 69, 114].

Parameter	**Units**	**Value**
Density of blood	kg/m^3	1005
Density of tumor tissue (unfrozen)	kg/m^3	998
Density of tumor tissue (frozen)	kg/m^3	921
Density of lung tissue (unfrozen)	kg/m^3	161
Density of lung tissue (frozen)	kg/m^3	149
Thermal conductivity of tumor tissue (unfrozen)	$W/m\ ^0C$	0.552
Thermal conductivity of tumor tissue (frozen)	$W/m\ ^0C$	2.25
Thermal conductivity of lung tissue (unfrozen)	$W/m\ ^0C$	0.11
Thermal conductivity of lung tissue (frozen)	$W/m\ ^0C$	0.38
Specific heat of tumor tissue (unfrozen)	$J/kg\ ^0C$	4200
Specific heat of tumor tissue (frozen)	$J/kg\ ^0C$	1230
Specific heat of lung tissue (unfrozen)	$J/kg\ ^0C$	4174
Specific heat of lung tissue (frozen)	$J/kg\ ^0C$	1221
Blood perfusion in tumor tissue	ml/s/ml	0.002
Blood perfusion in lung tissue	ml/s/ml	0.0005
Metabolic heat generation in tumor	W/m^3	672
Metabolic heat generation in lung	W/m^3	42000
Latent heat	kJ/kg	333.00
Arterial blood temperature	^0C	37

Since the biological tissues show the non-ideal property, therefore phase change occurs over a wide range with upper phase change temperature -1 ^0C and lower phase change temperature -8 ^0C. Position of the interfaces (lower and upper interfaces) versus time in *x*-direction at *y* = 2.0 cm for different values of relaxation time are presented in figures 2.2 and 2.3, respectively. Figures 2.2 and 2.3 examine how freezing positions are affected due to change in the relaxation time. Phase change movement, i.e., slope of freezing position decreases on increasing the relaxation time and temperature gradient also decreases due to an increase in distance from the cryoprobe. In this situation, the relaxation time controls the behavior of thermal signal propagation. This shows that freezing position for hyperbolic solution moves slower than the parabolic one, which implies that phase change interface position for hyperbolic case at the same time is lower than that of parabolic case. For example, phase change interface position for $\tau_q = 5s$ and $\tau_q = 10s$ are lower than $\tau_q = 0s$ (see figures 2.2 and 2.3). Furthermore a decrease in freezing position is observed with an increase in the value of τ_q.

As can be observed from the figures 2.2 and 2.3 that both freezing interfaces suddenly accelerate as they move towards healthy lung tissue from tumor tissue, i.e., cross the lung-tumor boundary. This phenomenon can be explained by considering the densities and conductivities of healthy lung tissue and tumor tissue. Parameter values from Table 2.2 shows that the healthy lung tissue has low density and smaller thermal conductivity as compared to the density and thermal conductivity of tumor tissue. This difference in the thermal-physical properties of healthy lung tissue and tumor tissue causes the freezing interfaces to suddenly accelerate as they cross the lung-tumor boundary. Bischof et al. [12] have also observed the similar kind of phenomena in their earlier work where they have studied the freezing in the special case of a solid tumor embedded in porous lung. Also, the hyperbolic model reduces to parabolic bio-heat model when $\tau_q = 0$ which is studied in great detail by Kumar and Katiyar [69] in their previous work.

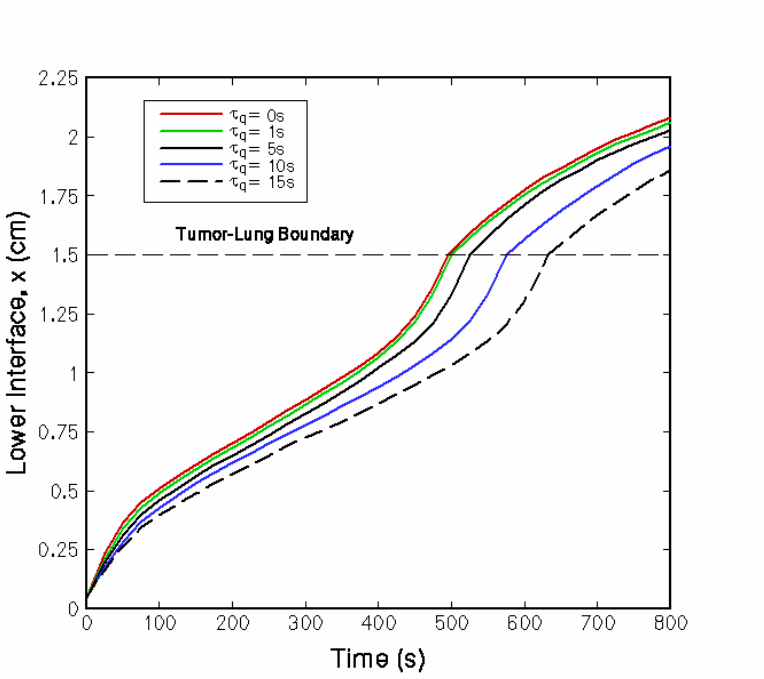

Figure 2.2: Position of lower interface during freezing versus time at y = 2.0 *cm* for the value of $\tau_q = 0s, \tau_q = 1s, \tau_q = 5s, \tau_q = 10s, \tau_q = 15s.$

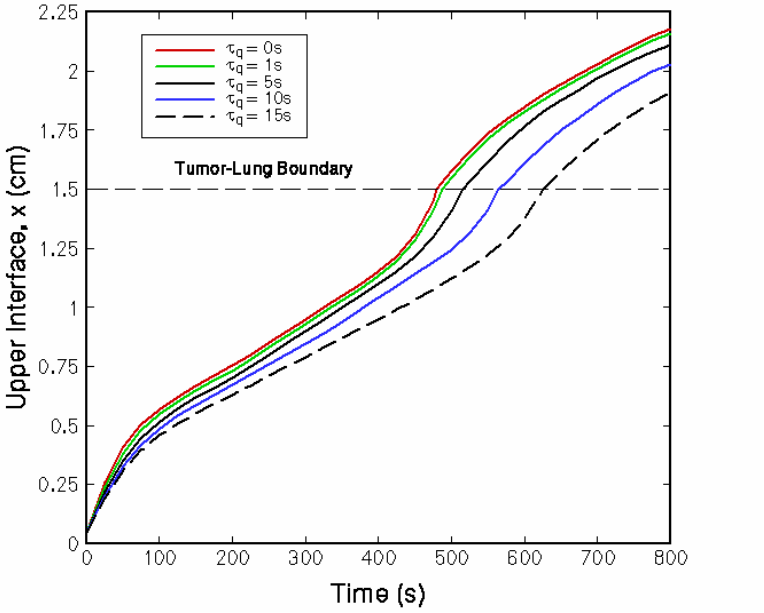

Figure 2.3: Position of upper interface during freezing versus time at y = 2.0 *cm* for the value of $\tau_q = 0s, \tau_q = 1s, \tau_q = 5s, \tau_q = 10s, \tau_q = 15s.$

Figures 2.4–2.8 are plotted for the temperature distribution within the tissue at time t = 200 *s*, 400 *s*, 600 *s* and 800 *s* during cryosurgery for different values of relaxation time i.e., $\tau_q = 0s, 1s, 5s, 10s$ and $15s.$ We know that when the value of τ_q tends to zero, hyperbolic

solution approaches to the parabolic solution. As can be seen from figures 2.4–2.5, the temperature distribution is almost similar for $\tau_q = 0s$ and $\tau_q = 1s$, i.e., the solutions of hyperbolic model and parabolic model predict almost same results for small value of the relaxation time. However, as we increase the relaxation time, both solutions differ significantly. Tissue temperature for hyperbolic model is higher than parabolic one at the same time. Temperature increases in the tissue with an increase in the relaxation time. A possible qualitative justification towards an increase in the temperature as follows. In the case of low relaxation time, heat diffuses into tissue much faster, hence tissue freezes quicker and its temperature decreases rapidly as compared to high relaxation time case. In addition to above, it can also be observed that in both hyperbolic and parabolic models, tissue temperature is much below the lethal temperature (- 30 ^0C) after time t = 800 s.

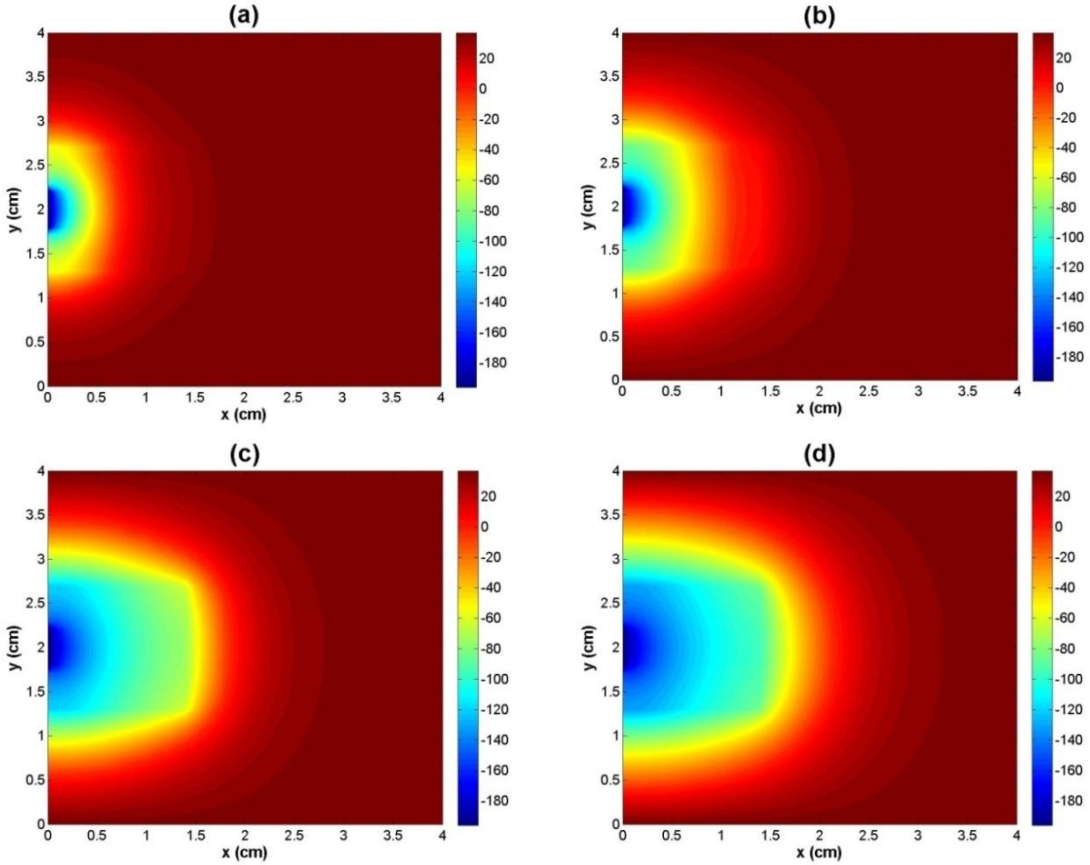

Figure 2.4: Temperature distribution along the tissue during freezing for $\tau_q = 0s$ at (a) t = 200 s, (b) t = 400 s, (c) t = 600 s and (d) t = 800 s.

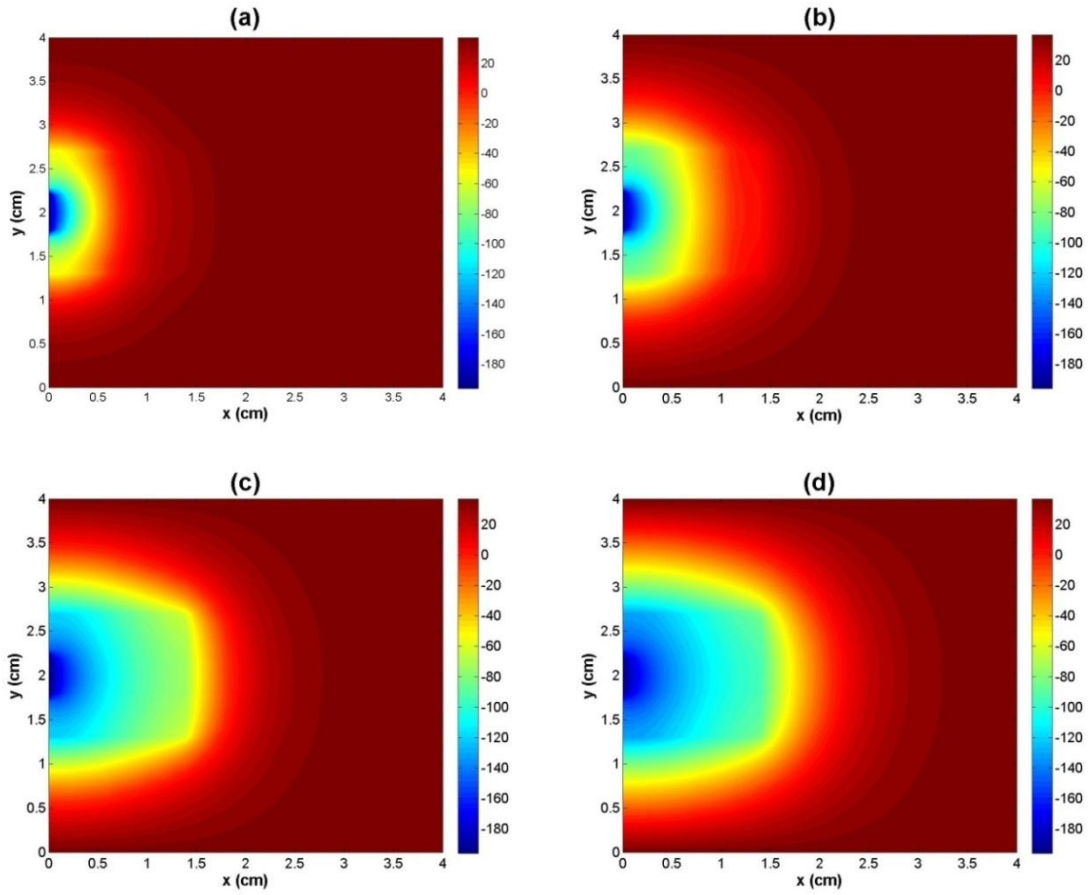

Figure 2.5: Temperature distribution along the tissue during freezing for $\tau_q = 1s$ at (a) t = 200 s, (b) t = 400 s, (c) t = 600 s and (d) t = 800 s.

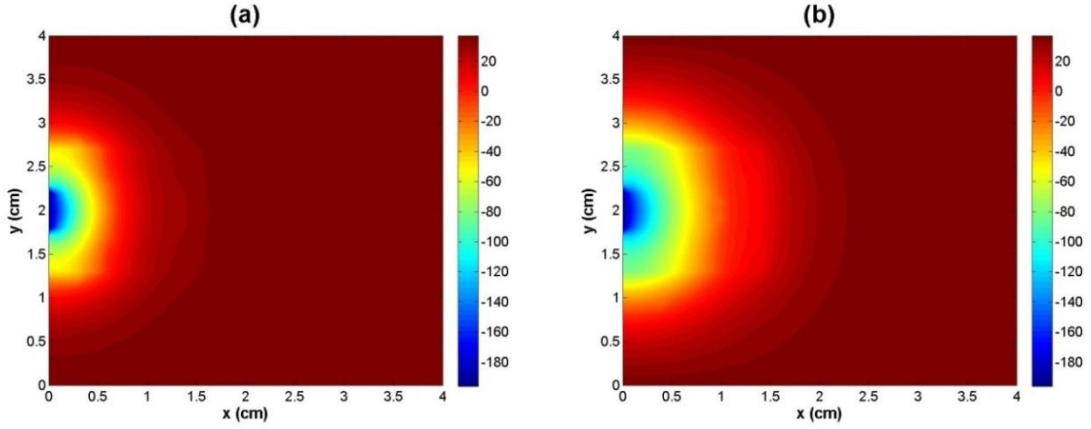

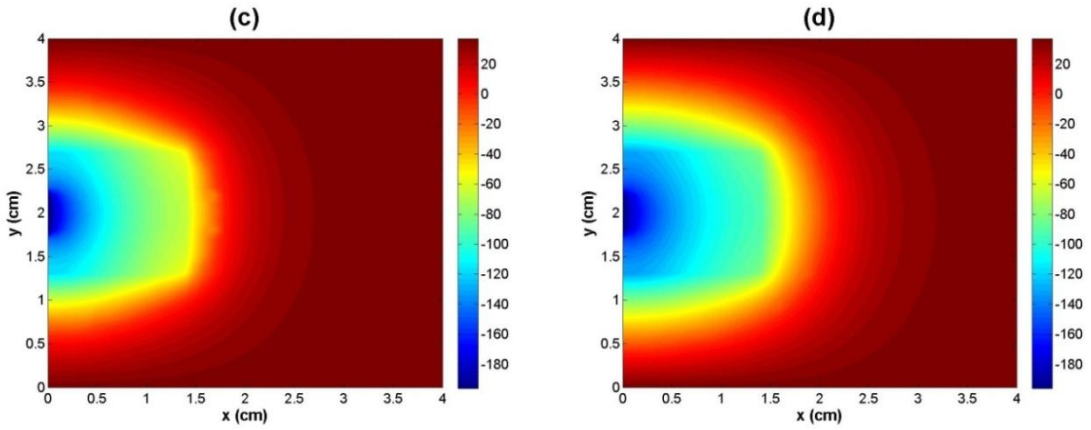

Figure 2.6: Temperature distribution along the tissue during freezing for $\tau_q = 5s$ at (a) t = 200 s, (b) t = 400 s, (c) t = 600 s and (d) t = 800 s.

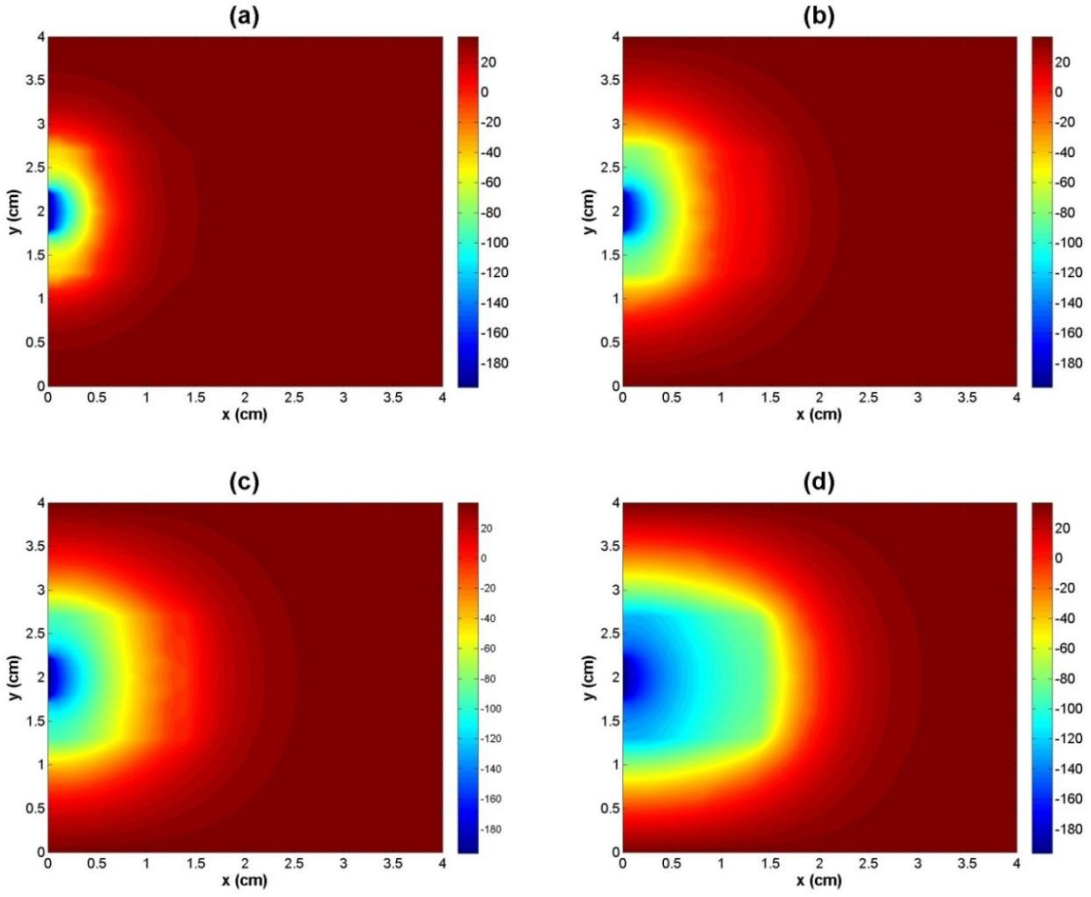

Figure 2.7: Temperature distribution along the tissue during freezing for $\tau_q = 10s$ at (a) t = 200 s, (b) t = 400 s, (c) t = 600 s and (d) t = 800 s.

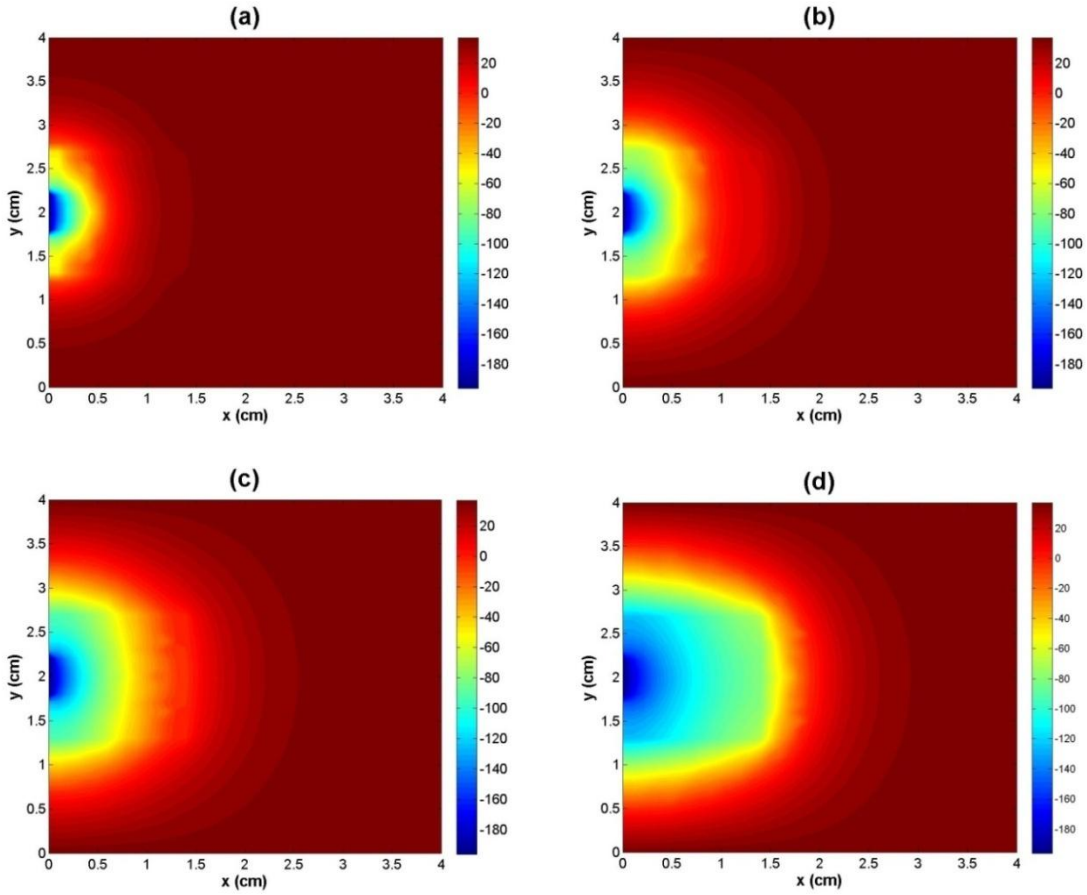

Figure 2.8: Temperature distribution along the tissue during freezing for $\tau_q = 15s$ at (a) t = 200 s, (b) t = 400 s, (c) t = 600 s and (d) t = 800 s.

Figures 2.9–2.12 show the positions of lower and upper freezing interfaces at time t = 200 s, 400 s, 600 s and 800 s with respect to the distance x and y for different values of relaxation time. Results in figures 2.9–2.12 clearly show the direction of ice growth and ice-ball history. It can be observed from the above figures that the phase change interfaces for hyperbolic model move faster as the value of relaxation time (τ_q) decreases. Freezing velocity of the thermal signals is retarded by relaxation time as it dominates the behavior of thermal signal propagation. Hence, the freezing is faster for smaller values of relaxation time for heat flux.

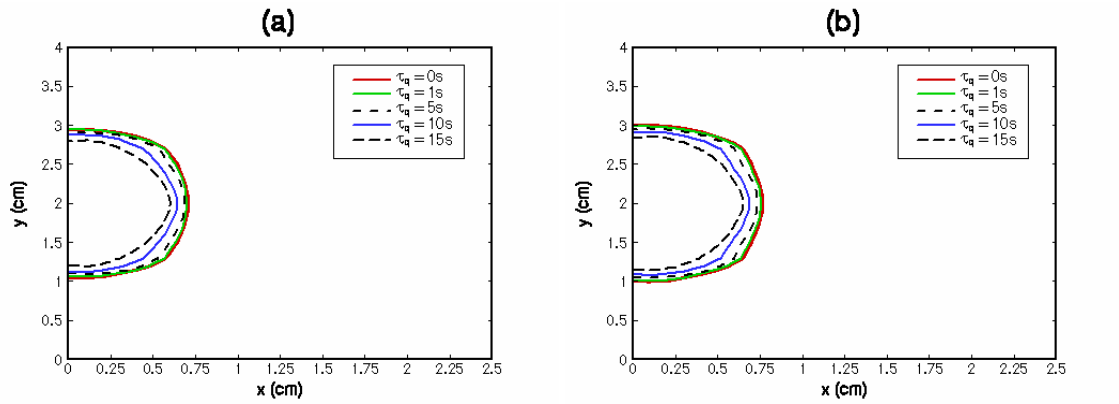

Figure 2.9: (a) Lower phase change interface and (b) Upper interface during freezing at t = 200 s, for $\tau_q = 0s, \tau_q = 1s, \tau_q = 5s, \tau_q = 10s, \tau_q = 15s$.

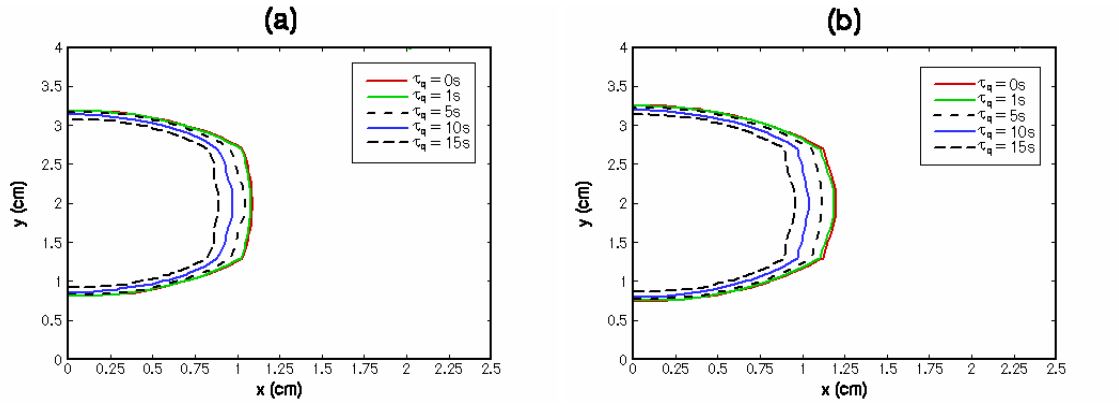

Figure 2.10: (a) Lower phase change interface and (b) Upper interface during freezing at t = 400 s, for $\tau_q = 0s, \tau_q = 1s, \tau_q = 5s, \tau_q = 10s, \tau_q = 15s$.

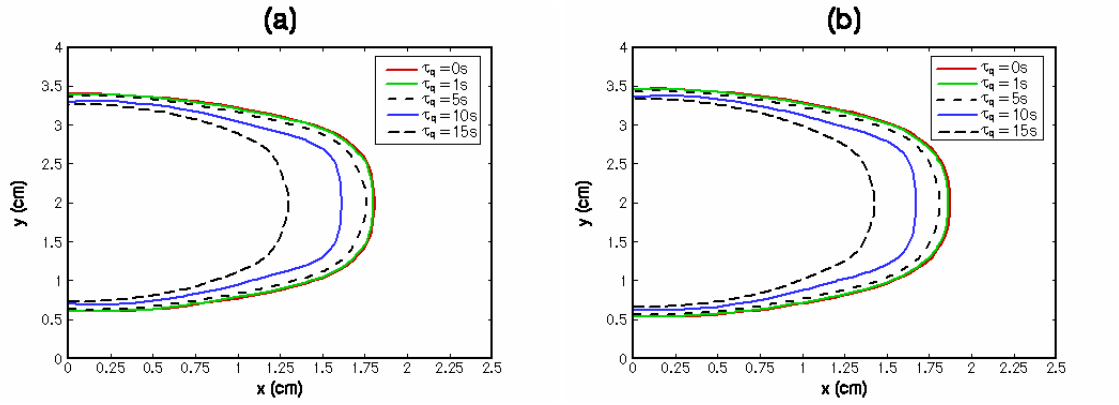

Figure 2.11: (a) Lower phase change interface and (b) Upper interface during freezing at t = 600 s, for $\tau_q = 0s, \tau_q = 1s, \tau_q = 5s, \tau_q = 10s, \tau_q = 15s$.

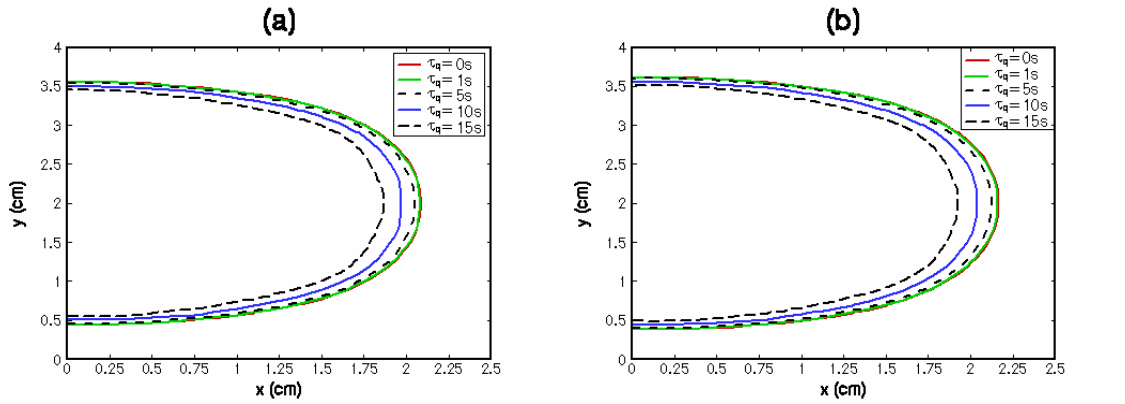

Figure 2.12: (a) Lower phase change interface and (b) Upper interface during freezing at t = 800 s, for $\tau_q = 0s, \tau_q = 1s, \tau_q = 5s, \tau_q = 10s, \tau_q = 15s$.

2.6 Conclusions

In this chapter, we have analyzed numerically the phase change interface and temperature distribution in a lung tumor tissue during cryosurgery. Due to infinite speed of heat propagation in the Fourier's law, a two-dimensional hyperbolic bio-heat model is considered. A comparison is also made between hyperbolic and parabolic models. By means of rigorous numerical experiments, we observe that relaxation time of heat flux has an important effect on freezing interfaces and temperature distribution. When the relaxation time tends to zero, the solution of hyperbolic model converges to the solution of the parabolic model. Phase change interface position decreases on increasing relaxation time, which implies that interface position for hyperbolic case at the same time is lower than that of parabolic case. Tissue temperature increases with an increase in the value of relaxation time. Hence non-Fourier effect becomes more effective as compared to Fourier effect. In the case of hyperbolic model freezing is fast for small values of relaxation time.

The above informations are important to know the extent of freezing in tumor necrosis. The knowledge of interface position and temperature distribution in biological tissue could be effective tool for a cryosurgeon to control the freezing in lung-tumor tissue within certain time period to minimize the damage to normal lung tissue. The present results may help in carrying out the cryosurgical treatment in lung cancer more effectively. The treatment can be so optimized that only the tumor tissue gets destroyed by freezing while causing least possible damage to the neighboring normal lung tissue due to over freezing.

Chapter 3

Dual Phase Lag Model for Cryosurgery of Lung Cancer: Comparison of Three Heat Transfer Models

3.1 Introduction

Many studies are available in the literature [2, 28, 134-135, 163] in which hyperbolic bio-heat model in biological tissues is used. Although a lot of experiments confirm that the hyperbolic bio-heat model produces more accurate and realistic results than the parabolic bio-heat model, it still creates an instantaneous behavior between heat transport and temperature gradient. It is also establishes that the temperature gradient is always the cause for heat flux while heat flux always effects the heat transfer process [142-143]. Further, hyperbolic model considers the micro scale response only in time, but it does not consider the micro scale response in space. Therefore, to consider the thermal behavior which is not captured by the Fourier's law and to take into account the microstructural effect in space, a new bio-heat model is introduced by Tzou [143]. This model is called as dual phase lag (DPL) model and it is based on dual-phase lag constitutive relation, which is given as

$$q\left(S,t+\tau_q\right)=-k\nabla T\left(S,t+\tau_T\right), \tag{3.1}$$

where, τ_T is the phase lag in temperature gradient. Using the Taylor's series, first order approximation of equation (3.1) is given by

$$q(S,t)+\tau_q\frac{\partial q(S,t)}{\partial t}=-k\nabla\left\{T(S,t)+\tau_T\frac{\partial T(S,t)}{\partial t}\right\}, \tag{3.2}$$

Equation (3.2) is called the dual phase lag constitutive relation. Eliminating q from energy balance equation (2.1), the dual phase lag constitutive relation leads to the following equation:

$$\tau_q\rho c\frac{\partial^2 T}{\partial t^2}+\left(\rho c+\rho_b w_b c_b\tau_q\right)\frac{\partial T}{\partial t}=k\nabla^2\left\{T(S,t)+\tau_T\frac{\partial T(S,t)}{\partial t}\right\}+\rho_b w_b c_b(T_b-T)+Q_m. \tag{3.3}$$

The above equation is known as a dual phase lag bio-heat equation. If phase lag in temperature gradient (τ_T) is equal to 0*s*, then it becomes hyperbolic bio-heat equation and if $\tau_q = \tau_T = 0\,s$ then parabolic bio-heat equation.

Dual phase lag model has been used by many researchers [80, 87, 161-162] without phase change. To investigate the non-Fourier heat conduction in processed meat, a dual phase lag model is proposed by Antaki [5]. Liu and Chen [80] have investigated the temperature rise behavior in biological tissues during hyperthermia treatment using the DPL model. They have ignored the effect of metabolic heat generation. To describe the heat transfer in living biological tissues, Zhou et al. [162] have used a 2D axisymmetric DPL model. In their study, they have obtained that the DPL bio-heat model shows a different thermal behavior from the other bio-heat models. Askarizadeh and Ahmadikia [7] have presented an analytical solution of DPL model to study the transient heat transfer in skin tissue. Singh and Kumar [136] have proposed a DPL bio-heat model to examine the important effect of phase lags of temperature gradient and heat flux in triple layer skin tissue during cryosurgery. Moradi and Ahmadikia [94] have studied the freezing process in biological tissue using one dimensional DPL model with metabolic heat generation and blood flow. They have obtained the temperature distribution and phase change interface positions in biological tissue for different values of phase lag in heat flux and temperature gradient. A dual phase lag equation has been used by Mochnacki and Majchrzak [93] to study the thermal interactions between biological tissue and cylindrical cryoprobe.

In this chapter, we propose a dual phase lag model to study the effect of two phase lags i.e., phase lag in heat flux and phase lag in temperature gradient on freezing process in cryosurgery. The model includes the discontinuity of temperature at the solid-liquid interface. For different values of phase lag in heat flux and temperature gradient, the graph of the temperature distribution and freezing interfaces in lung-tumor tissue are plotted. Cryosurgery in lung tumor tissue is performed by considering non-ideal property of tissue, blood perfusion and metabolism. The finite difference method is used to solve the enthalpy formulation of the dual phase lag bio-heat equation. A comparative study of DPL, parabolic and hyperbolic bio-heat models is thoroughly investigated.

3.2 Problem Description

The problem consists of a lung tissue of dimension $4.0cm \times 4.0cm$ in which a tumor tissue of dimension $1.5cm \times 1.5cm$ is embedded. A cryoprobe is situated at position $x = 0,\ 1.8\ cm \le y \le 2.2\ cm$. The corresponding schematic diagram of the physical model is shown in figure 2.1 [69].

3.3 Mathematical Formulation

3.3.1 Assumptions

- Heat conduction in tissue takes place through non-Fourier conduction law [2].
- The initial temperature of tissue is considered as an arterial temperature (37 ^0C).
- Non-ideal property of tissue is used with upper and lower phase change interface at temperatures -1^0C and -8^0C, respectively [114].
- Heat source appears due to blood perfusion and metabolism when tissue is unfrozen [27, 29].
- Thermo-physical properties of normal lung and tumor tissue are different for both frozen and unfrozen regions.

3.3.2 Governing Equations

The governing equations of two-dimensional dual phase lag model in frozen and unfrozen regions are given as

$$\tau_q \rho_f c_f \frac{\partial^2 T_f}{\partial t^2} + \rho_f c_f \frac{\partial T_f}{\partial t} = k_f \left(\frac{\partial^2 T_f}{\partial x^2} + \frac{\partial^2 T_f}{\partial y^2} \right) + \tau_T k_f \left(\frac{\partial^3 T_f}{\partial t \partial x^2} + \frac{\partial^3 T_f}{\partial t \partial y^2} \right), \tag{3.4}$$

$$\tau_q \rho_u c_u \frac{\partial^2 T_u}{\partial t^2} + \left(\rho_u c_u + \tau_q \rho_b c_b w_b \right) \frac{\partial T_u}{\partial t} = k_u \left(\frac{\partial^2 T_u}{\partial x^2} + \frac{\partial^2 T_u}{\partial y^2} \right) + \tau_T k_u \left(\frac{\partial^3 T_u}{\partial t \partial x^2} + \frac{\partial^3 T_u}{\partial t \partial y^2} \right) + \rho_b c_b w_b \left(T_b - T_u \right) + Q_m, \tag{3.5}$$

respectively. The subscripts *f*, *u* and *b* stand for frozen, unfrozen and blood of tissue, respectively.

Conditions at phase change interface are

$$k_f\left(\frac{\partial T_f}{\partial n}+\tau_T\frac{\partial^2 T_f}{\partial t\partial n}\right)-k_u\left(\frac{\partial T_u}{\partial n}+\tau_T\frac{\partial^2 T_u}{\partial t\partial n}\right)=\rho_f L v_n+\tau_q\rho_f L\dot{v}_n, \tag{3.6}$$

$$T_u(S,t)=T_f(S,t)=T_{ph}. \tag{3.7}$$

Using enthalpy $H(T)=\int_{T_r}^{T} c\,dT,$ where T_r is the reference temperature. Relation between enthalpy and temperature of tissue is given as

$$H=\begin{cases} c_f(T-T_{ms}) & T<T_{ms} \\ (T-T_{ms})\left\{\frac{1}{2}\left(c_f+c_u\right)+\frac{L}{(T_{ml}-T_{ms})}\right\} & T_{ms}\le T\le T_{ml}, \\ L+\frac{1}{2}\left(c_f+c_u\right)(T_{ml}-T_{ms})+c_u(T-T_{ml}) & T>T_{ml} \end{cases} \tag{3.8}$$

where, T_{ml} and T_{ms} are upper (-1 ^0C) and lower (-8 ^0C) phase change temperatures. Using equation (3.8), equations (3.4) – (3.7) reduce into a single equation as

$$\tau_q\rho\frac{\partial^2 H}{\partial t^2}+\left(\rho+\frac{\tau_q\rho_b c_b w_b}{c}\right)\frac{\partial H}{\partial t}=k\left(\frac{\partial^2 T}{\partial x^2}+\frac{\partial^2 T}{\partial y^2}\right)+k\tau_T\left(\frac{\partial^3 T}{\partial t\partial x^2}+\frac{\partial^3 T}{\partial t\partial y^2}\right)$$
$$+\rho_b c_b w_b\left(T_b-T\right)+Q_m. \tag{3.9}$$

3.3.3 Initial and Boundary Conditions

(a) The condition at initial time t = 0 as follows:

$$T_f(x,y,0)=T_0=37\ ^0C \text{ and } \left.\frac{\partial T_f}{\partial t}\right|_{t=0}=0,$$

$$T_u(x,y,0)=T_0 \text{ and } \left.\frac{\partial T_u}{\partial t}\right|_{t=0}=0,$$

(b) The conditions on the boundary of the tissue are defined as follows:

(i) At x = 0 and $1.8cm\le y\le 2.2cm$

$$T(0, y, t) = T_c = -196\ ^0C.$$

(ii) At $x = 0, 0 \le y < 1.8cm$ and $2.2cm < y \le 4.0cm$, adiabatic condition has been assumed, i.e.,

$$\frac{\partial T(x,y,t)}{\partial x} = 0.$$

(iii) At $y = 0$, $y = 4.0\ cm$ and $0 \le x \le 4.0cm$; $x = 4.0\ cm$, $0 \le y \le 4.0cm$

$$T\ (x, y, t) = 37\ ^0C.$$

(iv) At $y = 1.25$ cm, $y = 2.75\ cm$ and $0 \le x \le 1.5cm$; $x = 1.5$ cm, $1.25\ cm \le y \le 2.75cm$

Continuity condition for heat flux and temperature at common boundary of lung and tumor is given as

$$k_t \frac{\partial T_t(x,y,t)}{\partial x} = k_l \frac{\partial T_l(x,y,t)}{\partial x} \qquad \text{and } T_t = T_l$$

where, subscripts *t* and *l* stand for tumor and normal lung tissue, respectively.

3.4 Numerical Solution

Taking $x_i = i\delta x,\ y_j = j\delta y (\delta x = \delta y)\ and\ t_n = n\delta t$, where *i*, *j* and *n* are the space and time index, respectively; $\delta x, \delta y$ and δt are grid spacing along *x*-axis, *y*-axis and time respectively. In equation (3.9) using forward difference approximation to first order time derivative and second order central difference approximation to time and space derivatives at point (x_i, y_j, t_n), the discretized form of the equation as follows

$$\begin{aligned} H_{i,j}^{n+1} = & \left(1 + \frac{A_{i,j}^n}{A_{i,j}^n + B_{i,j}^n}\right) H_{i,j}^n - \left(\frac{A_{i,j}^n}{A_{i,j}^n + B_{i,j}^n}\right) H_{i,j}^{n-1} - \left(\frac{4D_{i,j}^n + 4E_{i,j}^n + F_{i,j}^n}{A_{i,j}^n + B_{i,j}^n}\right) T_{i,j}^n \\ & + \left(\frac{D_{i,j}^n + E_{i,j}^n}{A_{i,j}^n + B_{i,j}^n}\right)\left(T_{i+1,j}^n + T_{i,j+1}^n + T_{i-1,j}^n + T_{i,j-1}^n\right) - \left(\frac{E_{i,j}^n}{A_{i,j}^n + B_{i,j}^n}\right)\left(T_{i+1,j}^{n-1} + T_{i,j+1}^{n-1} - 4T_{i,j}^{n-1} + T_{i-1,j}^{n-1} + T_{i,j-1}^{n-1}\right) \\ & + \left(\frac{F_{i,j}^n}{A_{i,j}^n + B_{i,j}^n}\right) T_b + \frac{Q_m}{A_{i,j}^n + B_{i,j}^n}, \end{aligned} \tag{3.10}$$

where,

$$A_{i,j}^n = \frac{\tau_q \rho_{i,j}^n}{(\delta t)^2};\quad B_{i,j}^n = \left\{\frac{\rho_{i,j}^n}{(\delta t)} + \frac{\tau_q \rho_b c_b w_{bi,j}^n}{c_{i,j}^n (\delta t)}\right\};\ D_{i,j}^n = \frac{k_{i,j}^n}{(\delta x)^2};\ E_{i,j}^n = \frac{k_{i,j}^n \tau_T}{(\delta t)(\delta x)^2};\ F_{i,j}^n = \rho_b c_b w_{bi,j}^n\ .$$

Equation (3.10) can be written as

$$H_{i,j}^{n+1} = \left(1+U_{i,j}^{n}\right)H_{i,j}^{n} - U_{i,j}^{n}H_{i,j}^{n-1} - \left(4V_{i,j}^{n} + 4W_{i,j}^{n} + Y_{i,j}^{n}\right)T_{i,j}^{n} + \left(V_{i,j}^{n} + W_{i,j}^{n}\right)\left(T_{i+1,j}^{n} + T_{i,j+1}^{n} + T_{i-1,j}^{n}T_{i,j-1}^{n}\right) - W_{i,j}^{n}\left(T_{i+1,j}^{n-1} + T_{i,j+1}^{n-1} - 4T_{i,j}^{n-1} + T_{i-1,j}^{n-1} + T_{i,j-1}^{n-1}\right) + Y_{i,j}^{n}T_{b} + Z_{i,j}^{n}. \tag{3.11}$$

where,

$$U_{i,j}^{n} = \frac{A_{i,j}^{n}}{A_{i,j}^{n} + B_{i,j}^{n}};\ V_{i,j}^{n} = \frac{D_{i,j}^{n}}{A_{i,j}^{n} + B_{i,j}^{n}};\ W_{i,j}^{n} = \frac{E_{i,j}^{n}}{A_{i,j}^{n} + B_{i,j}^{n}};\ Y_{i,j}^{n} = \frac{F_{i,j}^{n}}{A_{i,j}^{n} + B_{i,j}^{n}};\ Z_{i,j}^{n} = \frac{Q_{m}}{A_{i,j}^{n} + B_{i,j}^{n}}.$$

Enthalpy at $(n+1)^{th}$ time level in terms of enthalpy and temperature at n^{th} time level is given by equation (3.11). A stability condition for numerical solution is used to manage the space and time increments, which is given as

$$\max\left\{\frac{(\delta t)\left\{4k(\delta t) + 4k\tau_{T} + \rho_{b}\, w_{b}\, c_{b}\,(\delta t)(\delta x)^{2}\right\}}{(\delta x)^{2}\left\{2c\tau_{q}\rho + c\rho(\delta t) + \tau_{q}\rho_{b}\, w_{b}\, c_{b}\,(\delta t)\right\}}, \frac{(\delta t)\left\{4k(\delta t) + 4k\tau_{T} + \rho_{b}\, w_{b}\, c_{b}\,(\delta t)(\delta y)^{2}\right\}}{(\delta y)^{2}\left\{2c\tau_{q}\rho + c\rho(\delta t) + \tau_{q}\rho_{b}\, w_{b}\, c_{b}\,(\delta t)\right\}}\right\} \le 1.$$

Temperature at $(n+1)^{th}$ time level can obtain from the enthalpy at $(n+1)^{th}$ time level by reverting the equation (3.8) as follows:

$$T = \begin{cases} \dfrac{H}{c_{f}} + T_{ms}, & H < 0 \\ \dfrac{2H(T_{ml} - T_{ms})}{\left(c_{f} + c_{u}\right)\left(T_{ml} - T_{ms}\right) + 2L} + T_{ms}, & 0 \le H \le L + \dfrac{1}{2}\left(c_{f} + c_{u}\right)\left(T_{ml} - T_{ms}\right). \\ \dfrac{H}{c_{u}} - \dfrac{L}{c_{u}} - \dfrac{\left(c_{f} + c_{u}\right)}{2c_{u}}\left(T_{ml} - T_{ms}\right) + T_{ml}, & H > L + \dfrac{1}{2}\left(c_{f} + c_{u}\right)\left(T_{ml} - T_{ms}\right) \end{cases} \tag{3.12}$$

Once the new temperature field is known from the enthalpies, the procedure is repeated for next time level.

3.4.1 Numerical Code Validation

Before discussing the analysis of the present problem, a numerical code validation and accuracy are checked by comparing our general results with the published results [60]. The results are compared at $\tau_q = \tau_T = 0\,s$ (parabolic bio-heat model) as a special case. The results generated by present code are in good agreement with the published one (see Table 3.1). We have also checked the grid independence test by varying the grid size in *x* and *y* directions and found that the results remain consistent when the grid size is 40 x 40 or more. Therefore, grid size as 40 x 40 is fixed for all the computations.

Table 3.1: Comparison between published and present results at $\tau_q = \tau_T = 0\,s$.

Published results [60]			**Present results**	
Time (s)	Lower Interface (cm)	Upper Interface (cm)	Lower Interface (cm)	Upper Interface (cm)
25	0.30	0.34	0.30	0.34
50	0.39	0.42	0.40	0.43
100	0.52	0.57	0.52	0.57
150	0.60	0.66	0.61	0.66
200	0.69	0.73	0.70	0.74
250	0.79	0.85	0.79	0.85
300	0.89	0.95	0.89	0.95
350	0.98	1.05	0.98	1.05
400	1.08	1.15	1.09	1.15
450	1.23	1.29	1.23	1.30

3.5 Results and Discussion

In this section, the numerical results are shown for DPL, parabolic and hyperbolic bio-heat models with phase change during cryosurgery of lung cancer. Thermo–physical properties of lung tumor tissue are given in Table 2.2 [12, 69, 114]. The values of phase lag of heat flux (τ_q) are considered as $\tau_q = 0\,s, 5\,s, 10\,s$ and $15\,s$ and the values of phase lag in temperature gradient (τ_T) are $\tau_T = 0\,s, 5\,s$ and $10\,s$ [77, 87, 94]. During the cryosurgical treatment of lung-tumor tissue, temperature distribution and interface position are important for the prediction of maximum damage to diseased tissue and minimum damage to healthy lung tissue. Therefore, we have examined position of phase change interfaces for different values of phase lag of heat flux and temperature gradient.

Since the lung-tumor tissue shows non-ideal behavior, therefore phase change occurs over a broad range with upper phase change temperature -1 ^0C and lower phase change temperature -8 ^0C. Positions of phase change interfaces versus time during the cryosurgery process for DPL, parabolic and hyperbolic models in *x*-direction at *y* = 2.0 cm, for different values of phase lag in heat flux and temperature gradient are shown in figures 3.1 and 3.2, respectively. In figures 3.1 and 3.2 the freezing interfaces suddenly accelerate as they cross the lung-tumor boundary. This is because of the low density and smaller thermal conductivity of healthy lung tissue as compared to the density and thermal conductivity of tumor tissue. This phenomena is also observed in the earlier work of Bischof et al. [12], If both phase lag times related to heat flux and temperature gradient are zero ($\tau_q = \tau_T = 0\,s$), DPL model reduces to parabolic bio-heat model which is also considered by Kumar et al. [60] and Kumar and Katiyar [69] in their previous work. It is also clear from the figures 3.1 and 3.2 that the freezing interfaces for DPL model move faster than the hyperbolic model but slower than the parabolic bio-heat model. That is, the time required to freeze the required region is minimum for parabolic while it is maximum for hyperbolic model.

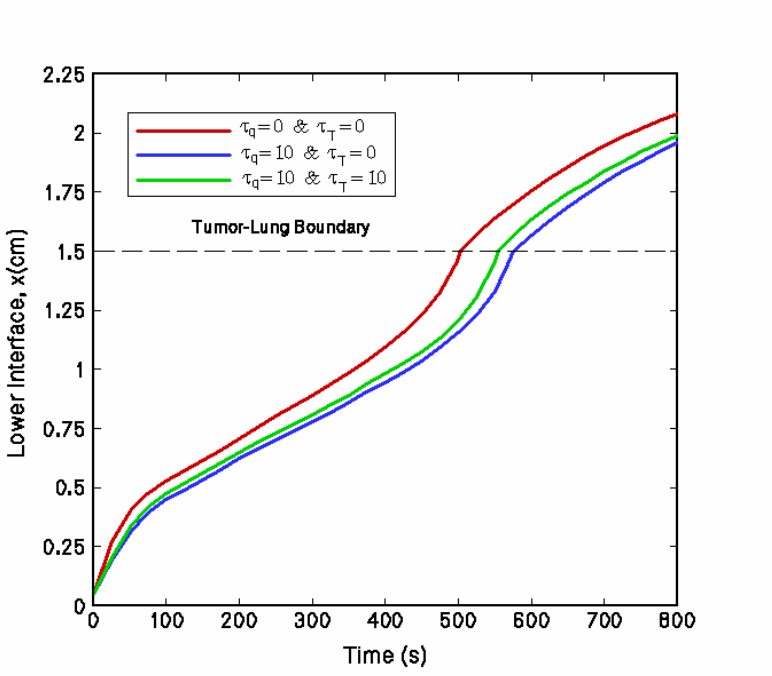

Figure 3.1: Position of lower interface during freezing versus time at *y* = 2.0 *cm* for DPL, parabolic and hyperbolic models.

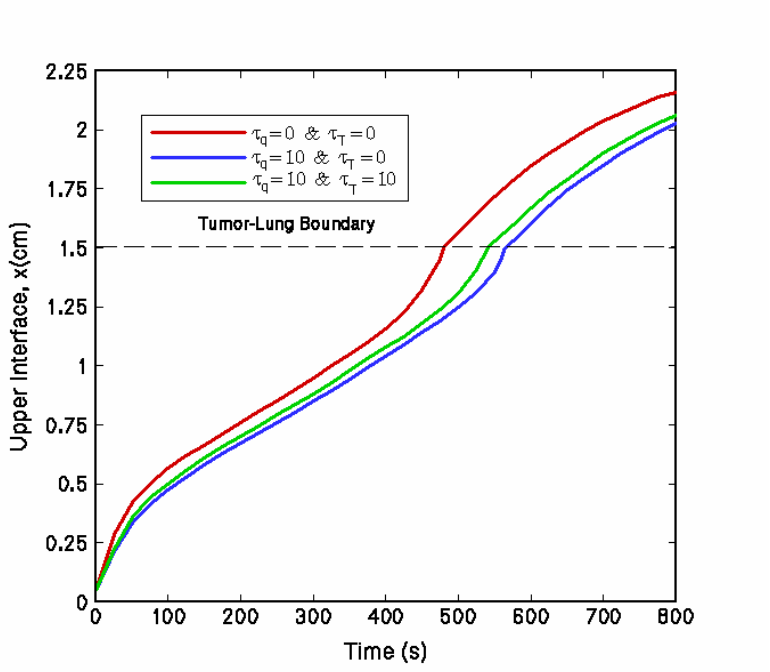

Figure 3.2: Position of upper interface during freezing versus time at y = 2.0 *cm* for DPL, parabolic and hyperbolic models.

Figures 3.3–3.5 show the temperature distribution in the subjected tissue at time, t = 200 *s*, 400 *s*, 600 *s* and 800 *s* for DPL, parabolic and hyperbolic models with respect to distance x and y for different values of phase lag in heat flux ($\tau_q = 0s, 5s, 10s$ and $15s$) and temperature gradient ($\tau_T = 0s, 5s$ and $10s$). Here, we have observed that in all the three models: DPL, parabolic and hyperbolic, after time t = 800 *s*, temperature of tumor tissue is much below the lethal temperature (-30 ^0C). In figures 3.3–3.5, it is also observed that the tissue temperature for DPL model is higher than the parabolic model and hyperbolic model has higher temperature than the DPL model. This implies that heat flow in the tissue is fastest in parabolic case and slowest for hyperbolic one.

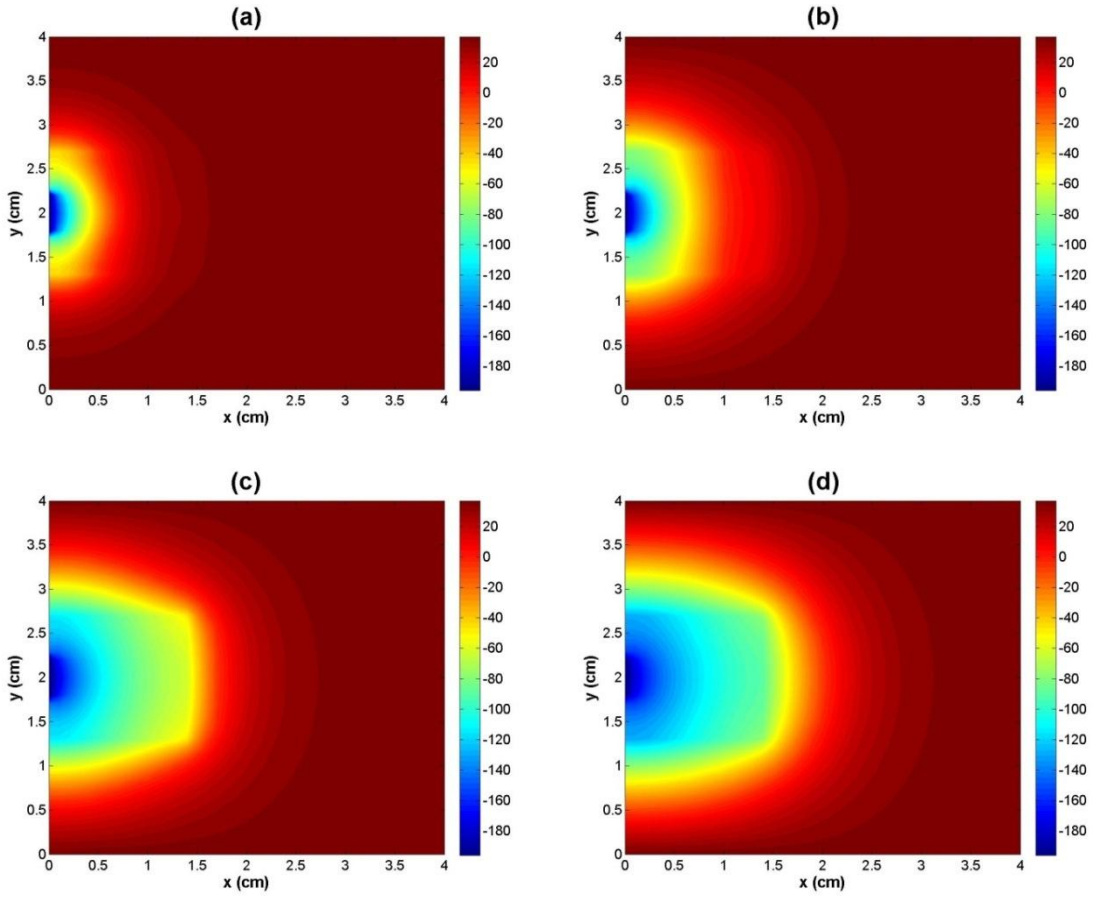

Figure 3.3: Temperature distribution along the tissue for DPL model ($\tau_q = 10\,s$ & $\tau_T = 10\,s$) at (a) t = 200 s, (b) t = 400 s, (c) t = 600 s and (d) t = 800 s.

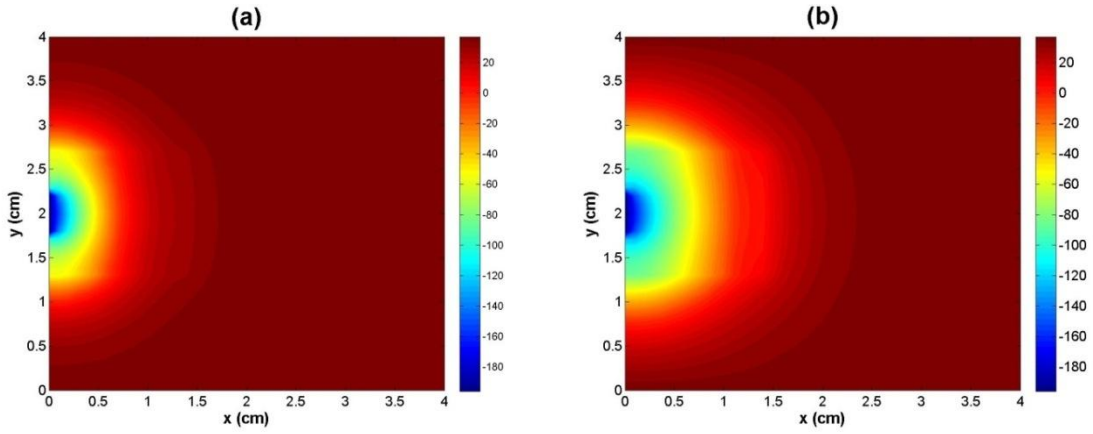

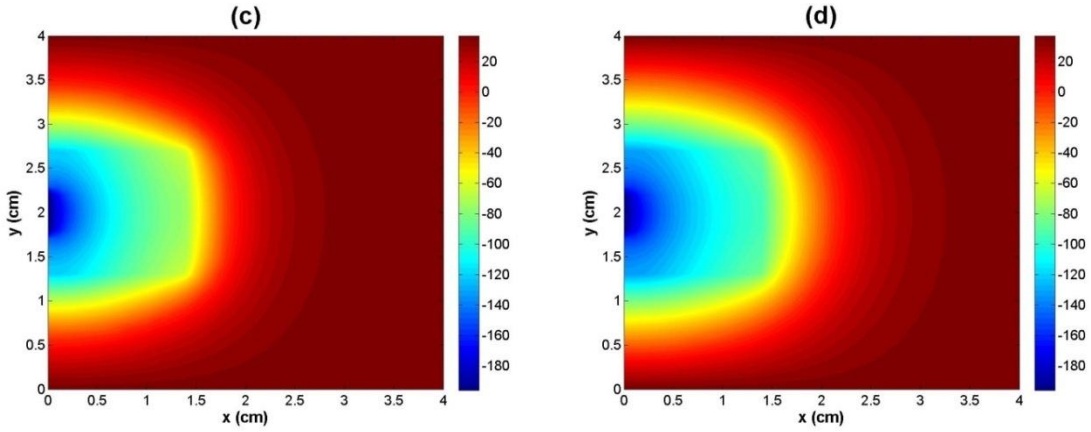

Figure 3.4: Temperature distribution along the tissue for parabolic model ($\tau_q = 0\,s$ & $\tau_T = 0\,s$) at (a) t = 200 s, (b) t = 400 s, (c) t = 600 s and (d) t = 800 s.

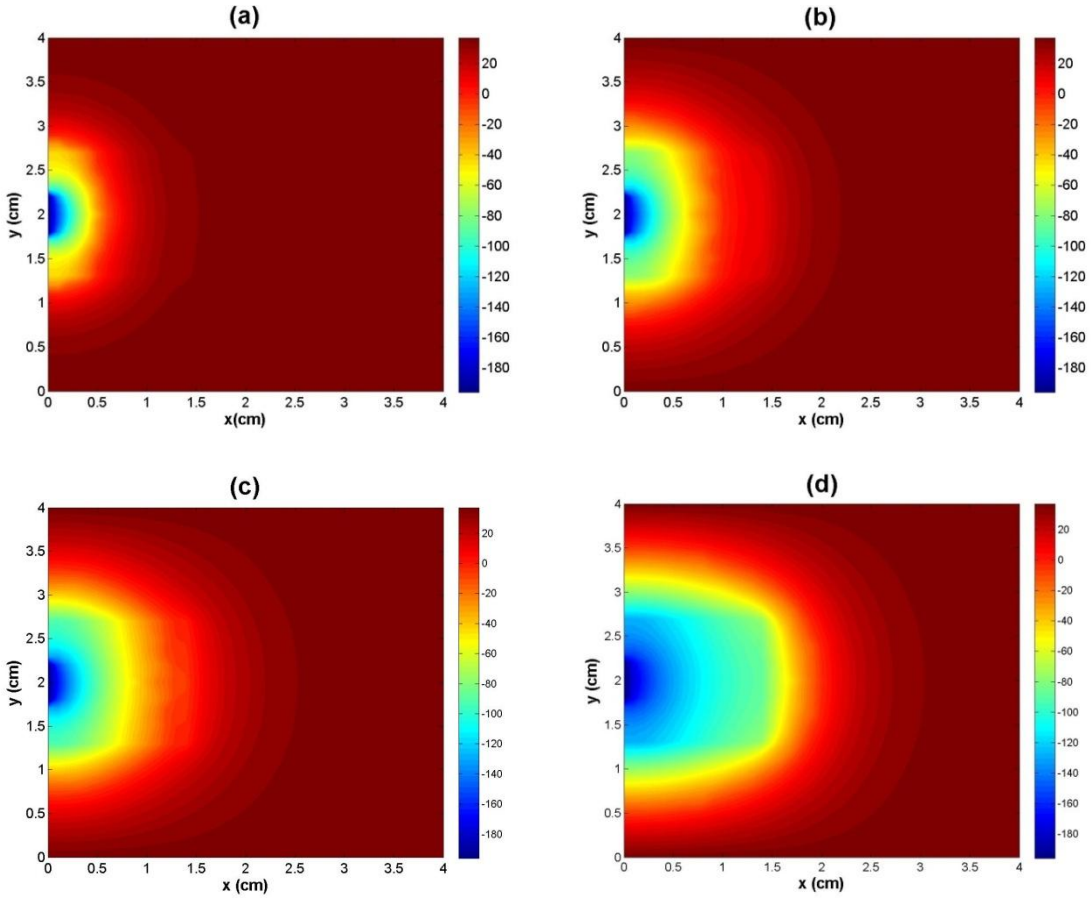

Figure 3.5: Temperature distribution along the tissue for hyperbolic model ($\tau_q = 10\,s$ & $\tau_T = 0\,s$) at (a) t = 200 s, (b) t = 400 s, (c) t = 600 s and (d) t = 800 s.

Figures 3.6–3.9 show the position of lower and upper freezing interfaces at time, t = 200 s, 400 s, 600 s and 800 s for DPL, parabolic and hyperbolic models with respect to distance x

and *y* for different values of phase lag in heat flux and temperature gradient. The direction of ice growth and ice ball history are clearly shown in figures 3.6–3.9.

From the results, it is observed that for parabolic model freezing process is fast as compare to the other two models i.e., DPL and hyperbolic model. Since the parabolic model is based on the classical Fourier's law so the thermal signal propagates through tissue without any delay. On the other hand for hyperbolic case at particular time *t* heat flux depends on the whole behavior of temperature gradient due to phase lag in heat flux. Therefore, freezing is slower for hyperbolic model than the parabolic model. In DPL model two phase lags τ_q and τ_T exist. Phase lag in temperature gradient (τ_T) consider the microstructural effect and accounts diffusion like behavior and the characters of thermal wave decay in DPL model due to the phase lag in heat flux (τ_q). Hence DPL model observed faster freezing than the hyperbolic model.

Position of lower and upper interfaces for DPL model at time *t* = 400 *s* and *t* = 600 *s* for a fixed value of phase lag in temperature gradient $\tau_T = 5s$ and different values of phase lag in heat flux, $\tau_q = 5s, 10s$ and $15s$ are shown in figures 3.10 and 3.11, respectively. It is observed that phase change interfaces for DPL model move faster with decreasing value of τ_q. The phase lag τ_q slows down the freezing velocity of thermal signals as it dominates the behavior of thermal wave propagation, hence freezing is fast for small value of τ_q.

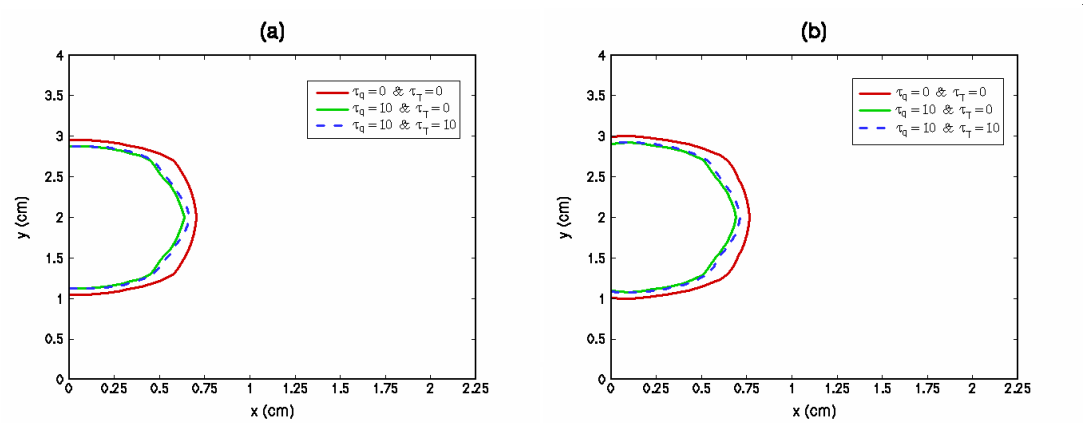

Figure 3.6: (a) Lower interface position and (b) Upper interface position for parabolic, hyperbolic and DPL model at *t* = 200 *s*.

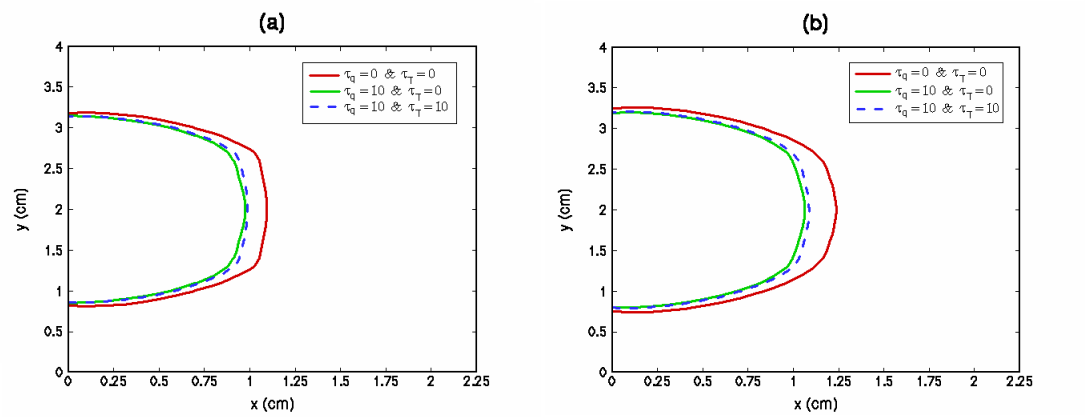

Figure 3.7: (a) Lower interface position and (b) Upper interface position for parabolic, hyperbolic and DPL model at t = 400 s.

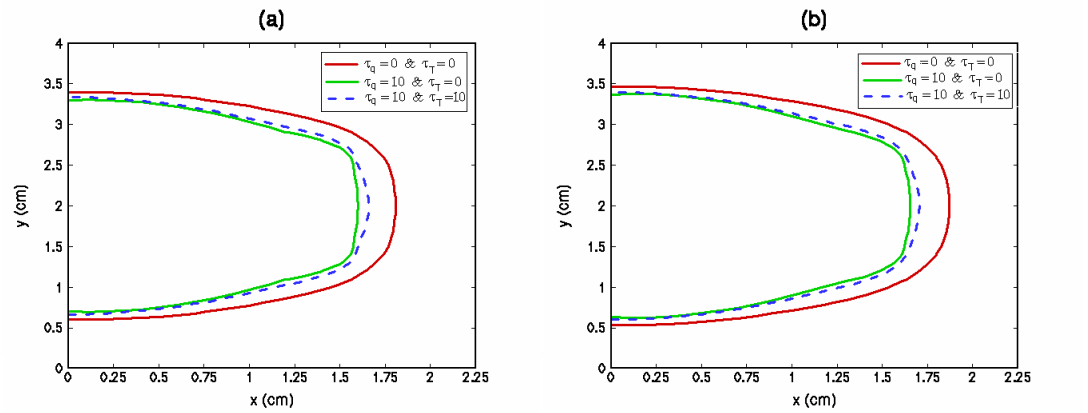

Figure 3.8: (a) Lower interface position and (b) Upper interface position for parabolic, hyperbolic and DPL model at t = 600 s.

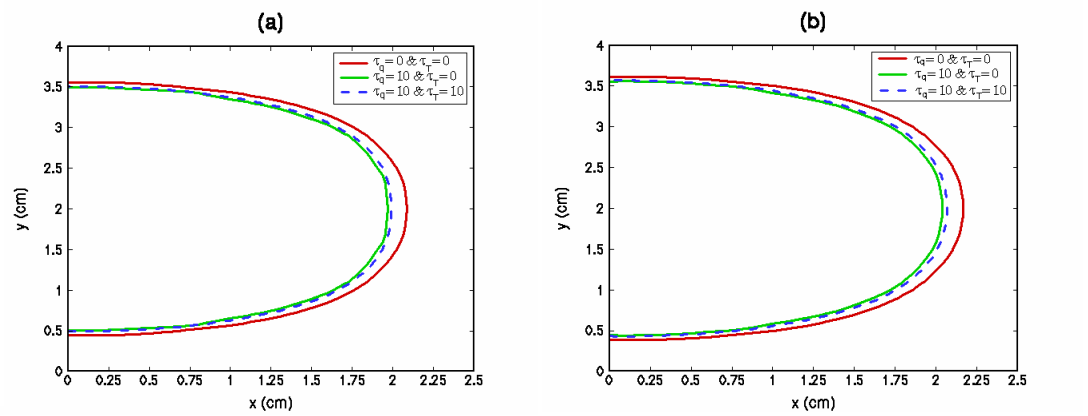

Figure 3.9: (a) Lower interface position and (b) Upper interface position for parabolic, hyperbolic and DPL model at t = 800 s.

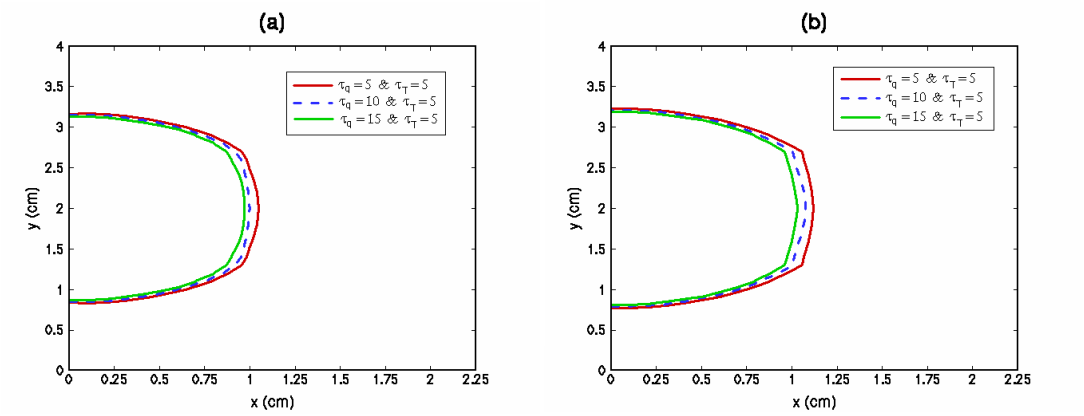

Figure 3.10: (a) Lower interface position and (b) Upper interface position for DPL model at t = 400 s for $\tau_q = 5s, 10s, 15s$ and $\tau_T = 5s$.

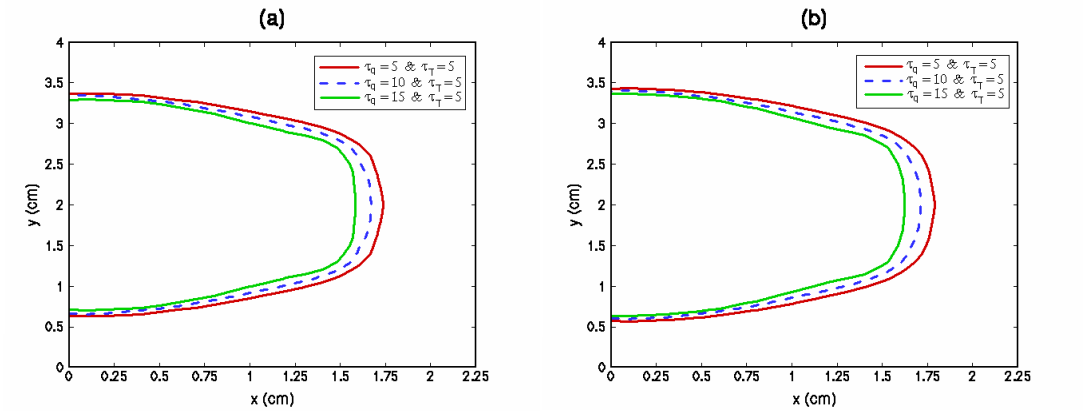

Figure 3.11: (a) Lower interface position and (b) Upper interface position for DPL model at t = 600 s for $\tau_q = 5s, 10s, 15s$ and $\tau_T = 5s$.

3.6 Conclusions

The Pennes bio-heat model is based on Fourier's law of heat conduction and it implies infinite speed of heat propagation which is unrealistic. Moreover, hyperbolic bio-heat model does not describe the microstructural interaction. Due to infinite speed and microstructural interaction effects, a dual phase lag model would be advantageous. By means of rigorous numerical experiments, it is found that the phase lags in temperature gradient and heat flux have significant effect on interface positions and temperature distribution. Phase change interfaces of three models, i.e., DPL, parabolic and hyperbolic accelerate at the lung-tumor boundary due to the change in thermo-physical properties of tissues and also the freezing interfaces for DPL case move faster than the hyperbolic case but slower than the parabolic one. It is observed that parabolic model gives lowest temperature in the tissue with comparison to DPL and hyperbolic model. The highest

temperature is obtained for hyperbolic model. It is also found in case of DPL model, at a fixed value of phase lag in temperature gradient and different values of phase lag in heat flux that the freezing is fast for small values of phase lag in heat flux.

Results obtained in this study regarding the phase change interface positions and temperature distribution in a lung tumor tissue may help in carrying out the cryosurgical treatment in lung cancer more effectively. Treatment can be optimized in a desired manner so that freezing process destroys only tumor tissue while the damage to neighboring normal lung tissues due to over freezing can be minimized.

Chapter 4

Three dimensional study on Freezing of Skin Tissue: A Three Layer Model

4.1 Introduction

Human skin is one of the main parts of the body. It plays various important roles such as thermoregulation, sensory, synthesis of vitamin D, host defense and insulation, etc. Thermoregulation is the most important among these roles, which works as protecting barrier between inner body and outside conditions. Skin is a composition of three layers namely, epidermis, dermis and subcutaneous. The exterior part of the skin is known as Epidermis which includes living as well as non-living cells. The thickness of this layer lies between 0.75-0.150 *mm* and is composed of keratinocytes (95%) and non-keratinocytes (5%) cells. Dermis is the second layer of skin whose thickness (0.001-0.004 *m*) is more than the epidermis layer. This layer plays the important function of thermoregulation and it contains blood vessels, nerves, lymph vessel, sebaceous and sweat glands. Subcutaneous fat is the third layer and composed of loose fatty connective tissue, major blood vessels and nerves. It is also known as hypodermis or subcutis. Hypodermis contains 50% of body fat. These layers help the skin to regulate body temperature. To cure diseased skin tissue, different thermal therapeutic treatments have been used in medicine [152]. The objective of all these treatments is to stimulate thermal injury accurately without affecting the neighboring healthy tissues.

Basically, heat transfer within skin tissue takes place through conduction mode combined with physiological process such as sweating, circulation of blood and metabolism, etc. There are several applications like cryosurgery, cryopreservation, cancer hyperthermia, skin cancer and burn injury evaluation, etc., in which heat transfer has been used [101, 102, 128-130, 133, 136, 153-154].In literature, many studies are available in which hyperbolic bio-heat conduction model has been used [1, 52, 77, 81-82, 163]. Deng and Liu [28] have numerically investigated the thermal stress and phase change behavior in skin tissue during freezing using the hyperbolic bio-heat model. In their results they have shown that thermal stress is maximum for large value of relaxation time. They have not considered the discontinuity in temperature at the phase change interface. To

investigate the temperature distribution in a biological tissue with different heating source under relaxation time, an analytical study is made by Shit and Bera [133]. The authors have analyzed the effect of different heating source both qualitatively and quantitatively. To describe the non-Fourier effect in the tissue during freezing a one dimensional hyperbolic model was discussed by Ahamdikia and Moradi [2]. They have used isothermal and non-isothermal phase change models in solidification procedure in vitro and vivo study. Mitra et al. [92] experimentally investigated the nature of heat propagation in processed meat using hyperbolic heat conduction model. They obtained that for processed meat the value of relaxation time is of the order of 15s.

Singh and Kumar [135] have proposed a hyperbolic bio-heat model to examine the effect of relaxation time for heat flux in triple layer skin tissue during freezing. They have restricted for one-dimensional model. Since the skin tissue is multi dimensional in nature. Therefore to be more realistic, an extended analysis has been performed. In this chapter, we have considered a three-dimensional hyperbolic bio-heat model with blood perfusion, metabolic heat generation and non-ideal property of tissue to investigate the freezing behavior in triple layer skin tissue. The complexity of the problem is due to moving interface, temperature discontinuity at the interface of solid-liquid and triple layer skin tissue which has different thermal properties in different layers. The finite difference method is adopted to study the effect of relaxation time on the motion of freezing front and temperature distribution in skin tissue. It is noted that relaxation time has significant effect on phase change interfaces and temperature distribution.

4.2 Problem Description

The problem considered a triple layer skin tissue of dimension $x_1 \times y_1 \times z_1$ (x_1=0.01208 m, y_1 = 0.002 m and z_1 = 0.001 m) and the dimension of epidermis, dermis and subcutaneous fat layers are $l_1 \times y_1 \times z_1$, $(l_2 - l_1) \times y_1 \times z_1$ and $(l - l_2) \times y_1 \times z_1$, respectively, which is shown in figure 4.1 [136]. where, l_1 = 0.00008 m, $(l_2 - l_1)$ = 0.002 m and $(l_2 - l_1)$ = 0.01 m.

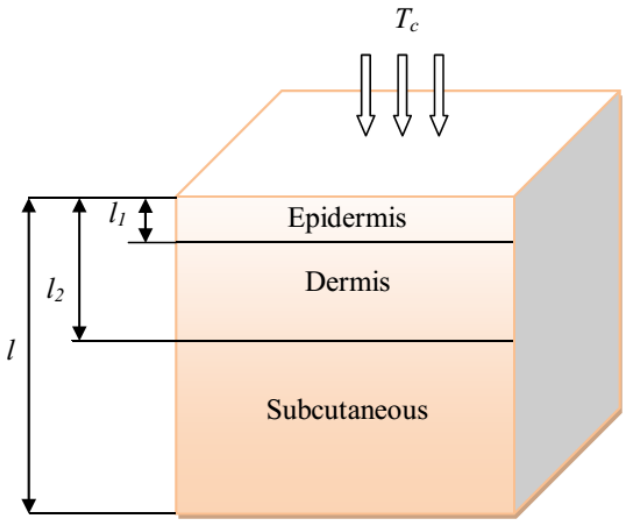

Figure 4.1: Physical sketch of triple layer skin tissue.

4.3 Mathematical Formulation

4.3.1 Assumptions

We consider the following assumptions to solve the three-dimensional hyperbolic bio-heat model.

- Heat transfer follows the non-Fourier's heat conduction.
- Initial temperature of tissue is considered as arterial temperature (37 ^0C).
- The upper and lower phase change interface occurs at temperatures -1 ^0C and -8 ^0C respectively [68, 114].
- The blood perfusion and metabolic heat generation are uniform through time and space. These phenomena vanish, however, in the frozen and in the mushy regions.
- In both frozen and unfrozen regions the thermal properties of skin layers are different and temperature dependent [53, 115].
- Specific heat and thermal conductivity for all layers are same in frozen region.

4.3.2 Governing Equations

The governing equations of 3D hyperbolic model for skin tissue in frozen and unfrozen regions are given below

$$\tau_q(\rho_p)_f(c_p)_f\frac{\partial^2(T_p)_f}{\partial t^2}+(\rho_p)_f(c_p)_f\frac{\partial(T_p)_f}{\partial t}=(k_p)_f\left(\frac{\partial^2(T_p)_f}{\partial x^2}+\frac{\partial^2(T_p)_f}{\partial y^2}+\frac{\partial^2(T_p)_f}{\partial z^2}\right), \tag{4.1}$$

$$\tau_q(\rho_p)_u(c_p)_u\frac{\partial^2(T_p)_u}{\partial t^2}+\left\{(\rho_p)_u(c_p)_u+\tau_q(\rho_b w_b)_p c_b\right\}\frac{\partial(T_p)_u}{\partial t}$$
$$=(k_p)_u\left(\frac{\partial^2(T_p)_u}{\partial x^2}+\frac{\partial^2(T_p)_u}{\partial y^2}+\frac{\partial^2(T_p)_u}{\partial z^2}\right)+(\rho_b w_b)_p c_b\left\{T_b-\left(T_p\right)_u\right\}+Q_{mp}, \tag{4.2}$$

In the above equations, subscripts p = e, d and s stand for epidermis, dermis and subcutaneous, respectively.

The conditions at interface are

$$(k_p)_f\frac{\partial\left\{(T_p)_f(S(t),t)\right\}}{\partial n}-(k_p)_u\frac{\partial\left\{(T_p)_u(S(t),t)\right\}}{\partial n}=\rho_p L v_n+\tau\rho_p L\dot{v}_n, \tag{4.3}$$

$$\left\{(T_p)_f(S(t),t)\right\}=\left\{(T_p)_u(S(t),t)\right\}=T_{ph}, \tag{4.4}$$

where, $v_n=\frac{\partial S(t)}{\partial t}$ and $\dot{v}_n=\frac{\partial^2 S(t)}{\partial t^2}$, n is the unit outward normal, L is the latent heat of fusion.

We consider enthalpy formulation to avoid the discontinuity of temperature at phase change interface and unknown position of the solid-liquid interface. Defining enthalpy $H(T)=\int_{T_r}^{T}cdT$, equations (4.1) - (4.4) reduce to a single equation as

$$\tau_q\rho_p\frac{\partial^2 H_p}{\partial t^2}+\left(\rho_p+\frac{\tau_q(\rho_b w_b)_p c_b}{c_p}\right)\frac{\partial H_p}{\partial t}=k_p\left(\frac{\partial^2 T_p}{\partial x^2}+\frac{\partial^2 T_p}{\partial y^2}+\frac{\partial^2 T_p}{\partial z^2}\right)$$
$$+(\rho_b w_b)_p c_b(T_b-T_p)+Q_{mp}. \tag{4.5}$$

The relation between tissue temperature and enthalpy is given as [13, 47].

$$H_p=\begin{cases}(c_p)_f(T_p-T_{ms}) & T_p<T_{ms}\\ (T_p-T_{ms})\left\{\frac{(c_p)_f+(c_p)_u}{2}+\frac{L}{(T_{ml}-T_{ms})}\right\} & T_{ms}\le T_p\le T_{ml}\\ L+\left\{\frac{(c_p)_f+(c_p)_u}{2}\right\}(T_{ml}-T_{ms})+(c_p)_u(T_p-T_{ml}) & T_p>T_{ml}\end{cases}. \tag{4.6}$$

4.3.3 Initial and Boundary Conditions

Here x_1= 0.01208 m, y_1 = 0.002 m and z_1 = 0.001 m.

(a) Initial conditions

At $t = 0$,

$$T_p(x, y, z, 0) = T_0 \qquad \text{and} \qquad \left.\frac{\partial T_p(x, y, z, t)}{\partial t}\right|_{t=0} = 0$$

where, $0 \le x \le x_1;\ 0 \le y \le y_1;\ 0 \le z \le z_1$.

(b) Boundary conditions

(i) At $x = 0$ plane, i.e., $(0 \le y \le y_1;\ 0 \le z \le z_1)$

$$T_e(0, y, z, t) = T_c = -196\ ^0C$$

where, T_c is the cryoprobe temperature.

(ii) At $x = l$ plane, $\left.\frac{\partial T_p(x, y, z, t)}{\partial x}\right|_{x=l} = 0.$

(iii) At $y = 0$ plane, $\left.\frac{\partial T_p(x, y, z, t)}{\partial y}\right|_{y=0} = 0$ and

at $y = y_1$ plane, $\left.\frac{\partial T_p(x, y, z, t)}{\partial y}\right|_{y=y_1} = 0.$

(iv) At $z = 0$ plane, $\left.\frac{\partial T_p(x, y, z, t)}{\partial z}\right|_{z=0} = 0$ and

at $z = z_1$ plane, $\left.\frac{\partial T_p(x, y, z, t)}{\partial z}\right|_{z=z_1} = 0.$

(v) At interface boundary of epidermis and dermis, i.e., $x = l_1$ and $0 \le y \le y_1;\ 0 \le z \le z_1$.

$$k_e \left.\frac{\partial T_e(x, y, z, t)}{\partial x}\right|_{x=l_1} = k_d \left.\frac{\partial T_d(x, y, z, t)}{\partial x}\right|_{x=l_1}$$

$$T_e(l_1, y, z, t) = T_d(l_1, y, z, t).$$

(vi) At interface boundary of dermis and subcutaneous, i.e., $x = l_2$ and $0 \le y \le y_1;\ 0 \le z \le z_1$.

$$k_d \left.\frac{\partial T_d(x,y,z,t)}{\partial x}\right|_{x=l_2} = k_s \left.\frac{\partial T_s(x,y,z,t)}{\partial x}\right|_{x=l_2}$$
$$T_d(l_2,y,z,t) = T_s(l_2,y,z,t).$$

4.4 Numerical Solution

Explicit finite difference scheme is used to solve equation (4.5). Considering $x_i = i\delta x,\ y_j = j\delta y,\ z_k = k\delta z\ (\delta x = \delta y = \delta z)\ and\ t_n = n\delta t$, where i, j, k and n are the space and time index, respectively; $\delta x, \delta y, \delta z$ and δt are the grid spacing along *x*-axis, *y*-axis, *z*-axis and time respectively. Enthalpy at $(n+1)^{th}$ time level is given by

$$\begin{aligned}(H_p)_{ijk}^{n+1} &= \left(1+\frac{A_{ijk}^n}{A_{ijk}^n+B_{ijk}^n}\right)(H_p)_{ijk}^n - \left(\frac{A_{ijk}^n}{A_{ijk}^n+B_{ijk}^n}\right)(H_p)_{ijk}^{n-1} \\ &+\left(\frac{D_{ijk}^n}{A_{ijk}^n+B_{ijk}^n}\right)\left\{(T_p)_{i+1,j,k}^n+(T_p)_{i-1,j,k}^n+(T_p)_{i,j+1,k}^n+(T_p)_{i,j-1,k}^n+(T_p)_{i,j,k+1}^n\ldots\right. \\ &\left.+(T_p)_{i,j,k-1}^n-6(T_p)_{i,j,k}^n\right\}+\left(\frac{E_{ijk}^n}{A_{ijk}^n+B_{ijk}^n}\right)\left\{T_b-(T_p)_{i,j,k}^n\right\}+(Q_{mp})_{ijk}^n,\end{aligned} \tag{4.7}$$

where,

$$A_{ijk}^n=\frac{\tau(\rho_p)_{ijk}^n}{(\Delta t)^2};\ \ B_{ijk}^n=\left[\frac{(\rho_p)_{ijk}^n}{(\Delta t)}+\frac{\tau(\rho_b w_b)_p c_b}{(c_p)_{ijk}^n(\Delta t)}\right];\ D_{ijk}^n=\frac{(k_p)_{ijk}^n}{(\Delta x)^2};\ E_{ijk}^n=\left\{(\rho_b w_b)_p\right\}_{ijk}^n c_b.$$

Equation (4.7) can be re-written in the following form:

$$\begin{aligned}(H_p)_{ijk}^{n+1} &= (1+U_{ijk}^n)(H_p)_{ijk}^n - U_{ijk}^n(H_p)_{ijk}^{n-1} \\ &+V_{ijk}^n\left\{(T_p)_{i+1,j,k}^n+(T_p)_{i-1,j,k}^n+(T_p)_{i,j+1,k}^n+(T_p)_{i,j-1,k}^n+(T_p)_{i,j,k+1}^n+(T_p)_{i,j,k-1}^n-6(T_p)_{i,j,k}^n\right\} \\ &+W_{ijk}^n\left\{T_b-(T_p)_{i,j,k}^n\right\}+Y_{ijk}^n.\end{aligned} \tag{4.8}$$

where,

$$Z_{ijk}^n=\frac{1}{A_{ijk}^n+B_{ijk}^n};\ \ U_{ijk}^n = A_{ijk}^n Z_{ijk}^n;\ V_{ijk}^n=D_{ijk}^n Z_{ijk}^n;\ W_{ijk}^n=E_{ijk}^n Z_{ijk}^n;\ Y_{ijk}^n=(Q_{mp})_{ijk}^n Z_{ijk}^n.$$

The grid size and time step is considered in such a way that the following stability criteria is satisfied,

$$\max\left[\frac{(\Delta t)^2\left\{6k_p+(\rho_b w_b)_p c_b(\Delta x)^2\right\}}{(\Delta x)^2\left\{2c_p\tau\rho_p+c_p\rho_p(\Delta t)+\tau(\rho_b w_b)_p c_b(\Delta t)\right\}},\frac{(\Delta t)^2\left\{6k_p+(\rho_b w_b)_p c_b(\Delta y)^2\right\}}{(\Delta y)^2\left\{2c_p\tau\rho_p+c_p\rho_p(\Delta t)+\tau(\rho_b w_b)_p c_b(\Delta t)\right\}},\frac{(\Delta t)^2\left\{6k_p+(\rho_b w_b)_p c_b(\Delta z)^2\right\}}{(\Delta z)^2\left\{2c_p\tau\rho_p+c_p\rho_p(\Delta t)+\tau(\rho_b w_b)_p c_b(\Delta t)\right\}}\right]\le 1$$

for numerical solution. After finding the enthalpy at $(n+1)^{th}$ time level, one can obtain the temperature at $(n+1)^{th}$ time level by reverting the equation (4.6) as follows:

$$T_p=\begin{cases}\dfrac{H_p}{(c_p)_f}+T_{ms} & H_p<0\\ \dfrac{2H_p(T_{ml}-T_{ms})}{\{(c_p)_f+(c_p)_u\}(T_{ml}-T_{ms})+2L}+T_{ms} & 0\le H_p\le L+\dfrac{1}{2}\{(c_p)_f+(c_p)_u\}(T_{ml}-T_{ms}).\\ \dfrac{H_p}{(c_p)_u}-\dfrac{L}{(c_p)_u}-\dfrac{\{(c_p)_f+(c_p)_u\}(T_{ml}-T_{ms})}{2(c_p)_u}+T_{ml} & H_p>L+\dfrac{1}{2}\{(c_p)_f+(c_p)_u\}(T_{ml}-T_{ms})\end{cases} \tag{4.9}$$

Isotherms at -8^0C and -1^0C show the position of lower and upper phase change interfaces respectively.

4.4.1 Numerical Code Validation

The 3D hyperbolic model reduces to the 1D hyperbolic model at $y=z=0$. A validation of numerical code is made by comparing our particular results with the published results [135]. Results for interface positions are compared at relaxation time for heat flux, $\tau_q=1s$. Table 4.1 shows the comparison of present and published results. It can be seen that the agreement is good.

Table 4.1: Comparison between published and present results at $\tau_q=1s$.

	Published results [135]		**Present results**	
Time (s)	Upper Interface (m)	Lower Interface (m)	Upper Interface (m)	Lower Interface (m)
50	0.0043	0.0040	0.0043	0.0039
100	0.0062	0.0059	0.0063	0.0059
150	0.0077	0.0073	0.0078	0.0072
200	0.0089	0.0085	0.0090	0.0084
250	0.0102	0.0098	0.0102	0.0097

4.5 Results and Discussion

Results in this section illustrate the effects of relaxation time for heat flux on interfaces of phase change and temperature distribution during freezing process of triple layer skin tissue. The values of thermo-physical properties of skin tissue are given in Table 4.1 [136, 160]. $\tau_q = 0\text{s}, 1\text{s}, 3\text{s}$ and 5s are the values of relaxation time for heat flux, which are taken for the present study [28, 77]. Numerical simulations were carried out for grid space of $dx = dy = dz = 0.00004\,m$ and time step of $dt = 0.002\,s$.

At time $t = 0$, the cryogenic probe temperature is set equal to the freezing temperature T_c. As a result, heat is transferred from the diseased tissue to the cryoprobe. The temperature of the tissue decreases rapidly and starts freezing on the surface of the cryoprobe. As time passes, the thickness of the frozen layer increases. The freezing procedure continues until the entire layer of diseased tissue has been deeply frozen and its tumor cells destroyed. Figures 4.2 – 4.4 show the 3D temperature distribution in the skin tissue for hyperbolic bio-heat model at time, t = 100 s, 200 s and 300 s. Initially, the skin tissue does not freeze completely. The whole skin tissue freeze as time proceeds. This is due to the significant difference between the thermal conductivity and diffusivity of skin tissue in the frozen and unfrozen regions as in frozen region conductivity and diffusivity are high as compared to the unfrozen region.

Table 4.2: Thermo-physical properties of triple layer skin tissue [136, 160]

Thermal parameters	Units	Values of three layers		
		Epidermis	Dermis	Subcutaneous
Density in frozen region	kg/m^3	921.00	921.00	921.00
Density in unfrozen region	kg/m^3	1200	1200	1000
Thermal conductivity in frozen region	W/m ^0C	2.0	2.0	2.0
Thermal conductivity in unfrozen region	W/m ^0C	0.26	0.52	0.21
Specific heat in frozen region	J/kg ^0C	1800	1800	1800
Specific heat in unfrozen region	J/kg ^0C	3600	3400	3060
Latent heat	kJ/kg	250.00	250.00	250.00
Metabolic heat generation	W/m^3	0	2500.00	2500.00
Blood perfusion rate	kg/ m^3	0	0.5	0.5
Thickness of layer	m	0.00008	0.002	0.01
Specific heat of blood	J/kg ^0C	3770		
Arterial temperature	^0C	37		

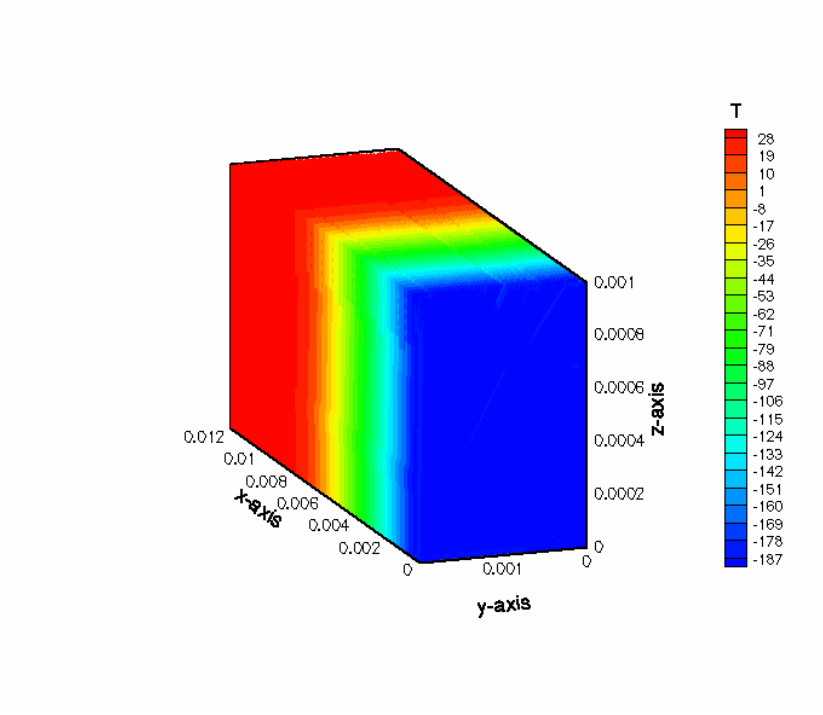

Figure 4.2: Temperature distribution along the skin tissue for relaxation time ($\tau_q = 1s$) at t =100 s.

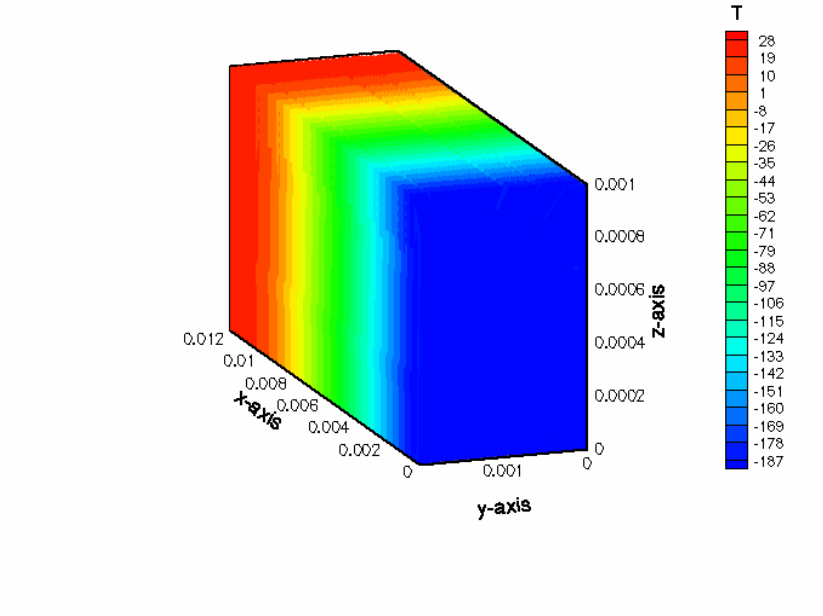

Figure 4.3: Temperature distribution along the skin tissue for relaxation time ($\tau_q = 1s$) at t =200 s.

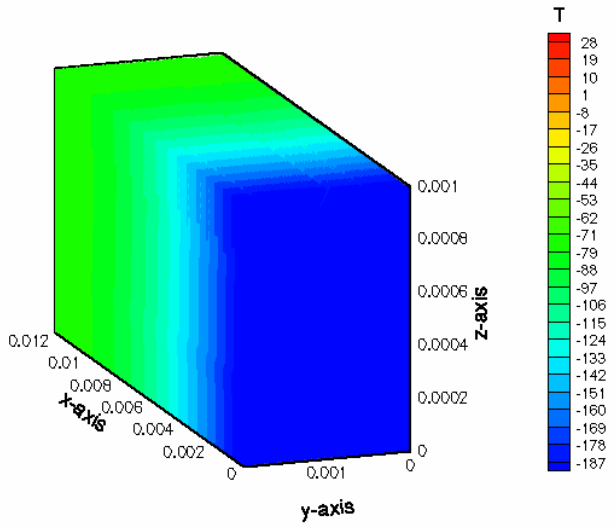

Figure 4.4: Temperature distribution along the skin tissue for relaxation time ($\tau_q = 1s$) at t =300 s.

Temperature distribution along the surface of skin tissue (at z = 0m) for different values of relaxation time for heat flux at different time, t = 100 s, 200 s and 300 s are given in figures 4.5 – 4.8. It is also observed that the tissue temperature increases with an increase in relaxation time for heat flux. The comparative study for hyperbolic and parabolic bio-heat models shows that the highest temperature for the hyperbolic case and lowest for the parabolic case occurs at the same time. A qualitative explanation of tissue temperature is given as: diffusion of heat into the skin tissue is much faster for low relaxation time, hence tissue freezes at a rapid rate and its temperature decreases quickly.

(a)

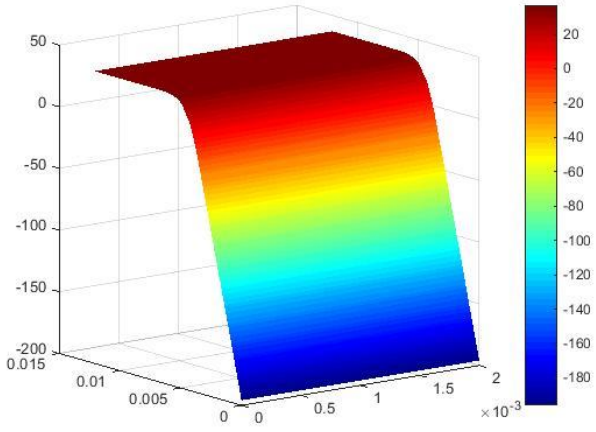

(b)

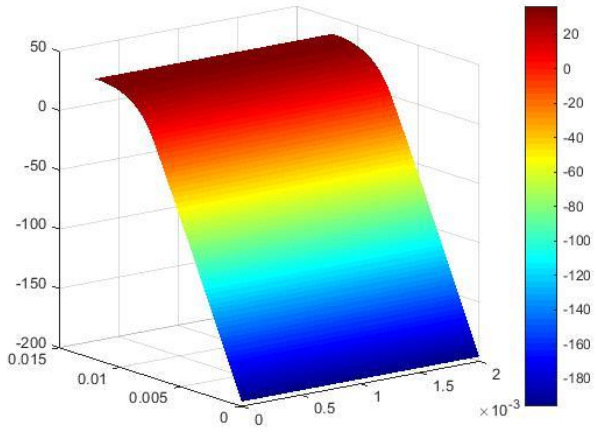

(c)

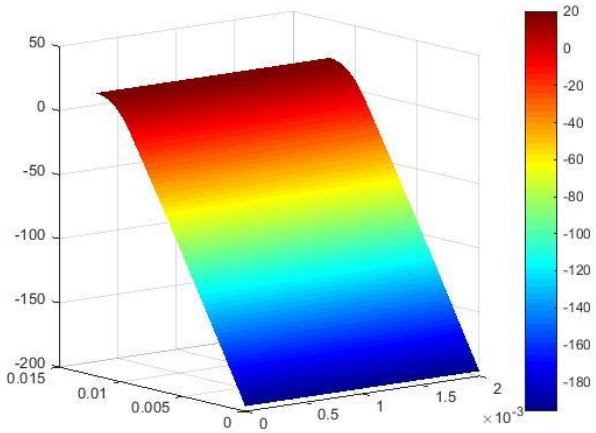

Figure 4.5: Temperature distribution along the skin tissue at z = 0 m for relaxation time ($\tau_q = 5\,s$) at time (a) t =100 s, (b) t =200 s and (c) t =300 s.

(a)

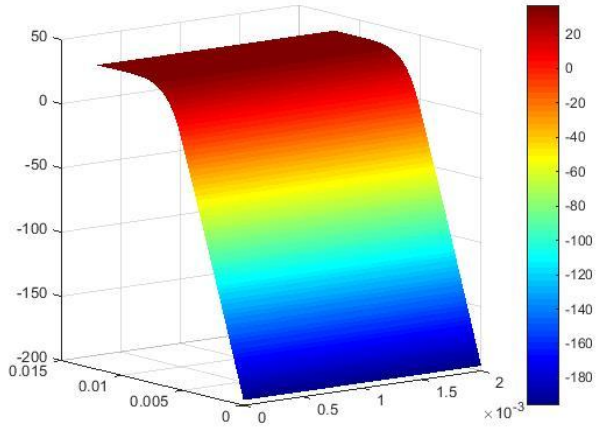

(b)

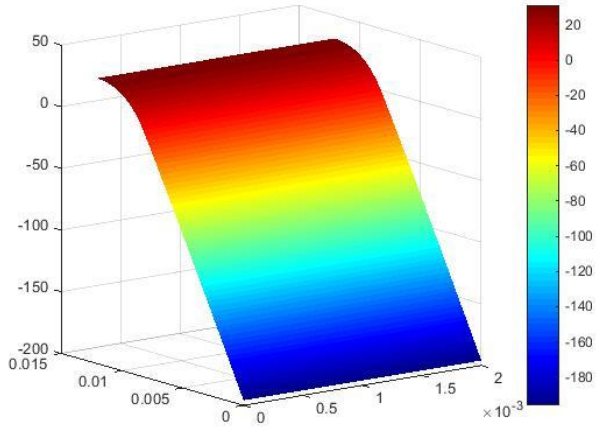

(c)

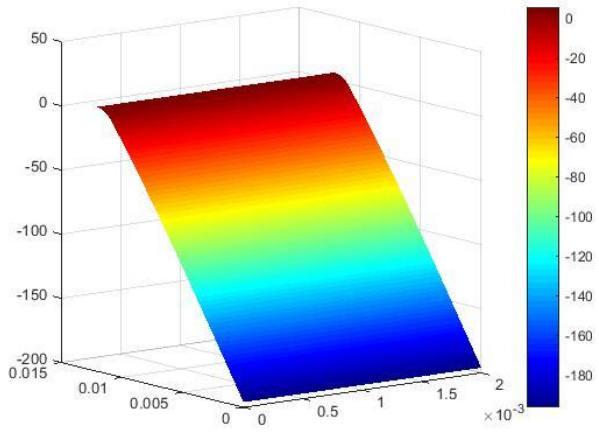

Figure 4.6: Temperature distribution along the skin tissue at z = 0 m for relaxation time ($\tau_q = 3s$) at time (a) t =100 s, (b) t =200 s and (c) t =300 s.

(a)

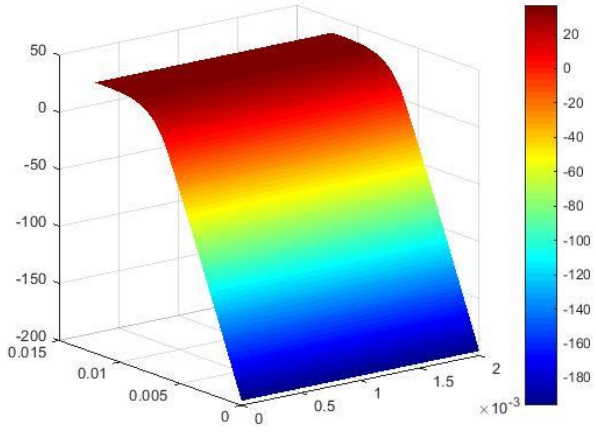

(b)

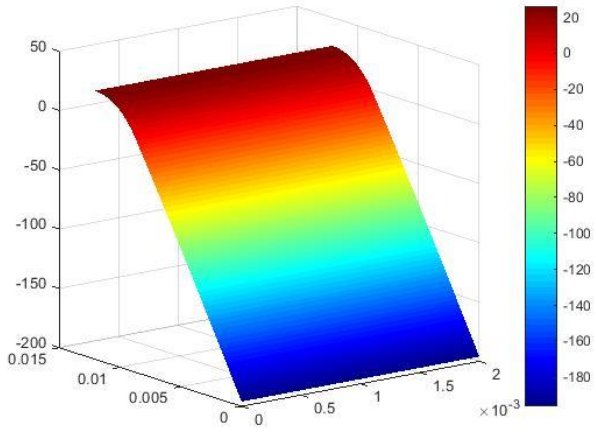

(c)

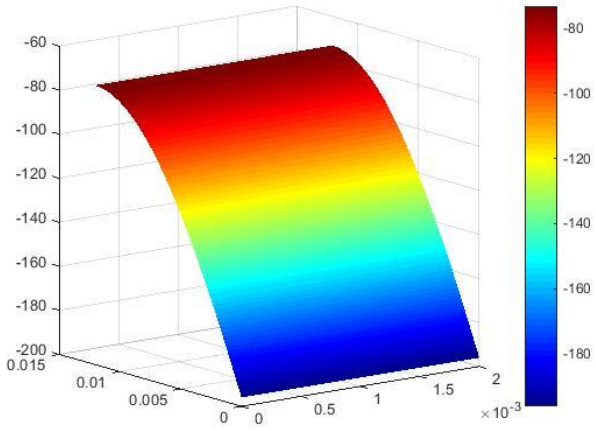

Figure 4.7: Temperature distribution along the skin tissue at $z = 0$ *m* for relaxation time ($\tau_q = 1\text{s}$) at time (a) $t = 100$ *s*, (b) $t = 200$ *s* and (c) $t = 300$ *s*.

(a)

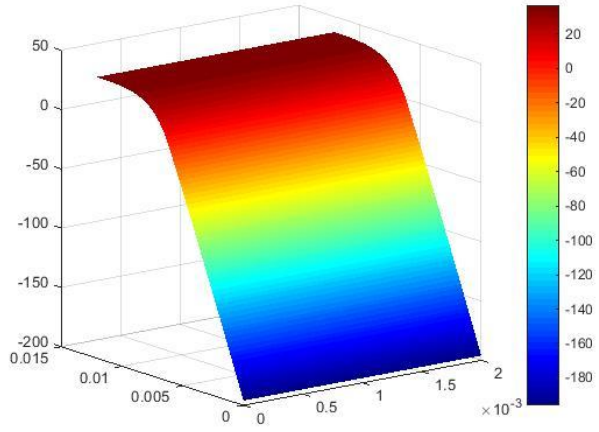

(b)

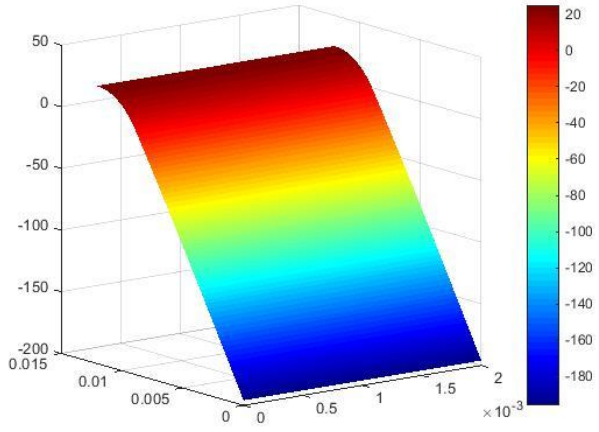

(c)

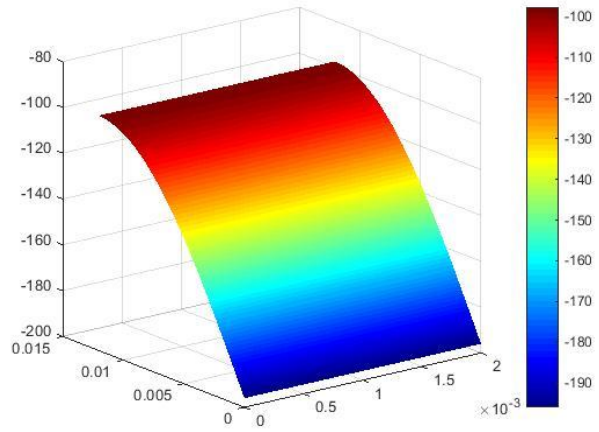

Figure 4.8: Temperature distribution along the skin tissue at z = 0 m for relaxation time ($\tau_q = 0\,s$) at time (a) t =100 s, (b) t =200 s and (c) t =300 s.

Since the triple layer skin tissue is a non-ideal material, phase change occurs over a specific range with upper phase change at temperature -1 ^0C and lower phase change at temperature -8 ^0C. Figures 4.9 and 4.10 show the position of phase change interfaces versus time during the freezing process in *x*-direction at $y = 0$ *m* and $z = 0$ *m* for different values of τ_q. How the relaxation time affects the freezing positions is examined in figures 4.9 and 4.10. The slope of freezing position decreases with an increase in time and also the temperature gradient becomes smaller due to an increase in distance from the cooling boundary.

The total time required to cover the entire tissue at $\tau_q = 0s, 1s, 3s$ and $5s$ for upper phase change interface are t = 257 *s*, 268 *s*, 303 *s* and 332 *s* and for lower phase change interface are t = 272 *s*, 283 *s*, 311 *s* and 354 *s*, respectively. This shows that total time required to cover the whole tissue for both upper and lower interfaces increases with increasing value of relaxation time. In this situation behavior of thermal signal propagation is controlled by relaxation time and fast freezing process observed for small values of relaxation time. Therefore, we can say that the motion of phase change interface position is slow for hyperbolic model as compared to the parabolic model.

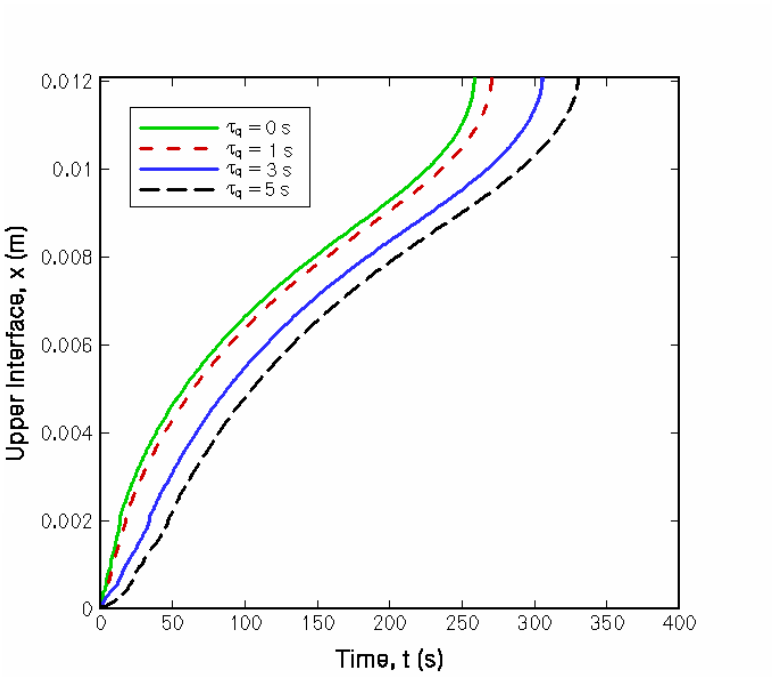

Figure 4.9: Position of upper interface during freezing versus time at $y = 0$ *m* and $z = 0$ *m* for $\tau_q = 0s, 1s, 3s$ and $5s$.

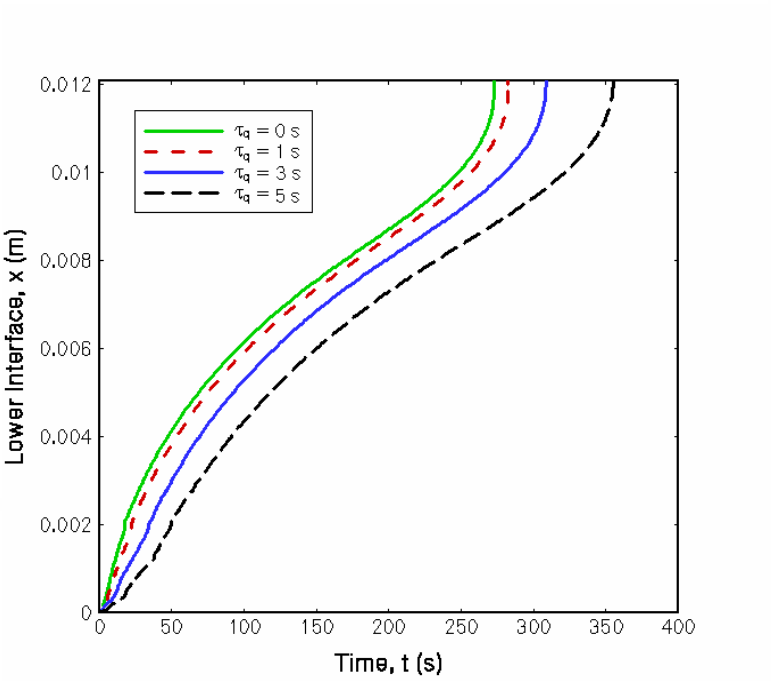

Figure 4.10: Position of lower interface during freezing versus time at $y = 0$ *m* and $z = 0$ *m* for $\tau_q = 0s, 1s, 3s$ and $5s$.

The above results show that freezing process is slower in hyperbolic bio-heat model than parabolic model. Since the parabolic model is based on the classical Fourier's law of heat conduction, which assumes that the propagation speed of heat is infinite, i.e., heat passes through skin tissue without any delay. On the other hand, for the hyperbolic case at certain time *t* heat flux depends upon the complete history of temperature gradient. Due to relaxation time of heat flux, heat transfer takes place into skin tissue with delay. Therefore, freezing for parabolic bio-heat model is faster than the hyperbolic model.

4.6 Conclusions

In this work we have studied numerically the freezing procedure during cryosurgery in triple layer skin tissue using three-dimensional hyperbolic bio-heat model. We have more emphasis on the effect of relaxation time parameter for heat flux on interfaces of phase change and temperature profiles. Our study for hyperbolic and parabolic models conclude that the total time required for freezing the whole region is smaller in case of parabolic model as compared to the hyperbolic model. The non-Fourier effect becomes more dominant in case when the value of relaxation time for heat flux increases. Freezing interfaces accelerate with decreasing value of relaxation time for heat flux. If the value of

relaxation time for heat flux is kept small then the solution of hyperbolic model tends to the solution of the parabolic model.

As the triple layer skin tissue is multidimensional, so compared to 1D or 2D case, 3D model provided the more detailed and realistic information of triple layer skin tissue behavior. The knowledge of heat transfer phenomena in soft skin tissues has great importance and contribution to the variety of medical treatment.

Chapter 5

Three dimensional study on Dual Phase Lag Bio-heat Model for Triple Layer Skin Tissue Freezing

5.1 Introduction

Skin is the important part of our body and it helps to regulate the temperature of body and protects form pathogens, outdoor micro-organisms and excessive water loss. It functions thermally as a heat generator, transmitter, radiator, absorber, conductor and vaporizer. The thermal properties of skin vary in different layers.

Many researchers have used the dual phase lag model without phase change [80, 87, 159, 161-162]. Ziaei Poor et al. [164] have presented the analytic solution for dual phase lag bio-heat equation in skin tissue. In their study, they obtained a major discrepancy between the predicted temperatures of three bio-heat transfer models for high rate of heat flux. To study the transient heat transfer in skin tissue, an analytic solution of DPL model is given by Askarizadeh and Ahmadikia [7]. The obtained results show the importance of DPL model for the blood perfusion rate and prediction of thermal damage in skin tissue. Talukdar et al. [139] study the heat transfer effect in human skin tissue subjected to radiant heat exposure and high intensity flame using dual phase lag model. They have assumed that blood perfusion rate in skin layers is temperature dependent. Their results are more realistic in comparison with the experimental analysis using Stoll's criterion. Kumar et al. [63] have numerically studied the bio-heat transfer during hyperthermia treatment using dual phase lag model. They have also compared the dual phase lag model with Thermal wave and Pennes bio-heat model and found that large differences in the temperature at the hyperthermia position and time to achieve the hyperthermia temperature exist, when the value of phase lag in temperature gradient is increases.

Liu et al. [79] have also used DPL model to describe the non-Fourier heat conduction in tissue. Their results show that the inverse method can overcome the difficulties from the non-Fourier inverse heat conduction problem. Nobrega and Coelho [105] have used three bio-heat models to study the thermal therapy of skin tissue and

predicted that all three models have meaningful difference in thermal damage and temperature distribution. They showed that bio-heat model is more effective in comparison with laser effect modeling and thermal damage is higher for thermal wave model and lower in case of DPL model.

The present study is an extension of Singh and Kumar [136] in which they have considered one-dimensional DPL bio-heat model and analyze the freezing effect in triple layer skin tissue. Here, in this chapter we have taken three-dimensional model to study the effects of phase lags of temperature gradient and heat flux on temperature distribution and interface positions in skin tissue. The model includes the discontinuity of temperature at the solid-liquid interface using the enthalpy formulation. The finite difference method is used to solve the enthalpy formulation of the dual phase lag bio-heat equation. The effects of both the phase lags on temperatures profile and interface positions have been studied. A comparative investigation of three different models (DPL, hyperbolic and parabolic bio-heat models) is also presented.

5.2 Problem Description

Figure 4.1 illustrates a schematic diagram of a triple layer skin tissue of dimension $x_1 \times y_1 \times z_1$ and the dimension of three layers, i.e., epidermis, dermis and subcutaneous are $l_1 \times y_1 \times z_1$, $(l_2 - l_1) \times y_1 \times z_1$ and $(l - l_2) \times y_1 \times z_1$, respectively, where, $l_1 = 0.00008\ m$, $(l_2 - l_1) = 0.002\ m$ and $(l_2 - l_1) = 0.01\ m$.

5.3 Mathematical Formulation

The prediction of the temperature distribution and freezing process that take place inside the skin tissue is carried out with a three-dimensional dual phase lag model that is based on the following assumptions:

- Heat transfer follows the non-Fourier's heat conduction.
- Initial temperature of tissue is considered as arterial temperature (37 ^0C).
- The upper and lower phase change interface occurs at temperatures -1 ^0C and -8 ^0C respectively [68, 114].

- The blood perfusion and the metabolic heat generation are uniform through time and space. These phenomena vanish, however, in the frozen and in the mushy regions.
- In both frozen and unfrozen regions the thermal properties of skin layers are different and temperature dependent [53, 115].
- Specific heat and thermal conductivity for all layers are same in frozen region.

5.3.1 Governing Equations

The governing equations of three-dimensional dual phase lag model for both frozen and unfrozen regions are given as

$$\tau_q(\rho_p)_f(c_p)_f\frac{\partial^2(T_p)_f}{\partial t^2}+(\rho_p)_f(c_p)_f\frac{\partial(T_p)_f}{\partial t}=(k_p)_f\left(\frac{\partial^2(T_p)_f}{\partial x^2}+\frac{\partial^2(T_p)_f}{\partial y^2}+\frac{\partial^2(T_p)_f}{\partial z^2}\right)+\tau_T(k_p)_f\left(\frac{\partial^3(T_p)_f}{\partial t\partial x^2}+\frac{\partial^3(T_p)_f}{\partial t\partial y^2}+\frac{\partial^3(T_p)_f}{\partial t\partial z^2}\right), \tag{5.1}$$

$$\begin{aligned}&\tau_q(\rho_p)_u(c_p)_u\frac{\partial^2(T_p)_u}{\partial t^2}+\left\{(\rho_p)_u(c_p)_u+\tau_q(\rho_b w_b)_p c_b\right\}\frac{\partial(T_p)_u}{\partial t}\\&=(k_p)_u\left(\frac{\partial^2(T_p)_u}{\partial x^2}+\frac{\partial^2(T_p)_u}{\partial y^2}+\frac{\partial^2(T_p)_u}{\partial z^2}\right)+\tau_T(k_p)_u\left(\frac{\partial^3(T_p)_u}{\partial t\partial x^2}+\frac{\partial^3(T_p)_u}{\partial t\partial y^2}+\frac{\partial^3(T_p)_u}{\partial t\partial z^2}\right)\\&\quad+(\rho_b w_b)_p c_b\left\{T_b-\left(T_p\right)_u\right\}+Q_{mp},\end{aligned} \tag{5.2}$$

Conditions at phase change interface are

$$(k_p)_f\left(\frac{\partial(T_p)_f}{\partial n}+\tau_T\frac{\partial^2(T_p)_f}{\partial t\partial n}\right)-(k_p)_u\left(\frac{\partial(T_p)_u}{\partial n}+\tau_T\frac{\partial^2(T_p)_u}{\partial t\partial n}\right)=(\rho_p)_f L v_n+\tau_q(\rho_p)_f L\dot{v}_n, \tag{5.3}$$

$$\left\{(T_p)_f(S(t),t)\right\}=\left\{(T_p)_u(S(t),t)\right\}=T_{ph}, \tag{5.4}$$

Using enthalpy $H(T)=\int_{T_r}^{T}cdT$ where T_r is the reference value of temperature, enthalpy formulation of equations (5.1) – (5.4) gives

$$\begin{aligned}&\tau_q\rho_p\frac{\partial^2 H_p}{\partial t^2}+\left\{\rho_p+\frac{\tau_q(\rho_b w_b)_p c_b}{c_p}\right\}\frac{\partial H_p}{\partial t}=k_p\left(\frac{\partial^2 T_p}{\partial x^2}+\frac{\partial^2 T_p}{\partial y^2}+\frac{\partial^2 T_p}{\partial z^2}\right)\\&\quad+k_p\tau_T\left(\frac{\partial^3 T_p}{\partial t\partial x^2}+\frac{\partial^3 T_p}{\partial t\partial y^2}+\frac{\partial^3 T_p}{\partial t\partial z^2}\right)+(\rho_b w_b)_p c_b(T_b-T_p)+Q_{mp}.\end{aligned} \tag{5.5}$$

Enthalpy and tissue temperature are related as

$$H_p = \begin{cases} (c_p)_f (T_p - T_{ms}) & T_p < T_{ms} \\ (T_p - T_{ms}) \left\{ \dfrac{(c_p)_f + (c_p)_u}{2} + \dfrac{L}{(T_{ml} - T_{ms})} \right\} & T_{ms} \le T_p \le T_{ml} \\ L + \left\{ \dfrac{(c_p)_f + (c_p)_u}{2} \right\} (T_{ml} - T_{ms}) + (c_p)_u (T_p - T_{ml}) & T_p > T_{ml} \end{cases} . \qquad (5.6)$$

5.3.2 Initial and Boundary Conditions

(a) Initial conditions

At $t = 0$,

$$T_p(x, y, z, 0) = T_0 \quad \text{and} \quad \left. \frac{\partial T_p(x, y, z, t)}{\partial t} \right|_{t=0} = 0$$

where, $0 \le x \le x_1;\ 0 \le y \le y_1;\ 0 \le z \le z_1$.

(b) Boundary conditions

(i) At $x = 0$ plane, i.e., $(0 \le y \le y_1;\ 0 \le z \le z_1)$

$$T_e(0, y, z, t) = T_c = -196\ ^0C$$

(ii) At $x = l$ plane, $\left. \dfrac{\partial T_p(x, y, z, t)}{\partial x} \right|_{x=l} = 0.$

(iii) At $y = 0$ plane, $\left. \dfrac{\partial T_p(x, y, z, t)}{\partial y} \right|_{y=0} = 0$ and

at $y = y_1$ plane, $\left. \dfrac{\partial T_p(x, y, z, t)}{\partial y} \right|_{y=y_1} = 0.$

(iv) At $z = 0$ plane, $\left. \dfrac{\partial T_p(x, y, z, t)}{\partial z} \right|_{z=0} = 0$ and

at $z = z_1$ plane, $\left. \dfrac{\partial T_p(x, y, z, t)}{\partial z} \right|_{z=z_1} = 0.$

(v) At interface boundary of epidermis and dermis, i.e., $x = l_1$ and $0 \le y \le y_1;\ 0 \le z \le z_1$.

$$k_e \left.\frac{\partial T_e(x,y,z,t)}{\partial x}\right|_{x=l_1} = k_d \left.\frac{\partial T_d(x,y,z,t)}{\partial x}\right|_{x=l_1}$$
$$T_e(l_1,y,z,t) = T_d(l_1,y,z,t).$$

(vi) At interface boundary of dermis and subcutaneous, i.e., $x = l_2$ and $0 \le y \le y_1;\ 0 \le z \le z_1$.

$$k_d \left.\frac{\partial T_d(x,y,z,t)}{\partial x}\right|_{x=l_2} = k_s \left.\frac{\partial T_s(x,y,z,t)}{\partial x}\right|_{x=l_2}$$
$$T_d(l_2,y,z,t) = T_s(l_2,y,z,t).$$

5.4 Numerical Solution

Considering $x_i = i\delta x,\ y_j = j\delta y,\ z_k = k\delta z\ (\delta x = \delta y = \delta z)\ and\ t_n = n\delta t$, where i, j, k and n are the space and time index, respectively; $\delta x, \delta y, \delta z$ and δt are the distance between grids along *x*-axis, *y*-axis, *z*-axis and time respectively. To discretize the equation (5.5), we have used the first-order forward difference for first order time derivative and second order central difference approximation for second order space and time derivatives at point (x_i, y_j, z_k, t_n), the discretized form of equation (5.5) is given as follows

$$\begin{aligned}
(H_p)_{ijk}^{n+1} &= \left(1+\frac{A_{ijk}^n}{A_{ijk}^n+B_{ijk}^n}\right)(H_p)_{ijk}^n - \left(\frac{A_{ijk}^n}{A_{ijk}^n+B_{ijk}^n}\right)(H_p)_{ijk}^{n-1} \\
&+\left(\frac{D_{ijk}^n+E_{ijk}^n}{A_{ijk}^n+B_{ijk}^n}\right)\left\{(T_p)_{i+1,j,k}^n+(T_p)_{i-1,j,k}^n+(T_p)_{i,j+1,k}^n+(T_p)_{i,j-1,k}^n+(T_p)_{i,j,k+1}^n+(T_p)_{i,j,k-1}^n-6(T_p)_{i,j,k}^n\right\} \\
&-\left(\frac{E_{ijk}^n}{A_{ijk}^n+B_{ijk}^n}\right)\left\{(T_p)_{i+1,j,k}^{n-1}+(T_p)_{i-1,j,k}^{n-1}+(T_p)_{i,j+1,k}^{n-1}+(T_p)_{i,j-1,k}^{n-1}+(T_p)_{i,j,k+1}^{n-1}+(T_p)_{i,j,k-1}^{n-1}-6(T_p)_{i,j,k}^{n-1}\right\} \\
&+\left(\frac{F_{ijk}^n}{A_{ijk}^n+B_{ijk}^n}\right)\left\{T_b-(T_p)_{i,j,k}^n\right\}+(Q_{mp})_{i,j,k}^n,
\end{aligned} \tag{5.7}$$

where,

$$A_{ijk}^n = \frac{\tau_q(\rho_p)_{ijk}^n}{(\delta t)^2};\ B_{ijk}^n = \left(\frac{(\rho_p)_{ijk}^n}{(\delta t)}+\frac{\tau_q(\rho_b w_b)_p c_b}{(c_p)_{ijk}^n(\delta t)}\right);\ D_{ijk}^n = \frac{(k_p)_{ijk}^n}{(\delta x)^2};$$
$$E_{ijk}^n = \frac{\tau_T(k_p)_{ijk}^n}{\delta t(\delta x)^2};\ F_{ijk}^n = \left\{(\rho_b w_b)_p\right\}_{ijk}^n c_b.$$

The above equation (5.7) can be written as:

$$
\begin{aligned}
(H_p)_{ijk}^{n+1} &= (1+U_{ijk}^n)(H_p)_{ijk}^n - U_{ijk}^n (H_p)_{ijk}^{n-1} \\
&+ V_{ijk}^n \left\{ (T_p)_{i+1,j,k}^n + (T_p)_{i-1,j,k}^n + (T_p)_{i,j+1,k}^n + (T_p)_{i,j-1,k}^n + (T_p)_{i,j,k+1}^n + (T_p)_{i,j,k-1}^n - 6(T_p)_{i,j,k}^n \right\} \\
&- W_{ijk}^n \left\{ (T_p)_{i+1,j,k}^{n-1} + (T_p)_{i-1,j,k}^{n-1} + (T_p)_{i,j+1,k}^{n-1} + (T_p)_{i,j-1,k}^{n-1} + (T_p)_{i,j,k+1}^{n-1} + (T_p)_{i,j,k-1}^{n-1} - 6(T_p)_{i,j,k}^{n-1} \right\} \\
&+ Y_{ijk}^n \left\{ T_b - (T_p)_{i,j,k}^n \right\} + Z_{ijk}^n .
\end{aligned}
\tag{5.8}
$$

where,

$$
U_{ijk}^n = \frac{A_{ijk}^n}{A_{ijk}^n + B_{ijk}^n}; \quad V_{ijk}^n = \frac{D_{ijk}^n}{A_{ijk}^n + B_{ijk}^n}; \quad W_{ijk}^n = \frac{E_{ijk}^n}{A_{ijk}^n + B_{ijk}^n}; \quad Y_{ijk}^n = \frac{F_{ijk}^n}{A_{ijk}^n + B_{ijk}^n}; \quad Z_{ijk}^n = \frac{(Q_{mp})_{ijk}^n}{A_{ijk}^n + B_{ijk}^n} .
$$

Equation (5.8) gives the value of enthalpy at $(n+1)^{th}$ time level. To manage the space and time increments, a stability condition for numerical solution is used, which is given as

$$
\max \left\{ \begin{array}{l}
\dfrac{(\delta t)\left\{6k(\delta t) + 6k\tau_T + (\rho_b w_b)_p c_b (\delta t)(\delta x)^2\right\}}{(\delta x)^2 \left\{2\tau_q c_p \rho_p + c_p \rho_p (\delta t) + \tau_q (\rho_b w_b)_p c_b (\delta t)\right\}}, \dfrac{(\delta t)\left\{6k(\delta t) + 6k\tau_T + (\rho_b w_b)_p c_b (\delta t)(\delta y)^2\right\}}{(\delta y)^2 \left\{2\tau_q c_p \rho_p + c_p \rho_p (\delta t) + \tau_q (\rho_b w_b)_p c_b (\delta t)\right\}}, \\
\dfrac{(\delta t)\left\{6k(\delta t) + 6k\tau_T + (\rho_b w_b)_p c_b (\delta t)(\delta z)^2\right\}}{(\delta z)^2 \left\{2\tau_q c_p \rho_p + c_p \rho_p (\delta t) + \tau_q (\rho_b w_b)_p c_b (\delta t)\right\}}
\end{array} \right\} \le 1.
$$

Temperature at $(n+1)^{th}$ time level can be obtained from the enthalpy at $(n+1)^{th}$ time level by inverting the equation (5.6) as follows:

$$
T_p = \begin{cases}
\dfrac{H_p}{(c_p)_f} + T_{ms} & H_p < 0 \\
\dfrac{2H_p (T_{ml} - T_{ms})}{\{(c_p)_f + (c_p)_u\}(T_{ml} - T_{ms}) + 2L} + T_{ms} & 0 \le H_p \le L + \dfrac{1}{2}\{(c_p)_f + (c_p)_u\}(T_{ml} - T_{ms}). \\
\dfrac{H_p}{(c_p)_u} - \dfrac{L}{(c_p)_u} - \dfrac{\{(c_p)_f + (c_p)_u\}(T_{ml} - T_{ms})}{2(c_p)_u} + T_{ml} & H_p > L + \dfrac{1}{2}\{(c_p)_f + (c_p)_u\}(T_{ml} - T_{ms})
\end{cases}
\tag{5.9}
$$

5.4.1 Numerical Code Validation

At $y = z = 0$, 3D dual phase lag model reduces to the 1D dual phase lag model. A numerical code validation is made by comparing the present results with published results [136], Results are compared for DPL model at $\tau_q = 3s$ and $\tau_T = 0.1s$, as a special case.

Solution generated by present code is in good agreement with published results. A comparison table is given below.

Table 5.1: Comparison between published and present results at $\tau_q = 3s$ and $\tau_T = 0.1s$.

	Published results [136]		**Present results**	
Time (s)	Upper Interface (m)	Lower Interface (m)	Upper Interface (m)	Lower Interface (m)
50	0.0038	0.0037	0.0038	0.0036
100	0.0058	0.0056	0.0060	0.0055
150	0.0070	0.0069	0.0071	0.0070
200	0.0084	0.0081	0.0085	0.0082
250	0.0098	0.0091	0.0098	0.0091

5.5 Results and Discussion

The results obtained for the two phase lag effects, namely phase lag in heat flux and phase lag of temperature gradient during the freezing process of triple layer skin tissue. For a subjected skin tissue, the thermo-physical properties used in the present simulation are listed in Table 4.1. For the numerical solution, values of the phase lag in heat flux are $\tau_q = 5s, 3s, 1s, 0s$ and values of the phase lag in temperature gradient are $\tau_T = 0.1s, 0s$ [28, 60, 161-162]. Numerical simulations were carried out for grid space of $dx = dy = dz = 0.00002\ m$ and time step of $dt = 0.002s$. The analysis of temperature distribution, upper and lower interfaces is important because of their significant role in freezing process.

The graphical representation of 3D temperature distribution in the skin tissue for DPL model at time, *t* = 100 *s*, 200 *s* and 300 *s* is shown in Figures 5.1–5.3. It is found that the end sections of skin tissue do not freeze at the start of freezing process. Due to the higher thermal conductivity and diffusivity of skin tissue in the frozen region, skin tissue solidifies as the time moves ahead. The thickness of the frozen layer increases with passage of time.

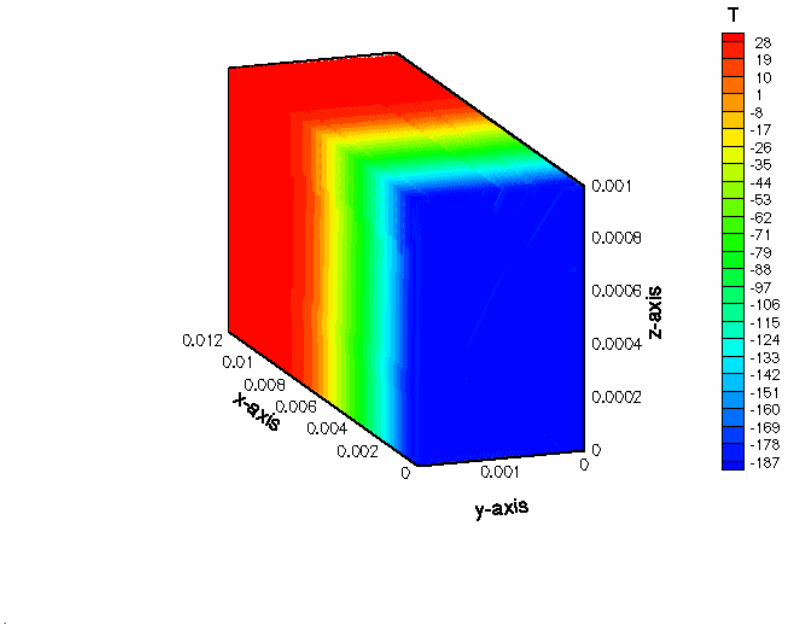

Figure 5.1: Temperature distribution along the skin tissue for DPL model ($\tau_q = 3s$ and $\tau_T = 0.1s$) at t =100 s.

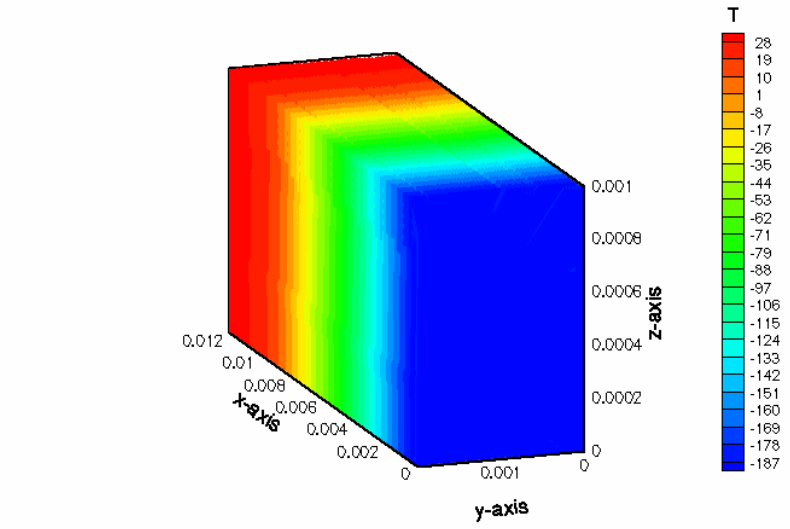

Figure 5.2: Temperature distribution along the skin tissue for DPL model ($\tau_q = 3s$ and $\tau_T = 0.1s$) at t =200 s.

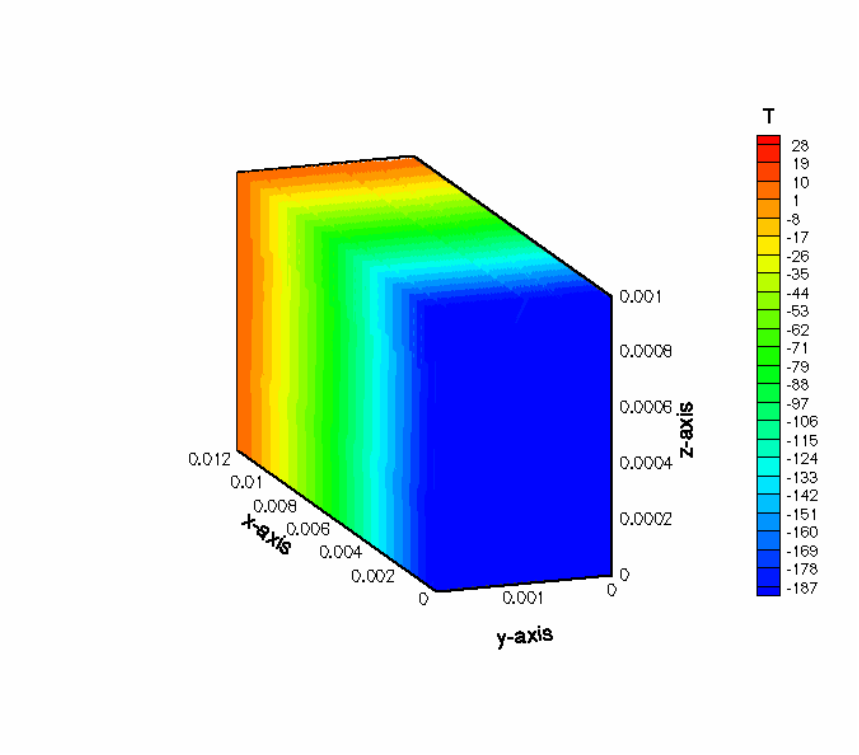

Figure 5.3: Temperature distribution along the skin tissue for DPL model ($\tau_q = 3s$ and $\tau_T = 0.1s$) at t =300 s.

Figures 5.4 – 5.6 show the temperature distribution at the surface of skin tissue (at z = 0m) for DPL, hyperbolic and parabolic models at time level t = 100 s, 200 s and 300 s. For different values of phase lag in heat flux and temperature gradient, the prediction of temperature distribution shows similar behavior but differ at different values of τ_q and τ_T. The comparative study of three bio-heat models, i.e., DPL, hyperbolic and parabolic, shows that the highest temperature of tissue for hyperbolic case and lowest for the parabolic case while moderate in case of DPL model at the same time.

(a)

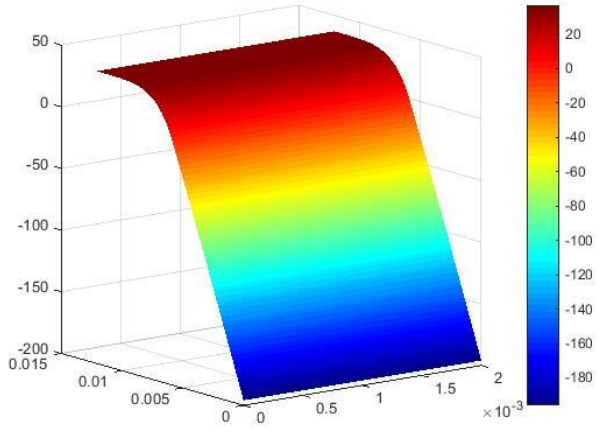

(b)

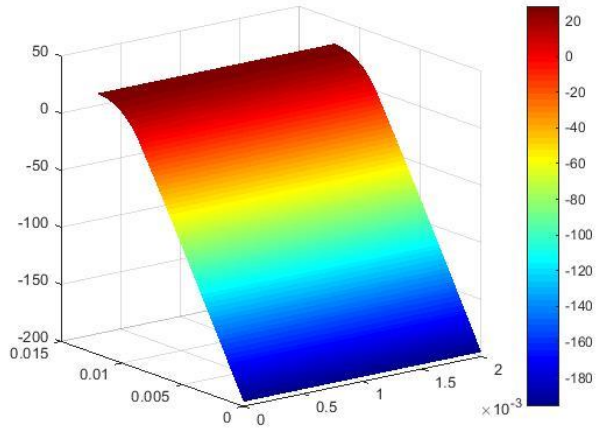

(c)

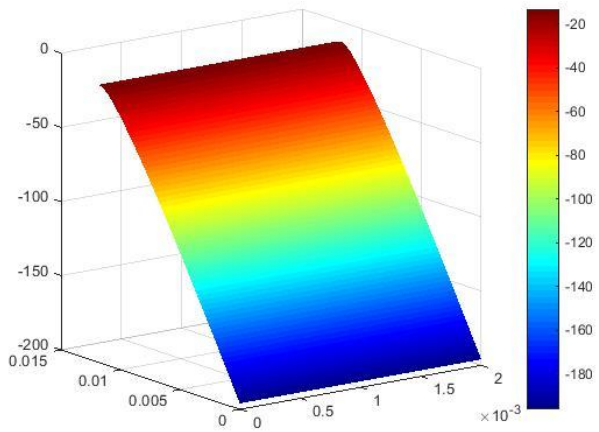

Figure 5.4: Temperature distribution along the skin tissue at z = 0 m for DPL model ($\tau_q = 3s$ & $\tau_T = 0.1s$) at time (a) t =100 s, (b) t =200 s and (c) t =300 s.

(a)

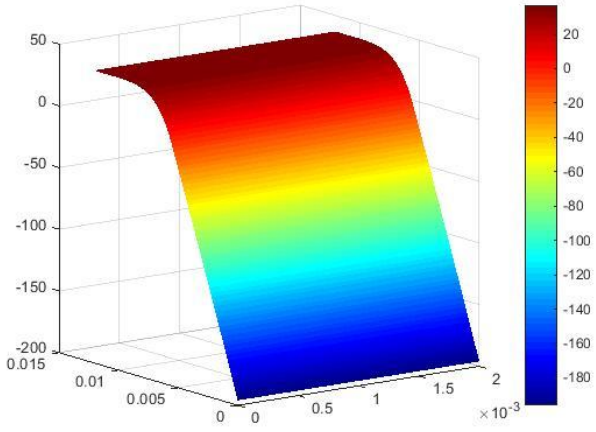

(b)

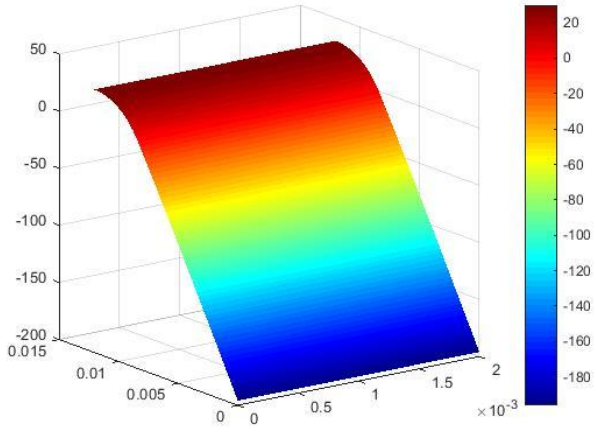

(c)

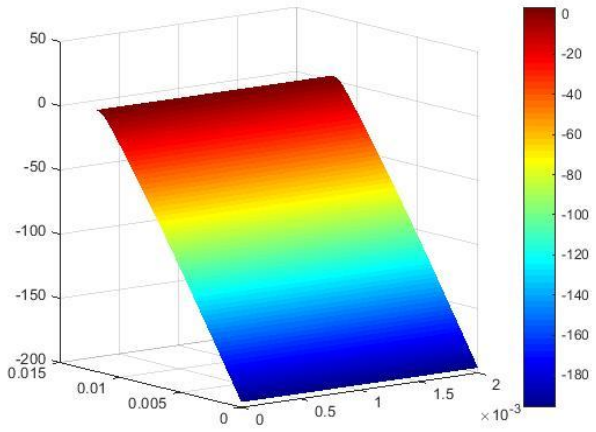

Figure 5.5: Temperature distribution along the skin tissue at z = 0 m for hyperbolic model ($\tau_q = 3s$ & $\tau_T = 0s$) at time (a) t =100 s, (b) t =200 s and (c) t =300 s.

(a)

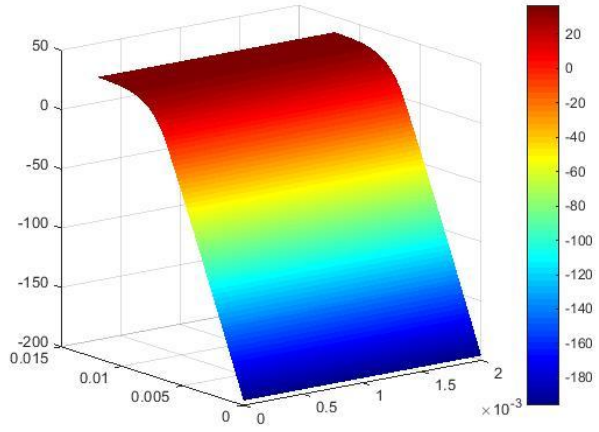

(b)

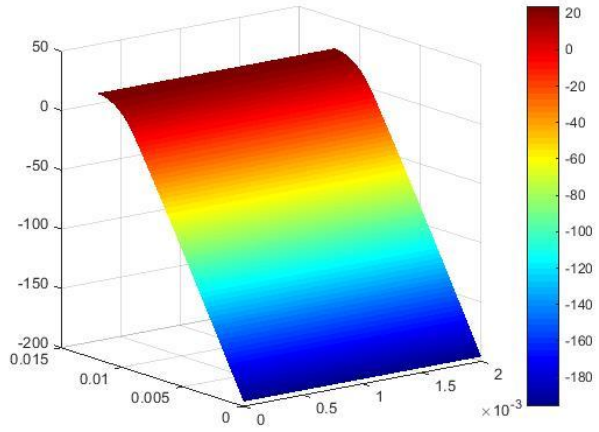

(c)

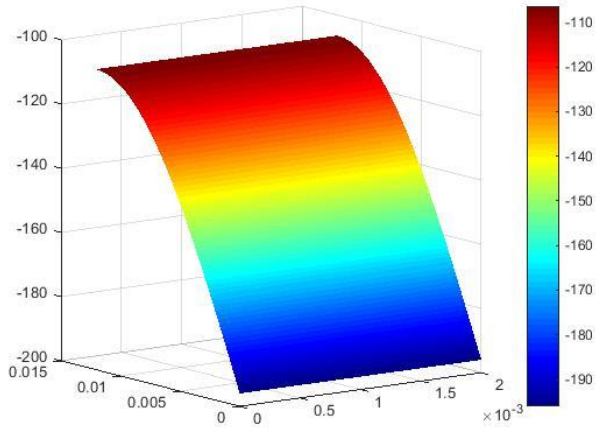

Figure 5.6: Temperature distribution along the skin tissue at z = 0 m for parabolic model ($\tau_q = 0\,s$ & $\tau_T = 0\,s$) at time (a) t =100 s, (b) t =200 s and (c) t =300 s.

As the triple layer skin tissue shows the non-ideal behavior, phase transition from one phase to another occurs over a broad range with upper phase change temperature at -1 ^0C and lower phase change temperature at -8 ^0C. Upper and lower phase change interface for DPL, hyperbolic and parabolic models are plotted at y = 0 m and z = 0 m in figures 5.7 and 5.8, respectively. Here it is observed that to cover the whole tissue for upper interface, total time taken are t = 284 s, 307 s, and 256 s and for lower interface are t = 302 s, 325 s, and 271 s at $\tau_q = 5s, 3s, 1s$ for DPL, hyperbolic and parabolic models, respectively.

Figures 5.9 and 5.10 show the interface positions for DPL model for fixed value of phase lag in temperature gradient $(\tau_T = 0.1s)$ and different values of phase lag in heat flux $(\tau_q = 5s, 3s, 1s)$ at different time. We observed that both upper and lower interface cover the whole skin tissue with total time, t = 300 s, 284 s, 267 s and t = 320 s, 303 s, 283 s, respectively. Therefore, interface positions of upper and lower interface decreases with increasing value of τ_q. It implies that for small values of τ_q, freezing is fast. This is due to dominance of phase lag in heat flux over the propagation of thermal signal.

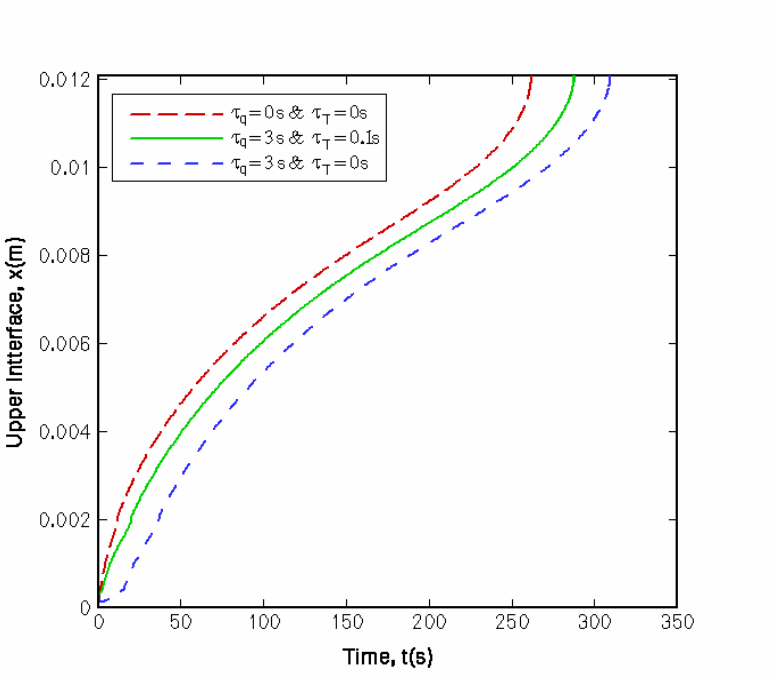

Figure 5.7: Position of upper interface during freezing versus time at y = 0 m and z = 0 m for DPL, hyperbolic and parabolic model.

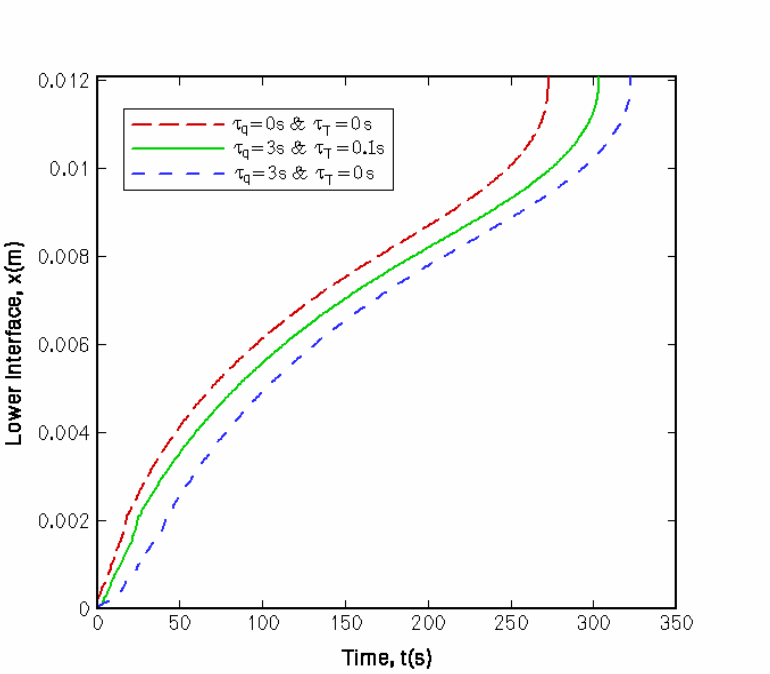

Figure 5.8: Position of lower interface during freezing versus time at $y = 0\ m$ and $z = 0\ m$ for DPL, hyperbolic and parabolic model.

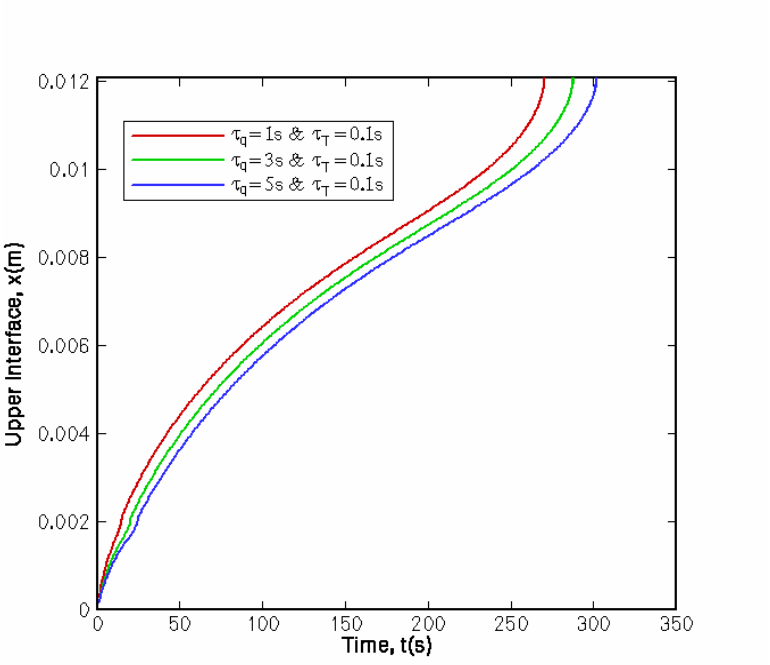

Figure 5.9: Position of upper interface during freezing versus time at $y = 0\ m$ and $z = 0\ m$ for DPL model at $\tau_q = 5s, 3s, 1s$ and $\tau_T = 0.1s$.

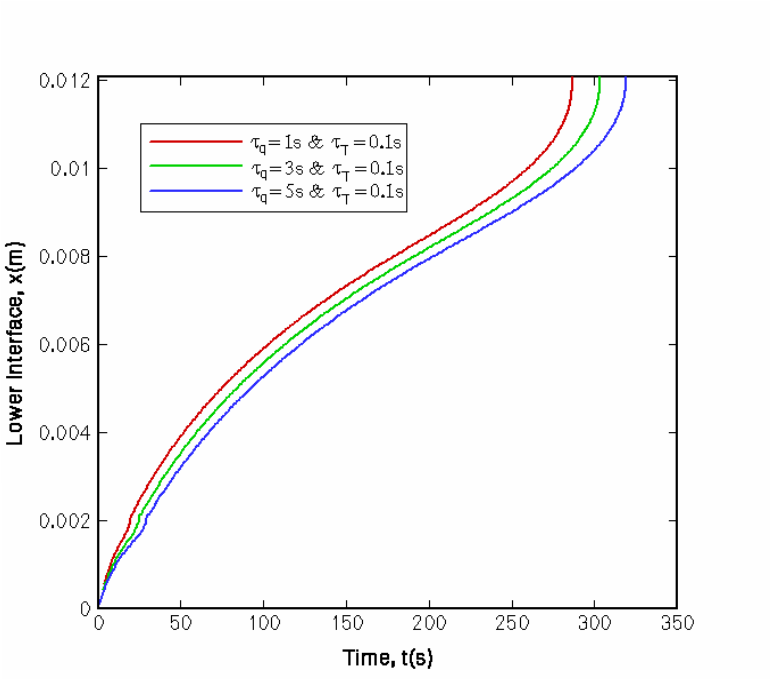

Figure 5.10: Position of lower interface during freezing versus time at $y = 0$ *m* and $z = 0$ *m* for DPL model at $\tau_q = 5s, 3s, 1s$ and $\tau_T = 0.1s$.

5.6 Conclusions

In summary, the effect of phase lag in heat flux and phase lag in temperature gradient on heat transfer process during freezing of triple layered skin tissue has been analyzed using dual phase lag bio-heat model. The governing nonlinear partial differential equations are solved numerically using finite difference scheme. Comparison of the three bio-heat models has also been studied. Results show that among of the three models DPL, parabolic and hyperbolic models, the time taken for complete freezing of the tissue is (i) lowest in case of parabolic model (ii) highest in case of hyperbolic and (iii) moderate for DPL model. Both the phase lags have a significant effect on interface positions and temperature distribution. In DPL case, at fixed value of τ_q and different values of τ_T, freezing interface decreases with increasing value of phase lag in heat flux. Results obtained are expected to be helpful in preselecting the parameters to optimize the freezing protocols.

Chapter 6

Conclusions and Future Scope

6.1 Conclusions

In the present thesis, an attempt has been made to understand the phase change heat transfer phenomena in biological tissues undergoing cryosurgery process. This work presents the mathematical models to study the effects of single phase lag (relaxation time for heat flux) and dual phase lag (phase lag of heat flux and phase lag of temperature gradient) parameters on interface positions and temperature distribution in subjected tissues. The finite difference method based on temperature dependent enthalpy has been adopted to solve the governing equations. We have focused on two types of problems: (i) phase change heat transfer in biological tissues using two and three-dimensional hyperbolic bio-heat model and (ii) phase change heat transfer in biological tissues using two and three-dimensional dual phase lag model.

In chapter 2, phase change heat transfer during cryosurgery of lung tumor tissue has been studied using two-dimensional hyperbolic bio-heat model. This chapter is mainly concerned with effects of relaxation time on temperature profiles and motion of freezing interfaces. In Chapter 3, a dual phase lag model is used to develop the constitutive relation to explore the effects of phase lag in heat flux and phase lag in temperature gradient on interface positions and temperature distribution in cryosurgery of lung cancer.

To analyze the freezing behavior of triple layer skin tissue, a three-dimensional hyperbolic bio-heat model is given in Chapter 4. Temperature distribution and position of interfaces are calculated for different values of relaxation time. The three-dimensional numerical study on dual phase lag model for freezing behavior of triple layer skin tissue is presented in Chapter 5. Temperature profiles and motion of freezing interfaces are plotted to see the effects of both the phase lags in freezing procedure. Since the triple layer skin tissue is multidimensional, 3D model gives more details of heat transfer, i.e., finer resolution of heat flow conditions within study area.

The following conclusions have been drawn from this study:

- Relaxation time for heat flux is an important factor which affects the temperature distribution and phase change interfaces. On comparing the two bio-heat models, it

is observed that hyperbolic solution reduces to parabolic solution for small value of relaxation time. The freezing interface decreases on increasing relaxation time for heat flux, which implies that interface position for hyperbolic model moves slower than the parabolic model.

- The tissue temperature is also increased with increasing value of relaxation time, which makes the non-Fourier's effect more dominant. Freezing is fast for small value of relaxation time in case of hyperbolic model.
- In case of dual phase lag model from the results, it is observed that due to the effects of two phase lags, phase change interfaces for DPL model move faster than the hyperbolic model but slower than the parabolic model. Tissue temperature is lowest for parabolic model with comparison to DPL and hyperbolic model. The highest temperature is obtained for hyperbolic model. This shows that parabolic model gives fastest heat flow in the media while it is slowest for hyperbolic model.
- It is observed that for different values of phase lag in heat flux and fixed value of phase lag in temperature gradient, freezing process is fast for small values of phase lag in heat flux.
- For performing effective treatment, the above informations are very useful to control temperature level accurately at the target tumor tissue because over freezing of tissue may cause an irreversible injury to the surrounding normal tissues.
- In triple layer skin tissue for hyperbolic model, the total time required for freezing the whole region is smaller in case of parabolic model as compared to the hyperbolic model.
- Further, among of the three models DPL, parabolic and hyperbolic models, the time taken for complete freezing of the tissue is lowest for parabolic model, highest for hyperbolic and moderate in case of DPL model.
- A successful understanding of parameters, which are responsible for tumor tissue damage, can help to develop suitable methodology for damage control of neighboring normal tissues.
- The results of present work are beneficial to understand the heat transfer mechanism during cryosurgical treatment.

6.2 Scope for Further Research

Research is an iterative and continuous process. The field of heat transfer with phase change in biological tissues is a vast area. This thesis has addressed only a few aspects of it. Some more potential extension of the work in this thesis is also possible.

- Future research will focus on the extension of the 2D-model to multi-dimensional so as to predict the freezing of lung-tumor tissue.
- Future efforts could also be made to develop the mathematical model for cryosurgery of tumor tissues with irregular domain or complex-shaped tumors.
- Multidimensional study with detailed numerical analysis using others numerical methods like finite element, finite volume method and boundary element method on their efficiency, accuracy and convergence.

These problems are left for the future study.

Bibliography

[1] Ahmadikia, H., Fazlali, R., Moradi, A., Analytical solution of the parabolic and hyperbolic heat transfer equations with constant and transient heat flux conditions on skin tissue, *International Communications in Heat and Mass Transfer*, 39(1) (2012) 121–130.

[2] Ahmadikia, H., Moradi, A., Non-Fourier phase change heat transfer in biological tissues during solidification, *Heat and Mass Transfer*, 48(9) (2012) 1559-1568.

[3] Alexiades, V., Solomon, A.D., *Mathematical Modeling of Melting and Freezing Process*, Hemisphere Publication, Washington DC, 1993.

[4] Allington, H.V., Liquid nitrogen in the treatment of skin diseases, *California Medicine*, 72(3) (1950) 153.

[5] Antaki, P.J., New interpretation of non-Fourier heat conduction in processed meat. *Transactions of the ASME-C-Journal of Heat Transfer*, 127(2) (2005) 189-193.

[6] Arnott, J., Practical illustrations of the remedial efficacy of a very low or anaesthetic temperature—I. In cancer, *The Lancet*, 56(1411) (1850) 316-318.

[7] Askarizadeh, H., Ahmadikia, H., Analytical analysis of dual-phase-lag model of bioheat transfer equation during transient heating of skin tissue, *Heat and Mass Transfer*, 50(12) (2014) 1673-1684.

[8] Baish, J.W., Ayyaswami, P.S., Foster, K.R., Small scale temperature fluctuation in perfused tissue during local hyperthermia, *Journal of Biomechanical Engineering*, 108(3) (1986) 246-251.

[9] Baissalov, R., Sandison, G.A., Donnelly, B.J., Saliken, J.C., McKinnon, J.G., Muldrew, K., Rewcastle, J.C., A semi-empirical treatment planning model for optimization of multiprobe cryosurgery, *Physics in Medicine and Biology*, 45(5) (2000) 1085.

[10] Baust, J., Gage, A.A., Ma, H., Zhang, C.M., Minimally invasive cryosurgery-technological advances, *Cryobiology*, 34(4) (1997) 373-384.

[11] Baust, J.G., Gage, A.A., Clarke, D., Baust, J.M., Buskirk, R.V., Cryosurgery-a putative approach to molecular based optimization, *Cryobiology*, 48(2) (2004) 190-204.

[12] Bischof, J.C., Bastacky, J., Rubinsky, B., An analytical study of cryosurgery in the lung, *Journal of Biomechanical Engineering*, 114(4) (1992) 467-472.

[13] Bonacina, C., Comini, G., Numerical solution of phase change problems, *International Journal of Heat and Mass Transfer*, 16(10) (1973) 1825-1832.

[14] Budhman, H.M., Dayan, J., Shitzer, A., Controlled freezing of non-ideal solution with application to cryosurgical processes, *Journal of Biomechanical Engineering*, 113(4) (1991) 430-437.

[15] Caldwell, J., Kwan, Y.Y., On the perturbation method for the Stefan problem with time-dependent boundary conditions, *International Journal of Heat and Mass Transfer*, 46(8) (2003) 1497-1501.

[16] Cancer facts and figures 2017. American Cancer Society. Available at: http://www.cancer.org/research/cancerfactsstatistics/cancerfactsfigures2017/

[17] Carslaw, H.S., Jaeger, J.C., *Conduction of Heat in Solids*, Second Edition, Oxford University Press, 1959.

[18] Cattaneo, C., A form of heat conduction equation which eliminates the paradox of instantaneous propagation, *Compte Rendus,* 247(4) (1958) 431-433.

[19] Charny, C. K., Levin, R. L., Bioheat transfer in a branching countercurrent network during hyperthermia, *Journal of Biomechanical Engineering*, 111(4) (1989) 263-270.

[20] Chen, M.M., Holmes, K.R., Microvascular contributions in tissue heat transfer, *Annals of the New York Academy of Sciences*, 335(1) (1980) 137-150.

[21] Chua, K.J., Chou, S.K., Ho, J.C., An analytical study on the thermal effects of cryosurgery on selective cell destruction, *Journal of Biomechanics*, 40(1) (2007) 100-116.

[22] Chun, C.K., Park, S.O., A fixed-grid finite-difference method for phase change problems, *Numerical Heat Transfer: Part B: Fundamentals*, 38(1) (2000) 59-73.

[23] Cooper, S.M., Dawber, R.P.R., The history of cryosurgery, *Journal of the Royal Society of Medicine*, 94(4) (2001) 196-201.

[24] Crank, J., *Free and Moving Boundary Problems*, University Press, New York, 1984.

[25] De Socio, L.M., Gualtieri, G., A hyperbolic Stefan problem, *Quarterly of Applied Mathematics*, 41(2) (1983) 253-259.

[26] Delgado, A.E., Sun, D.W., Heat and mass transfer model for predicting freezing processes a review, *Journal of Food Engineering*, 47(3) (2001) 157-174.

[27] Deng, Z.S., Liu, J., Modeling of multidimensional freezing problem during cryosurgery by the dual reciprocity boundary element method, *Engineering Analysis with Boundary Elements*, 28(2) (2004) 97-108.

[28] Deng, Z.S., Liu, J., Non-Fourier heat conduction effect on prediction of temperature transients and thermal stress in skin cryopreservation, *Journal of Thermal Stresses*, 26(8) (2003) 779-798.

[29] Deng, Z.S., Liu, J., Numerical simulation of 3-D freezing and heating problems for combined cryosurgery and hyperthermia therapy, *Numerical Heat Transfer, Part A: Applications*, 46(6) (2004) 587-611.

[30] Deng, Z.S., Liu, J., Numerical simulation of selective freezing of target biological tissues following injection of solutions with specific thermal properties, *Cryobiology*, 50(2) (2005) 183-192.

[31] Devireddy, R.V., Smith, D.J., Bischof, J.C., Effect of microscale mass transport and phase change on numerical prediction of freezing in biological tissue, *Journal of Heat Transfer*, 124(2) (2002) 365-374.

[32] Dey, S.K., A finite difference algorithm for coupled nonlinear ordinary differential equations, *International Journal of Computer Mathematics*, 10(1) (1981) 45-54.

[33] Dey, S.K., A novel explicit finite difference scheme for partial differential equations, *Mathematical Modelling and Analysis*, 4(1) (1999) 70-78.

[34] Dey, S.K., Finite-difference solution of boundary-layer equations, *Numerical Heat Transfer*, 3(4) (1980) 505-512.

[35] Diller, K.R., Engineering based contribution in cryobiology, *Cryobiology*, 34(4) (1997) 304-314.

[36] Elliott, C.M., Ockendon, J.R., *Weak and Variational Method for Moving Boundary Problems*, Pitman Publishing, Vol. 59, 1982.

[37] Evans, G.W., Issacson, E., MacDonald, J.K.L., Stefan-like problems, *Quarterly of Applied Mathematics*, 8(3) (1950) 312-319.

[38] Gage, A.A., Baust, J., Mechanism of tissue injury in cryosurgery, *Cryobiology*, 37(3) (1998) 171-186.

[39] Gage, A.A., Current issues in cryosurgery, *Cryobiology*, 19(3) (1982) 219-222.

[40] Ghosh, M., Chandra, P., Sinha, P., Shukla, J.B., Modelling the spread of bacterial disease: effect of service providers from an environmentally degraded region, *Applied Mathematics and Computation*, 160(3) (2005) 615-647.

[41] Ghosh, M., Chandra, P., Sinha, P., Shukla, J.B., Modelling the spread of carrier-dependent infectious diseases with environmental effect, *Applied Mathematics and Computation*, 152(2) (2004) 385–402.

[42] Globocan (2012), Estimated cancer incidence, mortality and prevalence worldwide in 2012, Available at: http://globocan.iarc.fr/Pages/fact_sheets_cancer.aspx?cancer=lung.

[43] Gupta, S.C., A moving grid numerical scheme for multi-dimensional solidification with transition temperature range, *Computer Methods in Applied Mechanics and Engineering*, 189(2) (2000) 525-544.

[44] Hafid, M., Lacroix, M., Fast inverse prediction of the freezing front in cryosurgery, *Journal of Thermal Biology*, 69 (2017) 13–22.

[45] Han, B., Bischof, J.C., Direct cell injury associated with eutectic crystallization during freezing, *Cryobiology*, 48(1) (2004) 8-21.

[46] Hanert, E., Piret, C., Numerical solution of the space-time fractional diffusion equation: Alternatives to finite differences, In *5th IFAC Symposium on Fractional Differentiation and Its Applications-FDA2012*, Hohai University, Nanjing, China, 14-17 May 2012.

[47] Hoffmann, N.E., Bischof, J.C., Cryosurgery of normal and tumor tissue in the dorsal skin flap chamber: Part I–thermal response, *Journal of Biomechanical Engineering*, 123(4) (2001) 301–309.

[48] Honnor, M.E., Davies, A.J., Nonlinear transient field problems with phase change using the boundary element method, *Engineering Analysis with Boundary Elements*, 28(6) (2004) 561-570.

[49] Ismail, K.A.R., Henriquez, J.R., Solidification of PCM inside a spherical capsule , *Energy Conversion and Management*, 41(2) (2000) 173-187.

[50] Jain, R.K., Gullino, P.M., Analysis of transient temperature distribution in a perfused medium due to a spherical heat source with application to heat transfer in tumors: homogeneous and infinite medium, *Chemical Engineering Communications*, 4(1-3) (1980) 95-118.

[51] Jain, R.K., Mass and heat transfer in tumors: applications in detection and treatment, *Advances in Transport Processes*, 3 (1984) 205-339.

[52] Jaunich, M., Raje, S., Kim, K., Mitra, K., Guo, Z., Bio-heat transfer analysis during short pulse laser irradiation of tissues, *International Journal of Heat and Mass Transfer*, 51(23) (2008) 5511–5521.

[53] Jiao, J., Guo, Z., Thermal interaction of short-pulsed laser focused beams with skin tissues, *Physics in Medicine and Biology*, 54(13) (2009) 4225.

[54] Jiji, L.M., Gaye, S., Analysis of solidification and melting of PCM with energy generation, *Applied Thermal Engineering*, 26(5) (2006) 568-575.

[55] Jiji, L.M., Weinbaum, S., Lemons, D.E., Theory and experiment for the effect of vascular microstructure on surface tissue heat transfer—part II: model formulation and solution, *Journal of Biomechanical Engineering*, 106(4) (1984) 331-341.

[56] Kapur, J.N., *Mathematical Modeling*, New Age International, Taj Press, New Delhi, 1998.

[57] Katiyar, V.K., Mohanty, B., Transient heat transfer analysis for moving boundary transport problem in finite media, *International Journal of Heat and Fluid Flow*, 10(1) (1989) 28-31.

[58] Ku, J.Y., Chan, S.H., A generalized Laplace transform technique for phase change problem, *Journal of Heat Transfer*, 112(2) (1990) 495-497.

[59] Kumar, A., Kumar, S., Katiyar, V. K., Telles, S., Dual phase lag bio-heat transfer during cryosurgery of lung cancer: Comparison of three heat transfer models, *Journal of Thermal Biology*, 69 (2017) 228-237.

[60] Kumar, A., Kumar, S., Katiyar, V.K., Telles, S., Phase change heat transfer during cryosurgery of lung cancer using hyperbolic heat conduction model, *Computers in Biology and Medicine*, 84 (2017) 20-29.

[61] Kumar, B.V.R., Rao, P.S., Sinha, P., A numerical study of performance of a slider bearing with heat conduction to the pad, *Finite Elements in Analysis and Design*, 37(6) (2001) 533-547.

[62] Kumar, M., A fourth order finite difference method for a class of singular two-point boundary value problems, *Applied Mathematics and Computation*,133(2) (2002) 539-545.

[63] Kumar, P., Kumar, D., Rai, K.N., A numerical study on dual-phase-lag model of bio-heat transfer during hyperthermia treatment, *Journal of Thermal Biology*, 49 (2015) 98-105.

[64] Kumar, R., Kumar, J., Finite volume scheme for multiple fragmentation equations, *International Journal of Numerical Analysis and Modeling*, Series B, 3(3) (2012) 270-284.

[65] Kumar, R., Kumar, J., Numerical simulation and convergence analysis of a finite volume scheme for solving general breakage population balance equations, *Applied Mathematics and Computation*, 219(10) (2013) 5140-5151.

[66] Kumar, R., Kumar, J., Warnecke, G., Moment preserving finite volume schemes for solving population balance equations incorporating aggregation, breakage, growth and source terms, *Mathematical Models and Methods in Applied Sciences*, 23(07) (2013) 1235–1273.

[67] Kumar, S., Ali, S., Katiyar, V.K., A parametric study on phase change heat transfer process during cryosurgery of lung tumor, *Indian Jounal Biomechanics: Special Issue* (2009) 210-213.

[68] Kumar, S., Katiyar, V.K., Mathematical modeling of thawing problem in skin and subcutaneous tissue, *In 6th World Congress of Biomechanics (WCB 2010)*, August 1-6, 2010 (1611-1614) Singapore, Springer Berlin Heidelberg.

[69] Kumar, S., Katiyar, V.K., Numerical study on phase change heat transfer during combined hyperthermia and cryosurgical treatment of lung cancer, *International Journal of Applied Mathematics and Mechanics*, 3(3) (2007) 1-17.

[70] Lai, T., Morsi, Y., Mazumdar, J., Modelling and simulation of particle deposition in the human lung, *Profiles in Industrial Research Knowledge and Innovation*, (2002) 313-320.

[71] Lazaridis, A., A numerical solution of the multidimensional solidification (or melting) problem, *International Journal of Heat and Mass Transfer*, 13(9) (1970) 1459-1477.

[72] Li, E., Liu, G.R., Tan, V., He, Z.C., An efficient algorithm for phase change problem in tumor treatment using α FEM, *International Journal of Thermal Sciences*, 49(10) (2010) 1954-1967.

[73] Li, J., Tang, H., Warnecke, G., Zhang, L., Local oscillations in finite difference solutions of hyperbolic conservation laws, *Mathematics of Computation*, 78(268) (2009) 1997-2018.

[74] Liepsch, D., Moravec, S. T., Pulsatile flow of non-Newtonian fluid in distensible models of human arteries, *Biorheology*, 21(4) (1984) 571-586.

[75] Liepsch, D., Pflugbeil, G., Matsuo, T., Lesniak, B., Flow visualization and 1-and 3-D laser-Doppler-anemometer measurements in models of human carotid arteries, *Clinical Hemorheology and Microcirculation*, 18(1) (1998) 1-30.

[76] Liepsch, D., Thurston, G., Lee, M., Studies of fluids simulating blood-like rheological properties and applications in models of arterial branches 1, *Biorheology*, 28(1-2) (1991) 39-52.

[77] Liu, J., Chen, X., Xu, L.X., New thermal wave aspects on burn evaluation of skin subjected to instantaneous heating, *IEEE Transactions on Biomedical Engineering*, 46(4) (1999) 420-428.

[78] Liu, J., Zhou, Y.X., Analytical study on the freezing and thawing process of biological skin with finite thickness, *Heat and Mass Transfer*, 38(4) (2002) 319-326.

[79] Liu, K. C., Chen, H. T., Cheng, P. J., Inverse investigation of non-Fourier heat conduction in tissue, *Journal of Thermal Biology*, 62 (2016) 123-128.

[80] Liu, K.C., Chen, H., Investigation for the dual-phase lag behaviour of bio-heat transfer, *International Journal of Thermal Sciences*, 49(7) (2010) 1138-1146.

[81] Liu, K.C., Cheng, P.J., Finite propagation of heat transfer in a multilayer tissue, *Journal of Thermophysics and Heat Transfer*, 22(4) (2008) 775–782.

[82] Liu, K.C., Thermal propagation analysis for living tissue with surface heating, *International Journal of Thermal Sciences*, 47(5) (2008) 507-513.

[83] Liu, W., Makhviladze, G., Fornberg, B., Piret, C., Moyle, K. R., Ventikos, Y., Liu, B., et al., 2743 An implicit finite element solution of thermal flows at low Mach number.

[84] Lunardini, V.J., *Heat Transfer in Cold Climates*, Van Nostrand Reinhold Company, New York, 1981.

[85] Maglik, A., A moving boundary solution for solidification of lava lake and magma instrusion in the presence of time-varying contact temperature, *Journal of Earth System Science*, 114(2) (2005) 169-176.

[86] Mahjoob, S., Vafai, K., Analytical characterization of heat transport through biological media incorporating hyperthermia treatment, International *Journal of Heat and Mass Transfer*, 52(5) (2009) 1608-1618.

[87] Majchrzak, E., Numerical solution of dual phase lag model of bioheat transfer using the general boundary element method, *Computer Modeling in Engineering and Sciences*, 69(1) (2010) 43-60.

[88] Mazumdar, J., An *Introduction to Mathematical Physiology and Biology*, Cambridge University Press, Second Edition, 1999.

[89] Mazumdar, J., *Preface to Biomathematical Modelling and Computing*, Automedica-New York- 15 (1993)177-177.

[90] Mazur, P., Freezing of living cells: mechanism and implications, *American Journal of Physiology-Cell Physiology*, 247(3) (1984) C125-C142.

[91] Mazur, P., Fundamental cryobiology and preservation of organs by freezing, *Organ Preservation for Transplantation*, (1981) 143-175.

[92] Mitra, K., Kumar, S., Vedevarz, A., Moallemi, M.K., Experimental evidence of hyperbolic heat conduction in processed meat, *Heat and Mass Transfer*, 117(3) (1995) 568-573.

[93] Mochnacki, B., Majchrzak, E., Numerical model of thermal interactions between cylindrical cryoprobe and biological tissue using the dual-phase lag equation,*International Journal of Heat and Mass Transfer*, 108 (2017) 1-10.

[94] Moradi, A., Ahmadikia, H., Numerical study of the solidification process in biological tissue with blood flow and metabolism effects by the dual phase lag model, *Proceedings of the Institution of Mechanical Engineers, Part H: Journal of Engineering in Medicine*, 226(5) (2012) 406–416.

[95] Muehlbauer, J.C., Hatcher, J.D., Lyons, D.W., Sunderland, J.E., Transient heat transfer analysis of alloy solidification, *Journal of Heat Transfer*, 95(3) (1973) 324-331.

[96] Nakayama, A., Kuwahara, Y., The limiting radius for freezing a tumor during percutaneous cryoablation, *Journal of Heat Transfer*, 130(11) (2008) 111101-6.

[97] Neumann, F., Lectures Given in the 1860's, *Die Partiellen Differential-Gleichungen der Mthematischen Physik*, (1912) 117-121.

[98] Ng, E.K., Sudharsan, N.M., Effect of blood flow, tumour and cold stress in a female breast: a novel time-accurate computer simulation,*Proceedings of the Institution of Mechanical Engineers, Part H: Journal of Engineering in Medicine*, 215(4) (2001) 393-404.

[99] Ng, E.Y.K., Sudharsan, N. M., Numerical modelling in conjunction with thermography as an adjunct tool for breast tumour detection, *BMC Cancer*, 4(17) (2004) 1-26.

[100] Ng, E.Y.K., Sudharsan, N.M., Bench Marking the Bioheat Equation for Finite Element Analysis, *Proceedings of the 4th International Symposium On Computer Methods in Biomechanics and Biomedical Engineering*, Lisbon, Portugal, Oct. 13-16, (1999).

[101] Ng, E.Y.K., Sudharsan, N.M., Numerical uncertainity and perfusion induced instability in bioheat equation: its importance in thermographic interpretation, *Journal of Medical Engineering and Technology*, 25(5) (2001) 222-229.

[102] Ng, E.Y.K., Tan, H.M., Ooi, E.H., Boundary element method with bioheat equation for skin burn injury, *Burns*, 35(7) (2009) 987-997.

[103] Nithaiarasu, P., An adaptive finite element procedure for solidification problems, *Heat and Mass Transfer*, 36(3) (2000) 223-229.

[104] Niu, L., Xu, K., Mu, F., Cryosurgery for lung cancer, *Journal of Thoracic Disease*, 4(4) (2012) 408–419.

[105] Nóbrega, S., Coelho, P. J., A parametric study of thermal therapy of skin tissue, *Journal of Thermal Biology*, 63 (2017) 92-103.

[106] Ozisik, M.N., *Finite Difference Methods in Heat Transfer*, CRC Press, 1994.

[107] Ozisik, M.N., *Heat Transfer: A Basic Approach*, McGraw-Hill, International Edition, 1985.

[108] Pam, Q.T., Modelling heat and mass transfer in frozen foods: a review, *International Journal of Refrigeration*, 29(6) (2006) 876-888.

[109] Pardasani, K.R., Saxena, V.P., Steady-state radial heat flow in skin and underlying tissue layer of spherical regions of human or animal body, *Indian Journal of Technology*, 25(11) (1987) 501-505.

[110] Pardashani, K.R., Adlakha, N., Co-axial circular sector element to study two-dimensional heat distribution problem in dermal region of human limbs, *Mathematical and Computer Modelling*, 22(9) (1995) 127-140.

[111] Pardashani, K.R., Shakya, M., A two dimensional infinite element model to study temperature distribution in human dermal region due to tumors, *Journal of Mathematics and Statistics*, 1(3) (2005) 184-188.

[112] Pennes, H.H., Analysis of tissue and arterial blood temperature in the resting human forearm, *Journal of Applied Physiology*, 1(2) (1948) 93–122.

[113] Piret, C., Dunn, J., Fast RBF OGr for solving PDEs on arbitrary surfaces, *In AIP Conference Proceedings*, 1776 (1) (2016) 070005, AIP Publishing.

[114] Rabin Y., Shitzer A., Exact solution to the one-dimensional inverse-Stefan problem in non-ideal biological tissues, *Journal of Heat Transfer*, 117 (1995) 425–431.

[115] Rabin, Y., Shitzer, A., Combined solution of the inverse-Stefan problem for successive freezing/thawing in non-ideal biological tissues, *ASME Journal of Biomechanical Engineering*, 119 (1997) 146-152.

[116] Rabin, Y., Shitzer, A., Numerical solution of the multidimensional freezing problem during cryosurgery, *Journal of Biomechanical Engineering*, 120 (1998) 32–37.

[117] Rabin, Y., Taylor, M.J., Wolmark, N., Thermal expansion measurements of frozen biological tissues at cryogenic temperatures, *Journal of Biomechanical Engineering*, 120(2) (1998) 259-266.

[118] Rai, K.N., Rai, S. K., Numerical solution of moving boundary problem on finite domain, *Heat and Mass Transfer*, 34(4) (1998) 295-298.

[119] Rai, K.N., Rai, S.K., Effect of heat generation and blood perfusion on the heat transfer in tissue with a blood vessel, *Heat and Mass Transfer*, 35(1) (1999) 75-79.

[120] Rai, K.N., Rai, S.K., Heat transfer inside the tissue with a supplying vessel for the case when metabolic heat generation and blood perfusion are temperature dependent, *Heat and Mass Transfer*, 35(4) (1999) 345-350.

[121] Ramajayam, K.K., Kumar, A., A novel approach to improve the efficacy of tumor ablation during cryosurgery, *Cryobiology*, 67 (2) (2013) 201-213.

[122] Rao, S.K., *Numerical Methods for Scientists and Engineers*, Third Edition, PHI, 2009.

[123] Roemer, R.B., Cetas, T.C., Applications of bioheat transfer simulations in hyperthermia, *Cancer Research*, 44 (10 Supplement) (1984) 4788s-4798s.

[124] Rossi, M.R., Rabin Y., Analysis of a numerical scheme for bioheat simulations of cryosurgery and its experimental validation on a phantom material, In *MSV* (2007) 187-193, International Conference on Modeling, Simulation and Visualization methods, Las Vegas, Nevada, USA.

[125] Sastry, S.S., *Introductory Methods of Numerical Analysis*, Fourth Edition, PHI, 2005.

[126] Selim, M.S., Seagrave, R.C., Solution of moving-boundary transport problems in finite media by integral transform. I. Problems with a plane moving boundary, *Industrial and Engineering Chemistry Fundamentals*, 12(1) (1973) 1-8.

[127] Shamsunder, N., Sparrow, E.M., Analysis of multidimensional conduction phase change problem via the enthalpy model, *ASME Journal of Heat Transfer*, 97 (1975) 333-340.

[128] Sharma, P.R., Ali, S., Katiyar, V.K., Mathematical modeling of temperature distribution on skin surface and inside biological tissue with different heating, *In 13th International Conference on Biomedical Engineering*, (2009) 1957–1961, Springer Berlin Heidelberg.

[129] Sharma, P.R., Ali, S., Katiyar, V.K., Numerical study of temperature and thermal dose response of tumor tissue during hyperthermia treatment, *In 25th Southern Biomedical Engineering Conference*, (2009) 377-378, 15–17 May 2009, Miami, Florida, USA, Springer, Berlin, Heidelberg.

[130] Sharma, P.R., Sazid, A., Katiyar, V.K., Transient heat transfer analysis on skin surface and inside biological tissue, *International Journal of Applied Mathematics and Mechanics*, 5 (2009) 36-47.

[131] Shepherd, J., Dawber, R. P. R., The historical and scientific basis of cryosurgery, *Clinical and Experimental Dermatology*, 7 (1982) 321–328.

[132] Shih, T. C., Yuan, P., Lin, W. L., Kou, H. S., Analytical analysis of the Pennes bioheat transfer equation with sinusoidal heat flux condition on skin surface, *Medical Engineering and Physics*, 29(9) (2007) 946-953.

[133] Shit, G.C., Bera, A., Temperature response in a living tissue with different heating source at the skin surface under relaxation time, *International Journal of Applied and Computational Mathematics*, 3(2) (2017) 381-394.

[134] Singh, S., Kumar, S., Freezing of biological tissues during cryosurgery using hyperbolic heat conduction model, *Mathematical Modelling and Analysis*, 20(4) (2015) 443-456.

[135] Singh, S., Kumar, S., Numerical analysis of triple layer skin tissue freezing using non-Fourier heat conduction. *Journal of Mechanics in Medicine and Biology*, 16(2) (2016) 1650017.

[136] Singh, S., Kumar, S., Numerical study on triple layer skin tissue freezing using dual phase lag bio-heat model, *International Journal of Thermal Sciences*, 86 (2014) 12-20.

[137] Smith, G.D., *Numerical Solution of Partial Differential Equations*, Third edition, Oxford University Press, 1985.

[138] Stefan, J., Über die theorie der eisbildung inbesondee uber die eisbindung im polarmeere, *Annalen der Physik*, 278(2) (1891) 269-286.

[139] Talukdar, P., Alagirusamy, R., Das, A., Heat transfer analysis and second degree burn prediction in human skin exposed to flame and radiant heat using dual phase

lag phenomenon, *International Journal of Heat and Mass Transfer*, 78 (2014) 1068-1079.

[140] Tandon, P.N., Bali, R., A study on temperature regulation in synovialjoints, *Tribology Letters*, 3(2) (1997) 209-213.

[141] Tarwidi D., Godunov method for computerized lung cancer cryosurgery planning with efficient freezing time, *In Information and Communication Technology (ICoICT), 2015 3rd International Conference on IEEE*, (2015) 494-499.

[142] Tzou, D.Y., A unified field approach for heat conduction from macro to microscales, *ASME Journal of Heat Transfer*, 117 (1995) 8-16.

[143] Tzou, D.Y., *Macro to Micro-scale Heat Transfer: The Lagging Behaviour*, Taylor and Francis, Washington, DC. 1997.

[144] Vernotte, P., Paradoxes in the continuous theory of the heat equation, *CR Acad Sci* 246(3) (1958) 154-3.

[145] Voller, V., Cross, M., Accurate solution of moving boundary problems using the enthalpy method, *International Journal of Heat and Mass Transfer*, 24(3) (1981) 545-556.

[146] Voller, V., Cross, M., An explicit numerical method to track a moving phase change front, *International Journal of Heat and Mass Transfer*, 26(1) (1983) 147-150.

[147] Voller, V.R., Shadabi, L., Enthalpy methods for tracking phase change boundary in two dimensions, *International Communications in Heat and Mass Transfer*, 11(3) (1984) 239-249.

[148] Warnecke, G., (Ed.): *Analysis and Numerics for Conservation Laws*, Springer-Verlag Berlin Heidelberg, 2005.

[149] Weill, A., Shitzer, A., Bar-Yoseph, P., Finite element analysis of the temperature field around two adjacent cryo-probes, *Journal of Biomechanical Engineering*, 115(4A), (1993) 374–379.

[150] Weinbaum, S., Jiji, L.M., A new simplified bioheat equation for the effect of blood flow on local average tissue temperature, *Journal of Biomechanical Engineering*, 107(2) (1985) 131-139.

[151] Wissler, E.H., Comments on Weinbaum and Jiji discussion of their proposed bioheat equation, *Journal of Biomechanical Engineering* 109(4) (1987) 355-356.

[152] Xu, F., Lu, T., *Introduction to Skin Biothermomechanics and Thermal Pain*, Springer, Heidelberg Dordrech, London New York, 2011.

[153] Xu, F., Lu, T.J., Steffen, K.A., Ng, E.Y.K., Mathematical modeling of skin bioheat transfer, *Applied Mechanics Reviews*, 62(5) (2009) 50801-50835.

[154] Xu, F., Wen, T., Lu, T.J., Seffen, K.A., Skin biothermomechanics for medical treatments, *Journal of the Mechanical Behavior of Biomedical Materials*, 1(2) (2008) 172–187.

[155] Yoo, J., Rubinsky, B., A finite element method for the study of solidification process in the presence of natural convection, *International Journal for Numerical Methods in Engineering*, 23(10) (1986) 1785-1805.

[156] Zein, A., Hantke, M., Warnecke, G., Modeling phase transition for compressible two-phase flows applied to metastable liquids, *Journal of Computational Physics*, 229(8) (2010) 2964-2998.

[157] Zhang, J., Hua, T.C., Chen, E.T., Experimental measurement and theoretical analyses of the freezing-thawing processes around a probe, *Cryo-Letters*, 21(4) (2000) 245–254.

[158] Zhang, J., Sadison, G.A., Murthy, J.Y., Xu, L.X., Numerical simulation for heat transfer in prostate cancer cryosurgery, *Journal of Biomechanical Engineering*, 127(2) (2005) 279-294.

[159] Zhang, Y., Generalized dual-phase lag bio-heat equations based on nonequilibrium heat transfer in living biological tissues, *International Journal of Heat and Mass Transfer*, 52(21) (2009) 4829-4834.

[160] Zhang, Y.T., Liu, J., Numerical study on three-region thawing problem during cryosurgical re-warming, *Medical Engineering and Physics*, 24(4) (2002) 265-277.

[161] Zhou, J., Chen, J.K., Zhang, Y., Dual-phase lag effects on thermal damage to biological tissues caused by laser irradiation, *Computers in Biology and Medicine*, 39(3) (2009) 286-293.

[162] Zhou, J., Zhang, Y., Chen, J.K., An axisymmetric dual-phase-lag bioheat model for laser heating of living tissues, *International Journal of Thermal Sciences*, 48(8) (2009) 1477-1485.

[163] Zhou, J., Zhang, Y., Chen, J.K., Non-Fourier heat conduction effect on laser-induced thermal damage in biological tissues, *Numerical Heat Transfer, Part A: Applications*, 54 (1) (2008) 1-19.

[164] Ziaei Poor, H., Moosavi, H., Moradi, A., Analysis of the dual phase lag bio-heat transfer equation with constant and time-dependent heat flux conditions on skin surface, *Thermal Science*, 20(5) (2016) 1457-1472.